NONCIRCULAR FUSELAGES IN SUPERSONIC FLOW

Thesis by

Norman Charles Peterson

In Partial Fulfillment of the Requirements

For the Degree of

Doctor of Philosophy

California Institute of Technology

Pasadena, California

1949

ACKNOWLEDGEMENT

During the preparation of this thesis, the writer has had the benefit of stimulating discussions of several of its parts with his principal adviser, Professor P. A. Lagerstrom who suggested the general problem, and with Professors H. J. Stewart and H. W. Liepmann. The writer wishes also to thank his friend, Dr. C. N. Nosretep of the Rand Corporation, Santa Monica, for continuing interest and criticism as the work progressed. The detailed preparation of the manuscript has been ably done by Mrs. Elizabeth Fox.

SUMMARY

The applicability of linearized theory to the aerodynamic study of slender, three-dimensional bodies in supersonic flow is considered in detail, and figures are presented which show the limitations of body shape and Mach number to be observed if quantitatively reliable results are to be achieved. Then methods are developed and evaluated for calculating the supersonic flow about slender noncircular bodies, other than wings.

Sections I and II are concerned with the velocity and pressure predictions of the linearized theory. It is shown that these quantities do not converge to the corresponding predictions of the exact solutions for vanishing disturbance, and the reason therefor is found. In Section III the inapplicability of wing theory methods and the theory of slender circular bodies to the present study is reviewed, and the problem is carried to the fundamental nonrotationally symmetrical solutions of the wave equation; the properties of the noncircular functions are developed in Section IV. Section V contains a description of the Lorentz transformation for obtaining solutions singular on a yawed line, and Section VI a simple statement of the GÖthert transformation for changing the Mach number.

Sections VII and VIII contain an exposition of the use of the theory developed in the previous Sections. Bodies in supersonic flow are classified according to size and orientation, and appropriate methods for each are presented and evaluated.

The Appendices present tables of the functions used in the analysis, along with sample computations.

CONTENTS

INTRODUCTION

This thesis has the two-fold purpose of evaluating by detailed explicit calculation the applicability of linearized theory to the study of supersonic flow about slender bodies in three dimensions; and, having discovered the domain of applicability, of developing suitable methods for calculating the flow about such bodies when they are not rotationally symmetrical.

In recent years a copious literature on linearized supersonic flow has appeared, but unfortunately little attention has been directed toward establishing in a concise form the limitations on body shape and Mach number which must be observed if the numerical predictions of the linearized theory are to be quantitatively reliable. The evaluation consists of two parts: the determination of the velocities by the linearized theory, and the calculation of the pressure from the velocity. It is illuminating to realize that at least six distinct pressure formulas have been in use in the literature, each a simplification of the exact formula and supposedly correct within terms of a certain order of magnitude. But it is shown in the text that the linearized theory does not necessarily predict the velocities correctly even for very small disturbances in three dimensions, and hence the most accurate representation of the exact pressure formula is not necessarily the best formula to use. A particular formula is recommended.

It may be argued that a linearized theory should not be expected to yield quantitatively reliable predictions and that one should be satisfied if the theory properly indicates the trend of the various

calculated quantities and correctly locates the decimal point in the numbers. However it happens that the linearized approach to supersonic aerodynamics is the only feasible approach to many of the most important problems if an answer is required within finite time. Consequently it is necessary to know for what configurations the linearized theory does and does not produce an acceptable numerical prediction; and, when the prediction is in error, whether the prediction is too large or too small.

The main part of the thesis is concerned with the development of methods for the study of supersonic flow over nonrotationally symmetrical slender bodies other than wings. It is shown that the methods of wing theory and the theory of rotationally symmetrical bodies are in general inapplicable to the problem, and the study is thrown back to a consideration of the fundamental solutions of the linearized equation of flow that may be superimposed in a demonstrated manner to represent a rather general class of bodies. Thruout the thesis, attention is given to the numerical reliability of the methods and the practicality of their use as routine calculation tools. Every effort has been made to discover and present the simplest calculation procedure for many of the problems likely to be encountered, and to this end extensive tables of the most important functions have been prepared. These tables are very useful. The solutions of the linearized equation are, of course, tabulated in their exact form.

An excellent chronological summary of the development of supersonic aerodynamics, and in particular of the linearized theory is presented in the introduction to the doctoral dissertation of Wallace D.

Hayes (1). The fundamental work dealing with the flow over slender bodies in three dimensions has been published by: Kármán and Moore (2) who in 1932 introduced the concept of superposition of conical flows to represent nonconical flows; Tsien (3) who in 1938 applied the superposition method to the study of bodies of revolution at yaw and introduced the important idea of cross flow; Lighthill (4,5) who in 1945 reexamined the fundamental assumptions of the linearized theory and put several of the ideas on a firm footing (though some criticism of Lighhill's paper is offered in this thesis); R. T. Jones (6,7) who in 1946 introduced the very convenient "slender body" approximation for estimating the characteristics of certain configurations; and finally W. D. Hayes (1), whose comprehensive thesis furnished the inspiration for this investigation. Some familiarity with these papers and with the theory of compressible fluid flow as summarized by Liepmann and Puckett (8) and by Sauer (9) has necessarily been assumed by the writer.

Throughout this study several words are used with specialized meanings; these words are now defined. The words solid body are used to distinguish the set of bodies under present consideration, which are essentially fuselage-like, from wing-like bodies. Furthermore, a solid body is slender and pointed at the upstream end, is not necessarily closed downstream, and has no thin excrescences. The meridian contours of a solid body have continuous slope, but the cross section contours may have slope discontinuities, other than cusps. The cross section contours are assumed to be simple closed continuous curves touched only once by any straight line from a point on the body axis. The set of

solid bodies is further subdivided in the text. The words circular and noncircular are used to distinguish a solid body which is a body of revolution from one which is not. Also, by square body, elliptical body, etc., are meant solid bodies whose cross section contours are respectively square or elliptical, and so on. A ray is any straight line in the space which passes through the origin of coordinates. A conical velocity field is one in which the velocity is constant along any ray. In speaking of velocity potentials, the words conical and nonconical mean that the velocity field associated with the potential is, respectively, conical or nonconical.

In the text, underlined numbers in parenthesis (1) denote the references to literature, and decimal numbers (8.11) denote equations.

I. LIMITATIONS OF THE LINEARIZED THEORY IN THREE DIMENSIONS

This study is concerned with the steady supersonic flow over solid bodies as defined in the Introduction. On the assumption that this flow is isentropic (irrotational) and steady, that the effects of viscosity and heat transfer are negligible, and that the incremental velocities are small in comparison with the sonic velocity, the exact equation of motion may be linearized. There result the fundamental equations for linearized flow (8, Chapter 8)

$$\bar{q} = \bar{U} + \operatorname{grad}\varphi$$

$$(M^2-1)\frac{\partial^2\varphi}{\partial x^2} - \frac{\partial^2\varphi}{\partial y^2} - \frac{\partial^2\varphi}{\partial z^2} = 0 \qquad (1.1)$$

In (1.1) φ is the velocity potential of the perturbations, $\bar{U}$ is the free stream velocity (assumed parallel to the x-axis), M is the free stream Mach number, and x,y,z are Cartesian coordinates. When the free stream is supersonic, $M^2-1 \equiv B^2 > 0$ and (1.1) has the form of the wave equation, frequently written

$$\Box\,\varphi = 0$$

$$\Box = B^2\frac{\partial^2}{\partial x^2} - \frac{\partial^2}{\partial y^2} - \frac{\partial^2}{\partial z^2}$$

If the surface of the solid body is

$$S(x,y,z) = 0$$

then the problem is to construct the solution of (1.1) which satisfies the condition that the flow be tangent to the body surface:

$$(\bar{U} + \operatorname{grad}\varphi)\cdot\operatorname{grad} S\Big|_{S=0} = 0 \qquad (1.2)$$

The precision of the results to be deduced from the linearized theory may be estimated by comparison of the numerical values of a particular flow variable as obtained from solutions of both the linearized and exact (nonlinear) differential equations describing a representative problem. Denoting by q the magnitude of the local total velocity, the variable selected for comparison is $1 - \left(\frac{q}{U}\right)^2$, the argument of the exact isentropic pressure formula. $U^2\left[1 - \left(\frac{q}{U}\right)^2\right]$ is approximately proportional to twice the longitudinal perturbation. The formula of linear theory for q at the surface of an unyawed circular cone of half vertex angle θ_s in a steady supersonic stream is

$$q_s = U \cos\theta_s \left[1 - \frac{t_s^2}{B^2\sqrt{1-t_s^2}}\left(\cosh^{-1}\frac{1}{t_s} - \sqrt{1-t_s^2}\right)\right]$$

where $t_s = B \tan\theta_s$. This quantity according to the exact solution of the problem may be calculated from Kopal's tables (10).

If the maximum permissible error be established as 10% of the exact value, it is possible to plot as a function of M the maximum and minimum of t_s and θ_s for which the linearized theory yields an acceptable value of $1 - \left(\frac{q_s}{U}\right)^2$. The result is presented on Fig. 1, where the domain of applicability of the linear theory is labelled. The boundaries of the domain are not definite because the fundamental parameters of the linearized and exact solutions are not the same. The upper boundary is associated with those combinations of large cone angle and Mach number at which the assumption of isentropy is beginning to break down. The left boundary marks those Mach numbers below which the conical flow regime does not exist (bow wave detached). The lower boundary requires some discussion, for the existence of a lower limit of cone angle

below which, at a given Mach number, the linearized theory does not yield an acceptable prediction of the perturbation velocity challenges the validity of the linearizing assumptions.

Figure 2 presents a comparison of exact and linear theory predictions of $1 - \left(\frac{v_s}{U}\right)^2$ for unyawed cones of 5°, 7°.5, 10° and 15° half-vertex angle. Apparently the predictions of the linearized theory do not in general agree with those of the exact solution and, for small cone angles, the divergence increases as the cone angle decreases. The error in the longitudinal perturbation component is the order of 20% for a 5° cone at moderate supersonic speeds. This behavior suggests that there is something fundamentally incorrect in the linearized differential equation for rotationally symmetrical supersonic flows, for otherwise the exact and linearized predictions would coincide for vanishingly small disturbances.

Second order theory (11) produces perturbation predictions of greatly improved accuracy. It is, however, impossible to deduce from the results of the theory whether or not the functional dependence of the perturbations on the Mach number and cone angle is correctly given to a first approximation by the simple linear theory, for the iteration procedure is only a method of calculating correction terms to be applied to any initial function which fulfills the prescribed boundary conditions.

It will now be indicated that the linearized differential equation inadequately approximates the exact equation when the disturbance considered is very small. The exact differential equation of the problem

will be discussed, and an approximate integral of it found which is valid for very small disturbances and low supersonic speeds. The new solution agrees well with the exact solution; it can be transformed into the linearized theory result with an added correction term of order ε^2. The lowest order term of second order theory is of order $\varepsilon^4 (\log \varepsilon)^2$ (11).

The motion is considered on the hodograph plane, where the differential equation is ordinary with a single dependent variable. The exact hodograph equation describing the adiabatic compressive flow between the body surface and the bow wave of an unyawed circular cone is (12,13)

$$v v_{uu} = \left(1 - \frac{u^2}{a^2}\right) + \left(1 - \frac{v^2}{a^2}\right)(v_u)^2 - \frac{2uv v_u}{a^2} \qquad (1.3)$$

where u, v, and a are respectively the axial and radial components of velocity, and the local velocity of sound. The integral curves of (1.3), named meridian curves by Busemann, constitute a two-parameter family. Each curve joins a chord of the oblique shock polar to the locus (Busemann apple curve) of the end point of the final velocity vector on the cone surface. At the apple curve, the meridian curve is normal to a radius from the origin of the hodograph (12,13,10,14,15).

As the present interest centers on the portion of the apple curve associated with vanishing cone angle ($v \to 0$, $u \to u_1$ = free stream velocity) the following approximations, which are asymptotically exact, are made without altering in any way the character of equation (1.3):

$$1 - \frac{u^2}{a^2} = const. = 1 - M_1^2 \equiv -B^2$$

$$1 - \frac{v^2}{a^2} = 1$$

$$a^2 = const.$$

whereupon (1.3) becomes

$$v v_{uu} - (v_u)^2 = -B^2 - \frac{2uv v_u}{a^2} \quad . \tag{1.4}$$

Now the linearized differential equation describing the present problem, namely

$$-B^2 \frac{\partial u}{\partial x} + \frac{\partial v}{\partial r} + \frac{v}{r} = 0$$

becomes on the hodograph plane

$$v v_{uu} - (v_u)^2 = -B^2 \tag{1.5}$$

hence the difference between the asymptotically exact and the linearized equations describing the supersonic cone flow problem lies in the inclusion or omission of the term, $\frac{-2uv v_u}{a^2}$, on the right of (1.4), which term is presumed to be of second order in small quantities and ignorable in comparison with $-B^2$; this term arises essentially from the cross-product $-2a^{-2}\varphi_x \varphi_y \varphi_{xy}$ in the exact equation. Now at the intersection of a meridian curve and the apple curve the conditions are, without approximation:

$$u = u_3$$

$$v = \varepsilon u_3$$

$$v_u = -\frac{1}{\varepsilon}$$

therefore $-\frac{2uvv_u}{a^2} = \frac{2u_3^2}{a^2} > B^2$, independently of ε.

Here $\arctan \varepsilon = \theta_s$, the cone half vertex angle, and subscript 3 denotes final values. For the typical example of a 5° cone at M = 1.2, it is found that $\frac{2u_3^2}{a^2} \lesssim 2.8$, whereas $-B^2 \lesssim -0.44$, and hence over a portion of the course of the meridian curve, the right hand side assumed in the linearized treatment is not only of incorrect sign, but also of incorrect magnitude, for every ε, however small. It follows that the solutions to the linearized equation for circular cone flows cannot be asymptotically correct, and that the usual three-dimensional linearized theory is inapplicable to a vanishing rotationally symmetrical disturbance.

The solid line on the following sketch shows qualitatively the behavior of the quantity $-B^2 - \frac{2uvv_u}{a^2}$ as obtained from the tabulations of the exact solution for a typical cone angle and Mach number.

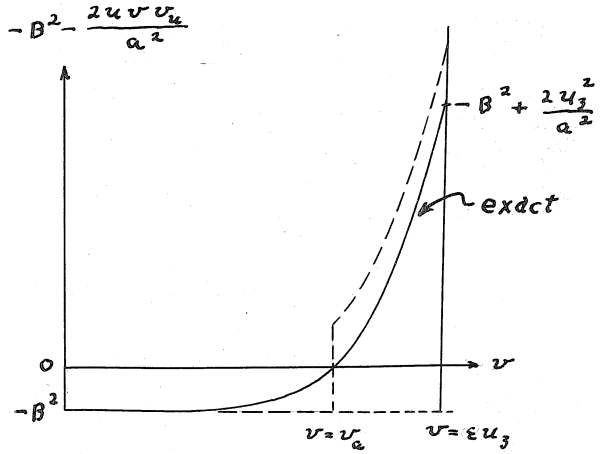

It is of course desirable to obtain an explicit integral of (1.4) but this is probably impossible in terms of elementary functions, for the equation can be shown to define an Abelian function of multiple periodicity (16, p. 26ff.). It is interesting, however, to construct an approximate integral of (1.4), without iteration, which in some measure

takes account of the actual behavior of the right hand side.

The differential equations

$$v v_{uu} - (v_u)^2 = -B^2 \tag{1.5}$$

$$v v_{uu} - (v_u)^2 = -\frac{2uv v_u}{a^2} \tag{1.6}$$

are explicitly integrable and each well approximates the exact equation (1.4) over a portion of the integral curve. It is proposed to patch the solutions of (1.5) and (1.6) in both v and v_u at the point (u_a, v_a), which is very near the point at which the quantity $-B^2 - \frac{2uv v_u}{a^2}$ of the exact solution vanishes. This procedure amounts to replacing the right hand side of the exact equation by the function depicted qualitatively by the dashed line on the preceding sketch. The solution thus obtained is not a true asymptotic integral of (1.4), but is certainly a closer approximation to the truth than the integral of (1.5).

Introduce new variables

$$x = \frac{u}{a} \quad , \quad y = \frac{v}{a}$$

in (1.4), (1.5), and (1.6). These equations become

$$yy'' - (y')^2 = -B^2 - 2xyy' \tag{1.4}$$

$$yy'' - (y')^2 = -B^2 \qquad (x_1 \leq x \leq x_a) \tag{1.5}$$

$$yy'' - (y')^2 = -2xyy' \qquad (x_a < x \leq x_3). \tag{1.6}$$

The end conditions are:

at $\quad x = x_1 \quad , \quad y_5 = 0 \quad , \quad y_5' = -B$ (1.7a)

$$\text{at} \quad x = x_a \;, \qquad y_5 = y_6 \;, \qquad y_5' = y_6' \tag{1.7b}$$

$$\text{at} \quad x = x_3 \;, \qquad y_6 = \varepsilon x_3 \;, \qquad y_6' = -\frac{1}{\varepsilon} \tag{1.7c}$$

where the subscripts 1 and 3 denote free stream and final surface conditions, respectively; and subscripts 5 and 6 denote the differential equation defining the function.

Equations (1.5) and (1.6) may be integrated by known methods, the results being respectively

$$y_5 = \alpha B \sinh \frac{x_1 - x}{\alpha} \tag{1.8}$$

and

$$y_6 = \delta e^{\lambda \operatorname{erf} x} \tag{1.9}$$

where α, δ, and λ are constants to be determined from conditions (1.7) and where the definition

$$\operatorname{erf} x = \frac{2}{\sqrt{\pi}} \int_0^x e^{-\xi^2} d\xi$$

has been employed. Conditions (1.7c) imposed on (1.9) require

$$\lambda = -\frac{\sqrt{\pi}}{2} \frac{e^{x_3^2}}{\varepsilon^2 x_3} \tag{1.10}$$

and

$$\delta = \varepsilon x_3 e^{\frac{\sqrt{\pi}}{2} \frac{e^{x_3^2}}{\varepsilon^2 x_3} \operatorname{erf} x_3} \;. \tag{1.11}$$

Point (x_a, y_a) is defined by the equation

$$-B^2 - 2 x_1 y_5 y_5' = 0$$

that is

$$\sinh 2\left(\frac{x_1 - x_a}{\alpha}\right) = \frac{1}{\alpha x_1}$$

from which it is found that

$$x_a = x_1 - \frac{\alpha}{2} \sinh^{-1} \frac{1}{\alpha x_1}$$

$$x_a \doteq x_1 - \frac{\alpha}{2} \log \frac{2}{\alpha x_1} \tag{1.12}$$

for α is very much less than unity (see equation (1.19)). Insertion of (1.12) in (1.8) then shows

$$y_a \doteq B\sqrt{\frac{\alpha}{2x_1}} \tag{1.13}$$

with completely negligible error.

Conditions (1.7b) may now be imposed and there appears

$$B\sqrt{\frac{\alpha}{2x_1}} = \delta e^{\lambda \operatorname{erf} x_a} \tag{1.14}$$

$$-\frac{B}{2}\sqrt{\frac{2}{\alpha x_1}} = \frac{2}{\sqrt{\pi}} \delta\lambda e^{-x_a^2} e^{\lambda \operatorname{erf} x_a} . \tag{1.15}$$

Using (1.12) to write x_a in terms of α and x_1 in (1.14) and (1.15), equations (1.1), (1.11), (1.14), and (1.15) could, in principle, be solved simultaneously to find α, δ, λ, and x_3 in terms of ϵ and x_1, thus permitting the new approximate expression for the meridian curve to be written explicitly. But interest is focused on only the locus of the end point, (x_3, y_3), of the meridian curve as a function of ϵ and x_1. This locus is calculated as follows: dividing (1.15) by (1.14) there results

$$\lambda = -\frac{\sqrt{\pi}}{2} \frac{e^{x_a^2}}{\alpha}$$

and upon comparing this expression with (1.10),

$$\alpha = \varepsilon^2 x_3 e^{x_a^2 - x_3^2} \tag{1.16}$$

without approximation. Finally equation (1.14) may be written

$$\delta = B\sqrt{\frac{\alpha}{2x_1}}\, e^{-\lambda \operatorname{erf} x_a}$$

and upon comparison with (1.11) it appears that

$$B^2 \frac{\alpha}{2x_1} \exp\left[\sqrt{\pi}\, \frac{e^{x_3^2}}{\varepsilon^2 x_3} \operatorname{erf} x_a\right] = \varepsilon^2 x_3^2 \exp\left[\sqrt{\pi}\, \frac{e^{x_3^2}}{\varepsilon^2 x_3} \operatorname{erf} x_3\right].$$

Using (1.16) to eliminate α from the left of this equation, and taking the logarithm on both sides, it is found

$$\frac{\sqrt{\pi}}{2} \frac{e^{x_3^2}}{\varepsilon^2 x_3} (\operatorname{erf} x_a - \operatorname{erf} x_3) + (x_a^2 - x_3^2) = \log \sqrt{\frac{2x_1 x_3}{B^2}}$$

which may be written

$$e^{x_3^2} \int_{x_3}^{x_a} e^{-\xi^2} d\xi = \varepsilon^2 x_3 \left[\log \sqrt{\frac{2x_1 x_3}{B^2}} - (x_a^2 - x_3^2)\right]. \tag{1.17}$$

It is apparent in the subsequent development that the quantity $(x_a^2 - x_3^2)$ is at most about $\frac{1}{12}\varepsilon^2 x_3 \log \frac{2}{B\varepsilon}$ and is therefore negligible in comparison with $\log \sqrt{\frac{2x_1 x_3}{B^2}}$; equation (1.17) becomes

$$e^{x_3^2} \int_{x_3}^{x_a} e^{-\xi^2} d\xi = \varepsilon^2 x_3 \log \frac{\sqrt{2x_1 x_3}}{B}. \tag{1.18}$$

Similarly, referring to (1.16)

$$\alpha = \varepsilon^2 x_3 \{1 - (x_a^2 - x_3^2) + \cdots\}$$

$$\alpha \doteq \varepsilon^2 x_3 . \tag{1.19}$$

Equation (1.18), using (1.19) and (1.12), relates x_1, x_3, and ε implicitly. Several points (x_1, x_3, ε) from the exact solution have been tested in (1.18) and found to be compatible with remarkable accuracy. Tables of error function were consulted in evaluating the integral. Unfortunately, the implicit relationship is not computable, and some sacrifice is required to make it so.

The familiar linear theory result can be obtained from (1.8) (15), and as well from (1.18) on the basis of an invalid assumption. Saying that inasmuch as x_a and x_3 are very nearly equal, the integrand in (1.18) is approximated by the constant $e^{-x_3^2}$, whence, using (1.19) and (1.12)

$$x_1 - x_3 \doteq \varepsilon^2 x_3 \log \frac{\sqrt{2x_1x_3}}{B} + \varepsilon^2 x_3 \log \sqrt{\frac{2}{\varepsilon^2 x_1 x_3}}$$

$$= \varepsilon^2 x_3 \log \frac{2}{B\varepsilon} \tag{1.20}$$

which is recognised as a simplification of the linearized result based on the exact boundary condition

$$y_3 = \varepsilon x_3 .$$

More accurately

$$e^{x_3^2} \int_{x_3}^{x_a} e^{-\xi^2} d\xi \equiv \int_{x_3}^{x_a} e^{x_3^2 - \xi^2} d\xi \doteq \int_{x_3}^{x_a} \left[1 + (x_3^2 - \xi^2) + \frac{(x_3^2 - \xi^2)^2}{2} \right] d\xi$$

the expression on the right has the value

$$(x_a - x_3) + \frac{x_a}{10}(x_a^2 - x_3^2) - \frac{1}{3}(x_a - x_3)^2 (x_a + 2x_3)\left(1 + \frac{2x_3^2}{5}\right) \tag{1.21a}$$

which, for $B\varepsilon < 0.20$ may be represented by

$$(x_a - x_3)\left(1 + \frac{x_1^2}{5}\right) \doteq e^{x_3^2}\int_{x_3}^{x_a} e^{-\xi^2}\, d\xi \,. \qquad (1.21b)$$

A more accurate representation of (1.21a) is required if $B\varepsilon > 0.20$. Now according to (1.12) and (1.19),

$$x_a = x_1 - \varepsilon^2 x_3 \log\sqrt{\frac{2}{\varepsilon^2 x_1 x_3}}$$

therefore, with reference to (1.21b) and (1.18)

$$(x_1 - x_3 - \varepsilon^2 x_3 \log\sqrt{\frac{2}{\varepsilon^2 x_1 x_3}} = \frac{1}{1 + \frac{x_1^2}{5}}\, \varepsilon^2 x_3 \log\sqrt{\frac{2 x_1 x_3}{B^2}}$$

or

$$(x_1 - x_3) = \varepsilon^2 x_3 \log\left\{\frac{\sqrt{2}}{\varepsilon\sqrt{x_1 x_3}}\left(\frac{\sqrt{2 x_1 x_3}}{B}\right)^{\frac{1}{1 + \frac{x_1^2}{5}}}\right\} . \qquad (1.22)$$

Comparing (1.20) and (1.22), the error committed in taking the integrand in (1.18) to be constant is apparent.

The quantities x_3 in the right of (1.22) appear because the exact boundary condition, $y_3 = \varepsilon x_3$, has been imposed. Use of the approximate boundary condition, $y_3 = \varepsilon x_1$, which is asymptotically exact, replaces x_3 by x_1 and introduces an error obviously self compensating to some degree. The error is certainly of minor consequence, though difficult to assess analytically with precision.

The ultimate approximate result, which is computable, to be compared over its range of validity with the exact and linear solutions for slender cones at low supersonic speeds is

$$x_1 - x_3 = \varepsilon^2 x_1 \log\left\{\frac{\sqrt{2}}{\varepsilon x_1}\left(\frac{\sqrt{2}\, x_1}{B}\right)^{\frac{1}{1 + \frac{x_1^2}{5}}}\right\} \qquad (1.23a)$$

which may be written

$$\frac{x_1 - x_3}{x_1} = \varepsilon^2 \log \frac{2}{B\varepsilon} - \frac{\varepsilon^2 x_1^2}{5 + x_1^2} \log \frac{\sqrt{2}\, x_1}{B} \quad . \tag{1.23b}$$

Formula (1.23) is compared graphically on Fig. 2 with the linearized and exact solutions. The formula for the exact calculation of the quantity $1 - \left(\frac{\beta_s}{2}\right)^2$ from the longitudinal perturbation is

$$1 - \left(\frac{\beta_s}{2}\right)^2 = 1 - (1 + \varepsilon^2)\left(1 - \frac{x_1 - x_3}{x_1}\right)^2 \quad .$$

It must be emphasized that the approximations made in deriving (1.23) from (1.18) are valid only at low supersonic speeds.

The foregoing analysis in conjunction with a thorough numerical investigation of the linearized, exact, and present solutions of the problem of the slender circular cone in supersonic flow suggests that the familiar linearized theory is quantitatively unreliable for the treatment of very slender, as well as thick, solid bodies. The domain of applicability is shown on Fig. 1. For very slender bodies, the simple Jones slender body theory (6), (7) is reasonably accurate for lift and moment calculation, and is considerably easier to apply than the general methods to be presented in this study; some comments on the Jones method are to be made subsequently. For thick bodies, resort must be taken to numerical integration of the exact equations. Except as explicitly noted, the remainder of this study is concerned with the class of solid bodies to which the linearized theory is applicable.

II. CALCULATION OF LOCAL PRESSURE

The various methods of deducing the local pressure from the velocity predictions of the linearized theory are now to be appraised. There are several formulae in use for this calculation; all are approximations, of varying accuracy, to the exact isentropic pressure relationship (8, Chapter 8)

$$C_p \equiv \frac{p-p_\infty}{\rho_\infty \frac{U^2}{2}} = \frac{2}{\gamma M_\infty^2}\left[\left\{\frac{1+\frac{\gamma-1}{2}M_\infty^2}{1+\frac{\gamma-1}{2}M^2}\right\}^{\frac{\gamma}{\gamma-1}} - 1\right] \tag{2.1}$$

$$= \frac{2}{\gamma M_\infty^2}\left[\left\{1+\frac{\gamma-1}{2}M_\infty^2\left(1-\frac{q^2}{U^2}\right)\right\}^{\frac{\gamma}{\gamma-1}} - 1\right] .$$

Here subscript ∞ denotes free stream conditions and q the local total velocity. The components of perturbation in the x(free stream), y, z (or x, r, θ) directions may be designated u, v, w, then

$$1-\frac{q^2}{U^2} = -\frac{2u}{U} - \frac{(u^2+v^2+w^2)}{U^2} .$$

Consider the expansion of the quantity in braces in (2.1) according to the binomial theorem. If terms linear in the perturbations are considered, the familiar Ackeret-Prandtl pressure formula results (8)

$$C_p = -\frac{2u}{U} . \tag{2.2}$$

Next taking into account all quantities in the first two terms of the expansion, the quadratic formula of Busemann appears (12)

$$C_p = -2\left(\frac{u}{U} + \frac{u^2+v^2+w^2}{2U^2}\right) \equiv 1-\frac{q^2}{U^2} , \tag{2.3}$$

and if the u^2 is arbitrarily dropped from the right of (2.3), the Hayes quadratic formula is obtained (1)

$$C_p = -2\left(\frac{u}{U} + \frac{v^2+w^2}{2U^2}\right). \tag{2.4}$$

Finally, including the term quadratic in the perturbations from the third term of the binomial expansion, a formula of Van Dyke is found (11)

$$C_p = -2\left(\frac{u}{U} + \frac{v^2+w^2-B^2u^2}{2U^2}\right). \tag{2.5a}$$

This formula may be written

$$C_p = 1 - \frac{\theta^2}{U^2} + M^2\frac{u^2}{U^2}. \tag{2.5b}$$

Formula (2.5) is a simplification of a quartic formula recommended by Kármán and Moore (2).

A comparison of the pressure predictions of these formulae for a 10° cone is presented on Fig. 3, along with the exact pressure prediction taken from Kopal's tables (10). Similar calculations for cones of 5°, $7^\circ.5$, $12^\circ.5$, and 15° indicate little variation of the qualitative behavior or accuracy of the several pressure formulae. The linear theory predictions of the perturbation velocities have, of course, been used in the formulae, and inasmuch as these velocities are not correct, it is not surprising that the exact isentropic pressure formula does not yield the best pressure prediction.

It is concluded from the numerical investigation that formula (2.5) should be used for pressure estimation in the linearized study of solid bodies. The inaccuracy of this formula tends to compensate well the inaccuracy of the velocity prediction. The use of this nonlinear formula

usually precludes an analytical integration of the pressure over the surface of a body, but this is no loss for it will be found that the velocity functions arising in all but the simplest problems are of such form as to rule out analytical pressure integration using even the linear pressure formula. Recommended procedures are described in the appropriate sections of this study.

It may be remarked that for small cone angles at moderate supersonic speeds, the error in the pressure prediction of the linear formula (2.2) increases as the cone angle decreases. This observation casts some doubt on the acceptability of portions of several investigations concerning rotationally symmetrical solid bodies, where this formula in conjunction with a passage to the limit of zero body thickness was used to simplify the analysis and derive closed expressions for lift, drag, and moment (17, 18, 3, 4, 19). In particular, the findings on optimum projectile shape are in question. In two recent papers M. J. Lighthill has used the more satisfactory quadratic formula (2.3) (5, 20).

III. MOTIVATION

In general, the methods of supersonic wing theory are inapplicable to the solid body problem; the reasons for this conclusion are to be brought forward. An exception is the Jones slender body method (6), to be discussed later.

Much use in wing theory is made of Green's formula for the wave equation (21, p. 430 ff):

$$\iiint_D (\varphi \Box \psi - \psi \Box \varphi)\, dV = \iint_S (\varphi \frac{\partial \psi}{\partial \nu} - \psi \frac{\partial \varphi}{\partial \nu} \tag{3.1}$$

where $\Box = \beta^2 \frac{\partial^2}{\partial x^2} - \frac{\partial^2}{\partial y^2} - \frac{\partial^2}{\partial z^2}$ and $\frac{\partial}{\partial \nu}$ is the symbol of conormal differentiation (1, 21, p. 434). Equation (3.1) relates the volume and surface integrals of two functions, φ and ψ, and their first and second partial derivatives, over the content and surface of the domain bounded by the retrograde Mach cone from the point of interest, P, a plane normal to the free stream upstream from all disturbances, and the surface of the body included by the retrograde Mach cone.

Without going into detail or mentioning the variations of the method applicable near wing tips, the philosophy of this approach and its limitations may be described briefly as follows. The function ψ can be so selected that the value of the volume integral on the left in (3.1) may be continued to the solution, $\varphi(P)$, of the wave equation (22), and such that the surface integral on the right extends only over the surface of the solid body included by the Mach cone from P. The difficulties arise in the right of (3.1); in wing theory use is made of the symmetry or antisymmetry of the problem in question to eliminate

the quantity $\varphi \frac{\partial \psi}{\partial \nu}$ by consideration of the solution, φ, at points symmetrically placed with respect to the plane of the wing. On the plane of the wing, the co-normal derivative becomes simply the normal derivative, hence the function φ is related to the integral over a portion of the plane of the wing of a function proportional to the normal derivative of φ, which is prescribed by the boundary condition.

In the consideration of solid bodies the simple relationship between the normal and conormal derivatives of φ at the body surface does not exist, and it is further impossible, in general, to construct the function ψ such that one of the terms in the right of (3.1) vanishes at the body surface. Thus (3.1) is at best transformable into an integral equation of the Volterra type and even though in principle a Volterra equation can always be solved in a step by step manner, in all but the simplest problem no further analytical progress can be made. The exception is the problem of the unyawed slender circular cone; but in this case the methods of conical flow are more efficient (13, 1, 23).

The powerful theory of conical supersonic flows (23, 1) capitalizes Busemann's observation (13) that the wave equation is transformable into the Laplace equation in planes normal to the free stream, provided the disturbance is conical. Thus the vast structure of potential theory may be brought to bear. But if the trace of the body in this normal plane is other than a circle concentric with the trace of the Mach cone, or a straight line very near a diameter of the Mach cone, the transformation warps the body trace and complicates the boundary condition equation. Nevertheless the formal solution of any conical problem fulfilling

the linearizing assumptions exists and may be written on the basis of the theorems of potential theory. However the explicit construction of the solution for a noncircular conical solid body is impractical, for one has to deal with a domain having literally irregular boundaries and boundary conditions. The calculations for an elliptic cone have been carried out by Laporte and Bartels(24).

To build a method capable of treating in a straightforward manner the aerodynamics of solid bodies, resort is taken to the superposition of solutions of the wave equation singular along one or more lines within the body. This method was inaugurated in one form by Th. von Kármán and N. B. Moore (2), who used the axis of the Mach cone as the line of singularities. The development of the method by various investigators has been sketched in the Introduction. The Kármán-Moore method is suitable for the consideration of conical or nonconical circular solid bodies, either yawed (3) or unyawed, provided the discussion of Section II (ante) hereof is kept in mind. S. H. Maslen has recently published an interesting approximate method for the study of noncircular cones (25). The cone is built up of several inclined source lines of common origin, each producing a conical velocity field.

It is now to be shown that the generalization of the Kármán method is in general unsuitable for noncircular solid bodies.

To construct, by superposition, the perturbation velocity potential, φ, which satisfies the wave equation

$$B^2 \frac{\partial^2 \varphi}{\partial x^2} - \frac{\partial^2 \varphi}{\partial r^2} - \frac{1}{r} \frac{\partial \varphi}{\partial r} - \frac{1}{r^2} \frac{\partial^2 \varphi}{\partial \theta^2} = 0 \qquad (3.2)$$

and which fulfills the boundary condition

$$(U + \text{grad}\,\varphi)\cdot \text{grad}\, S = 0 \tag{1.2}$$

on the surface, $S(x, r, \theta) = 0$, of a solid body, the separation of the azimuthal variable may be considered:

$$\varphi = \sum_s G_s(x, r)\,(C_s \cos s\theta + D_s \sin s\theta)\,. \tag{3.3}$$

Kármán's method arises from the assumption that

$$G_s(x, r) = F_s(x, r)\, r^s$$

which leads to the differential equation defining the $F_s(x, r)$ functions:

$$\frac{\partial^2 F_s}{\partial x^2} = \frac{1}{B^2}\left(\frac{\partial^2 F}{\partial r^2} + \frac{2s+1}{r}\frac{\partial F_s}{\partial r}\right). \tag{3.4}$$

It is easily seen that

$$F_{s+1} = \frac{1}{r}\frac{\partial}{\partial r} F_s$$

hence it follows that

$$F_s(x, r) = \left(\frac{1}{r}\frac{\partial}{\partial r}\right)^s F_o(x, r)\,. \tag{3.5}$$

By (3.4), $F_o(x, r)$ is defined by the equation

$$\frac{\partial^2 F_o}{\partial x^2} = \frac{1}{B^2}\left(\frac{\partial^2 F_o}{\partial r^2} + \frac{1}{r}\frac{\partial F_o}{\partial r}\right) \tag{3.6}$$

and this equation is, of course, the familiar wave equation for rotationally symmetrical waves. The solution of (3.6) as used by Karman and Moore, and others, is

$$\varphi_0 = F_0 = \frac{1}{2\pi}\int_{\cosh^{-1}\frac{x}{Br}}^{0} f(x - Br\cosh z)\,dz$$

$$\varphi_0 = \frac{1}{2\pi}\int_0^{x-Br} \frac{f(\xi)\,d\xi}{\sqrt{(x-\xi)^2 - B^2r^2}} \qquad (3.7)$$

which expression is interpreted as the result of superposition, along the axis of the Mach cone, of "supersonic sources" of yield $f(\xi)$ per unit length. As shown in references (2) and (25), the distribution is simply related to the body cross-section area by the approximate formula

$$f = \frac{V}{2\pi}\frac{dS}{dx} . \qquad (3.8)$$

For $s=1$ it follows from (3.5) that

$$\varphi_1 = -(C_1\cos\theta + D_1\sin\theta)\frac{1}{2\pi}\int_{\cosh^{-1}\frac{x}{Br}}^{0} f_1(x - Br\cosh z)\cosh z\,dz$$

which is the correction function, originally used by Tsien (3), to account for the cross flow over a yawed circular solid body. A relation similar to (3.8) determines the distribution f_1.

In order to study noncircular solid bodies, the functions $F_s(x,r)$ explicitly expressed in terms of the definite integrals, are required. These expressions rapidly increase in complexity as s increases, and for $s \geq 2$, the relationship between the distribution functions f_i and the body shape becomes obscure. It is found that

$$\left(\frac{1}{r}\frac{\partial}{\partial r}\right)^s = \sum_{j=0}^{s-1} \frac{(-1)^j(s+j-1)!}{2^j j!(s-j-1)!}\frac{1}{r^{s+j}}\left(\frac{\partial}{\partial r}\right)^{s-j}$$

hence $F_s(x,r)$ is of the form

$$F_s(x,r) = \frac{(-1)^s}{2\pi r^{2s}} \sum_{j=0}^{s-1} \frac{(s+j-1)!}{2^j j!(s-j-1)!} \int_0^{x-Br} \frac{f_s(\xi)(x-\xi)^{s-j}}{\sqrt{(x-\xi)^2 - B^2 r^2}}\, d\xi$$

$$+ \frac{(-1)^s}{2\pi} \sum_{j=0}^{s-1} \frac{(s+j-1)!}{2^j j!(s-j-1)!} \sum_{k=1}^{s-j} \left(\frac{-1}{x}\right)^k f_s^{(s-j-k)}(0) \sum_{l=0}^{k-1} \binom{k-1}{l} \frac{x\, r^l (s-j-l-1)!}{(s-j-k)!} \cdot$$

$$\cdot (-1)^{k-l} \frac{\partial^l}{\partial r^l} \frac{1}{\sqrt{x^2 - B^2 r^2}} \quad ,$$

with

$$\left(\frac{\partial}{\partial r}\right)^{2m} \frac{1}{\sqrt{x^2 - B^2 r^2}} = \frac{1}{B\left(\frac{x^2}{B^2} - r^2\right)^{m+\frac{1}{2}}} \sum_{\lambda=0}^{m} C_\lambda(m) \frac{\left(\frac{x^2}{B^2}\right)^{2\lambda}}{\left(\frac{x^2}{B^2} - r^2\right)^\lambda}$$

$$\left(\frac{\partial}{\partial r}\right)^{2m+1} = \frac{\partial}{\partial r}\left(\frac{\partial}{\partial r}\right)^{2m}$$

and

$$C_\lambda(m) = (-1)^{m+\lambda} \frac{(2m+2\lambda)!\,(m!)^2}{2^{2\lambda}(\lambda!)^2 (m-\lambda)!(m+\lambda)!} \quad .$$

Quite evidently the construction of solutions of the wave equation by definite integrals becomes impractical for frequencies, S , greater than 3 or 4. It may be pointed out that the functions f_s must be of degree s in ξ in order for the resulting potential function to describe a conical flow.

A separation of variables in the wave equation which avoids the previous difficulties can be found. It is obvious that both the total and perturbation velocity potentials of a conical flow are proportional to length along any straight line inside the Mach cone passing through the cone apex, for then the gradient of the potential is constant along

rays inside the Mach cone. It is natural to select the length as distance along the Mach cone axis and separate the variables in the wave equation in some set of conical coordinates. Let

$$x = x \quad , \quad t = \frac{\beta r}{x} \quad , \quad \theta = \theta \; ; \quad r = \sqrt{y^2 + z^2} \tag{3.9}$$

and, for conical flows, assume

$$\phi = U \sum_m x \mathcal{H}_m(t) \left(A_m \cos m\theta + B_m \sin m\theta \right) . \tag{3.10}$$

For nonconical flows, the generalization of (3.10) is of course

$$\phi = U \sum_j \sum_m x^j \mathcal{H}_m^{(j)}(t) \left(A_m^{(j)} \cos m\theta + B_m^{(j)} \sin m\theta \right) . \tag{3.12}$$

The variables (3.9) and assumption (3.10) are due to Hayes (1). A study of the H(t) functions is now undertaken.

IV. THE H(t) FUNCTIONS

The wave equation (1.1)

$$\left(-B^2\frac{\partial^2}{\partial x^2}+\frac{\partial^2}{\partial y^2}+\frac{\partial^2}{\partial z^2}\right)\varphi=0 \tag{4.1}$$

written in the nonorthogonal conical coordinates (3.9)

$$\begin{aligned} x &= x \\ t &= \frac{\sqrt{x^2+z^2}\,\sqrt{y^2+z^2}}{x} \equiv \frac{Br}{x} \\ \theta &= \theta \end{aligned} \tag{4.2}$$

becomes

$$\left(-x^2\frac{\partial^2}{\partial x^2}+2xt\frac{\partial^2}{\partial x\,\partial t}+(1-t^2)\frac{\partial^2}{\partial t^2}+\frac{1}{t}(1-2t^2)\frac{\partial}{\partial t}+\frac{1}{t^2}\frac{\partial^2}{\partial\theta^2}\right)\varphi=0\ . \tag{4.3}$$

If solutions of (4.3) are postulated in the form

$$\varphi=U\sum_j\sum_m A_m^{(j)}x^j\mathcal{H}_m^{(j)}(t)\begin{Bmatrix}\cos m\theta\\ \sin m\theta\end{Bmatrix} \tag{4.4}$$

the azimuthal and conical variables are separated and the differential equation defining the $\mathcal{H}_m^{(j)}(t)$ is found to be

$$t^2(1-t^2)\mathcal{H}_m^{(j)\prime\prime}(t)+t\left[1+2(j-1)t^2\right]\mathcal{H}_m^{(j)\prime}(t)-\left[j(j-1)t^2+m^2\right]\mathcal{H}_m^{(j)}(t)=0\ . \tag{4.5}$$

Equation (4.5) is essentially due to Hayes (1) who wrote its solution in terms of hypergeometric functions and mentioned that the solutions are proportional to associated Legendre functions.

Equation (4.5) is here solved synthetically by analogy with spherical harmonic functions. The wave equation and the Laplace equation can be said to be the same differential equation in spaces of different metric. The metric associated with the Laplace equation, $\varphi_{x_1x_1}+\varphi_{y_1y_1}+\varphi_{z_1z_1}=0$

is the Euclidean distance:

$$R_e = \sqrt{x_1^2 + y_1^2 + z_1^2}$$

and the metric associated with the wave equation

$$\frac{\partial^2 \varphi}{\partial \left(\frac{x}{\beta}\right)^2} - \frac{\partial^2 \varphi}{\partial y^2} - \frac{\partial^2 \varphi}{\partial z^2} = 0$$

is the hyperbolic distance of (x,y,z) from the origin

$$R_h = \sqrt{\left(\frac{x}{\beta}\right)^2 - y^2 - z^2} = \frac{x}{\beta}\sqrt{1 - r^2} \quad . \tag{4.6}$$

The solution of the Laplace equation in spherical coordinates is

$$\varphi = \sum A_m^{(n)} \begin{Bmatrix} R_e^n \\ R_e^{-(n+1)} \end{Bmatrix} \begin{Bmatrix} P_n^m(\cos\phi) \\ Q_n^m(\cos\phi) \end{Bmatrix} \begin{Bmatrix} \sin m\theta \\ \cos m\theta \end{Bmatrix} \quad . \tag{4.7}$$

These coordinates are as sketched:

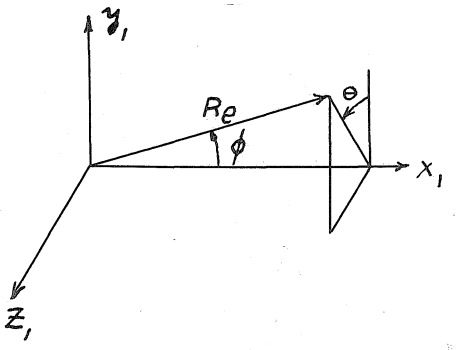

It appears from the sketch that

$$\cos\phi = \frac{x_1}{R_e} \quad .$$

If in (4.7) the Euclidean metric is replaced by the hyperbolic metric (4.6), the functions obtained are the harmonic solutions of the wave equation, as can be verified by substitution in (4.3). One obtains:

$$\varphi = \sum A_m^{(m)} \begin{Bmatrix} x^m (1-t^2)^{\frac{m}{2}} \\ x^{-m-1} (1-t^2)^{-\frac{(m+1)}{2}} \end{Bmatrix} \begin{Bmatrix} P_m^m\left(\frac{1}{\sqrt{1-t^2}}\right) \\ Q_m^m\left(\frac{1}{\sqrt{1-t^2}}\right) \end{Bmatrix} \begin{Bmatrix} \sin m\theta \\ \cos m\theta \end{Bmatrix} \qquad (4.8)$$

having absorbed into $A_m^{(m)}$ the multiplicative constants B^{-m}, B^{m+1} occurring with x^m and $x^{-(m+1)}$. In reference (26), H. J. Stewart presented the solutions of the wave equation in a form similar to that of (4.8). The functions P_m^m and Q_m^m above are associated Legendre functions of the first and second kind, respectively. Note that the argument of these functions is now greater than or equal to unity, owing to the introduction of the hyperbolic metric; Hobson's definition of the functions is therefore to be employed (27, section 15.6). The associated Legendre functions according to Hobson's definition obey recurrence relations, differentiation formulae, and so on, of the same form as the formulas for the Legendre functions of argument less than unity, but some signs are changed. Care is required.

The implicit boundary condition that all disturbances vanish on the apex Mach cone (where t = 1) requires that (4.8) be used in the form

$$\varphi = \sum A_m^{(j)} x^j (1-t^2)^{j/2} Q_j^m\left(\frac{1}{\sqrt{1-t^2}}\right) \begin{Bmatrix} \sin m\theta \\ \cos m\theta \end{Bmatrix}$$

and upon comparison of this equation with (4.4) it is found that

$$\mathcal{P}_m^{(j)}(t) = (1-t^2)^{j/2} Q_j^m\left(\frac{1}{\sqrt{1-t^2}}\right) \qquad (4.9)$$

which is thus the solution of interest of (4.5).

The functions $Q_j^m(u)$ are defined by the relation

$$Q_j^m(u) = (u^2-1)^{\frac{m}{2}} \left(\frac{d}{du}\right)^m Q_j(u) \tag{4.10}$$

(27, ante). The first four $Q_j(u)$ functions are (28):

$$Q_1(u) = \tfrac{1}{2} u \log \frac{u+1}{u-1} - 1 \tag{4.11a}$$

$$Q_2(u) = \tfrac{1}{4}(3u^2-1) \log \frac{u+1}{u-1} - \frac{3u}{2} \tag{4.11b}$$

$$Q_3(u) = \tfrac{1}{4}(5u^3-3u) \log \frac{u+1}{u-1} - \frac{5u^2}{2} + \frac{2}{3} \tag{4.11c}$$

$$Q_4(u) = \tfrac{1}{16}(35u^4-30u^2+3) \log \frac{u+1}{u-1} - \frac{35u^3}{8} + \frac{55u}{24} \,. \tag{4.11d}$$

The explicit calculation of the needed ~~$P_m^{(j)}(t)$~~ functions entails the prior derivation of the corresponding Legendre functions. Using (4.10), the functions $Q_j', Q_j^2, \cdots Q_j^{j+1}$ are obtained from (4.11). It happens that for $m \geq j+1$ a general explicit form of Q_j^m exists, and this formula is readily derived for $j = 1$. Then with reference to the recurrence relation

$$Q_{j+1}^m(u) = u\, Q_j^m(u) + (j+m)\sqrt{u^2-1}\, Q_j^{m-1}(u) \tag{4.12}$$

the general explicit formula for $Q_j^m(u)$ $(m \geq j+1)$ is obtained. The results are tabulated in Appendix A. The explicit general form of $Q_1^m(u)$ $(m \geq 2)$ is obtained as follows: According to (4.11a) and (4.10)

$$Q_1(u) = \tfrac{1}{2} u \log \frac{u+1}{u-1} - 1$$

$$Q_1'(u) = \frac{\sqrt{u^2-1}}{2}\left[\log(u+1) - \log(u-1) + u\left(\frac{1}{u+1} - \frac{1}{u-1}\right)\right]$$

$$Q_1^2(u) = \frac{u^2-1}{2}\left[\frac{2}{u+1} - \frac{2}{u-1} - u\left(\frac{1}{(u+1)^2} - \frac{1}{(u-1)^2}\right)\right]$$

$$Q_1^3(u) = \frac{(u^2-1)^{3/2}}{2}\left[\frac{-3}{(u+1)^2} + \frac{3}{(u-1)^2} + 2u\left(\frac{1}{(u+1)^3} - \frac{1}{(u-1)^3}\right)\right]$$

$$Q_1^4(u) = \frac{(u^2-1)^2}{2}\left[\frac{8}{(u+1)^3} - \frac{8}{(u-1)^3} - 6u\left(\frac{1}{(u+1)^4} - \frac{1}{(u-1)^4}\right)\right]$$

$$Q_1^5(u) = \frac{(u^2-1)^{5/2}}{2}\left[\frac{-30}{(u+1)^4} + \frac{30}{(u-1)^4} + 24u\left(\frac{1}{(u+1)^5} - \frac{1}{(u-1)^5}\right)\right] .$$

One may verify by induction that the foregoing functions generate the formula

$$Q_1^m(u) = \frac{(u^2-1)^{\frac{m}{2}}}{2}(m-2)!(-1)^m\left[\frac{m}{(u+1)^{m-1}} - \frac{m}{(u-1)^{m-1}} - (m+1)\left(\frac{u}{(u+1)^m} - \frac{u}{(u-1)^m}\right)\right]$$

or, simplifying

$$Q_1^m(u) = (-1)^m\frac{(m-2)!}{2}\left[(m+u)\left(\frac{u-1}{u+1}\right)^{\frac{m}{2}} + (m-u)\left(\frac{u+1}{u-1}\right)^{\frac{m}{2}}\right] . \qquad (4.13)$$

All the associated Legendre functions $Q_j^m(u)$ for $m \geq j+1$ are obtained from (4.13) and (4.12).

The $\mathcal{P}_m^{(j)}(t)$ functions arise from (4.9) and the functions tabulated in Appendix A by means of the substitution

$$u = \frac{1}{\sqrt{1-t^2}} .$$

In the simplification of the results, the identities

$$\log\frac{u+1}{u-1} \equiv \log\frac{1+\sqrt{1-t^2}}{1-\sqrt{1-t^2}} = 2\cosh^{-1}\frac{1}{t}$$

and

$$\frac{1-\sqrt{1-t^2}}{t} = \frac{t}{1+\sqrt{1-t^2}} = \sqrt{\frac{1-\sqrt{1-t^2}}{1+\sqrt{1-t^2}}}$$

and the definition

$$T = \frac{1-\sqrt{1-t^2}}{t}$$

have been used. T is the Tschaplygin transform of t and is of great importance in the theory of conical flows. In the coordinates (T, θ) the wave equation becomes the (elliptic) Laplace equation in planes x = const.

The $\mathcal{N}_m^{(j)}(t)$ functions obtained are:

$j=1$

$$\mathcal{N}_0^{(1)}(t) = \cosh^{-1}\frac{1}{t} - \sqrt{1-t^2} \tag{4.14a}$$

$$\mathcal{N}_1^{(1)}(t) = t\cosh^{-1}\frac{1}{t} - \frac{\sqrt{1-t^2}}{t} \tag{4.14b}$$

for $m \geq 2$

$$\mathcal{N}_m^{(1)}(t) = (-1)^m \frac{(m-2)!}{2}\left[(m\sqrt{1-t^2}+1)T^m + (m\sqrt{1-t^2}-1)T^{-m}\right] \tag{4.14c}$$

$j=2$

$$\mathcal{N}_0^{(2)}(t) = \frac{3-(1-t^2)}{2}\cosh^{-1}\frac{1}{t} - \frac{3}{2}\sqrt{1-t^2} \tag{4.14d}$$

$$\mathcal{N}_1^{(2)}(t) = 3t\cosh^{-1}\frac{1}{t} - \frac{\sqrt{1-t^2}}{t}\left\{3-2(1-t^2)\right\} \tag{4.14e}$$

$$\mathcal{N}_2^{(2)}(t) = 3t^2\cosh^{-1}\frac{1}{t} - \frac{\sqrt{1-t^2}}{t^2}\left\{3-5(1-t^2)\right\} \tag{4.14f}$$

for $m \geq 3$

$$\mathcal{N}_m^{(2)}(t) = (-1)^m \frac{(m-3)!}{2}\left[\left\{-3(m\sqrt{1-t^2}+1)-(m^2-1)(1-t^2)\right\}T^m + \left\{-3(m\sqrt{1-t^2}-1)+(m^2-1)(1-t^2)\right\}T^{-m}\right] \tag{4.14g}$$

$j=3$

$$\mathcal{N}_0^{(3)}(t) = \frac{1}{2}\left\{5-3(1-t^2)\right\}\cosh^{-1}\frac{1}{t} - \frac{\sqrt{1-t^2}}{6}\left\{15-4(1-t^2)\right\} \tag{4.14h}$$

$$\mathcal{N}_1^{(3)}(t) = \frac{3t}{2}\left\{5-(1-t^2)\right\}\cosh^{-1}\frac{1}{t} - \frac{\sqrt{1-t^2}}{2t}\left\{15-13(1-t^2)\right\} \tag{4.14i}$$

$$\mathcal{N}_2^{(3)}(t) = 15t^2\cosh^{-1}\frac{1}{t} - \frac{\sqrt{1-t^2}}{t^2}\left\{10-15(1-t^2)+3(1-t^2)^2\right\} \tag{4.14j}$$

$$\mathcal{H}_3^{(3)}(t) = 15t^3 \cosh^{-1}\frac{1}{t} - \frac{\sqrt{1-t^2}}{t^3}\left\{15 - 40(1-t^2) + 33(1-t^2)^2\right\} \tag{4.14k}$$

for $m \geq 4$

$$\mathcal{H}_m^{(3)}(t) = (-1)^m \frac{(m-4)!}{2}\Big[\left\{15(m\sqrt{1-t^2}+1) + (6m^2-9)(1-t^2) + m(m^2-4)(1-t^2)^{3/2}\right\}T^m$$

$$+ \left\{15(m\sqrt{1-t^2}-1) - (6m^2-9)(1-t^2) + m(m^2-4)(1-t^2)^{3/2}\right\}T^{-m}\Big] \tag{4.14l}$$

$j = 4$

$$\mathcal{H}_0^{(4)}(t) = \frac{1}{8}\left\{35 - 30(1-t^2) + 3(1-t^2)^2\right\}\cosh^{-1}\frac{1}{t} - \frac{\sqrt{1-t^2}}{24}\left\{105 - 55(1-t^2)\right\} \tag{4.14m}$$

$$\mathcal{H}_1^{(4)}(t) = \frac{5t}{2}\left\{7 - 3(1-t^2)\right\}\cosh^{-1}\frac{1}{t} - \frac{\sqrt{1-t^2}}{24t}\left\{420 - 405(1-t^2) + 64(1-t^2)^2\right\} \tag{4.14n}$$

$$\mathcal{H}_2^{(4)}(t) = \frac{15t^2}{2}\left\{7 - (1-t^2)\right\}\cosh^{-1}\frac{1}{t} - \frac{\sqrt{1-t^2}}{2t^2}\left\{105 - 190(1-t^2) + 81(1-t^2)^2\right\} \tag{4.14o}$$

$$\mathcal{H}_3^{(4)}(t) = 105t^3\cosh^{-1}\frac{1}{t} - \frac{\sqrt{1-t^2}}{4t^3}\left\{420 - 1120(1-t^2) + 924(1-t^2)^2 - 192(1-t^2)^3\right\} \tag{4.14p}$$

$$\mathcal{H}_4^{(4)}(t) = 105t^4\cosh^{-1}\frac{1}{t} - \frac{\sqrt{1-t^2}}{t^4}\left\{105 - 385(1-t^2) + 511(1-t^2)^2 - 279(1-t^2)^3\right\} \tag{4.14q}$$

for $m \geq 5$

$$\mathcal{H}_m^{(4)}(t) = (-1)^m \frac{(m-5)!}{2}\Big[\left\{-105 - (124m+45)\sqrt{1-t^2} - (57m^2+45m-63)(1-t^2)\right.$$

$$\left. - (9m^3+18m^2-37m-27)(1-t^2)^{3/2} - (m^4+3m^3-4m^2-12m)(1-t^2)^2\right\}T^m$$

$$+ \left\{105 + (-124m+45)\sqrt{1-t^2} + (57m^2-45m-63)(1-t^2)\right.$$

$$\left. + (-9m^3+18m^2+37m-27)(1-t^2)^{3/2} + (m^4-3m^3-4m^2+12m)(1-t^2)^2\right\}T^{-m}\Big] .$$

The recurrence relations, differentiation formulae, and so on, for the $\mathcal{H}_m^{(j)}(t)$ carry over from the theory of the Legendre functions, with the modifications imposed by (4.9). The formula of greatest utility is

$$\mathcal{H}_m^{(j+1)}(t) = \mathcal{H}_m^{(j)}(t) + (m+j)\,t\,\mathcal{H}_{m-1}^{(j)}(t) \tag{4.15}$$

which is subsequently to be of use for obtaining the numerical values of the $\mathcal{H}_m^{(j)}(t)$ functions for $j>1$ from the tables of modified $\mathcal{H}_m^{(1)}(t)$ herein presented.

The $\mathcal{H}_m^{(j)}(t)$ functions consist of two linearly independent parts, namely T^m and its coefficient, and T^{-m} and its coefficient. Each of these parts is, separately, a solution of the fundamental equation (4.5).

The conical multipoles $\mathcal{H}_m^{(1)}(t)$ will prove to be of paramount utility in this study and are now to be considered in some detail. The derivative of $\mathcal{H}_m^{(j)}(t)$ is denoted by a prime; it is found that

$$\mathcal{H}_0^{(1)\prime}(t) = -\frac{\sqrt{1-t^2}}{t} \tag{4.16a}$$

$$\mathcal{H}_1^{(1)\prime}(t) = \cosh^{-1}\frac{1}{t} + \frac{\sqrt{1-t^2}}{t^2} \tag{4.16b}$$

$m \geq 2$

$$\mathcal{H}_m^{(1)\prime}(t) = (-1)^m \frac{(m-2)!}{2}\frac{m}{t}\left[(m+\sqrt{1-t^2})T^m - (m-\sqrt{1-t^2})T^{-m}\right]. \tag{4.16c}$$

Now the (x,t,θ) coordinate system is not orthogonal but the (r,ν,θ) system, to which the perturbation velocities are referred, is orthogonal, hence in differentiating partially with respect to, say, x, it is necessary to specify whether t or r is to be held constant. The following notation prevents confusion:

$\left(\frac{\partial}{\partial x}\right)_t$ ⌣ t held constant

$\left(\frac{\partial}{\partial x}\right)_r$ ⌣ r held constant

Thus

$$\left.\begin{aligned}\frac{\partial}{\partial x_r} &= \frac{\partial}{\partial x_t} + \frac{\partial t}{\partial x_r}\frac{\partial}{\partial t_x} = \frac{\partial}{\partial x_t} - \frac{t}{x}\frac{\partial}{\partial t_x} \\ \text{and}\quad \frac{\partial}{\partial r_x} &= \frac{\partial t}{\partial r_x}\frac{\partial}{\partial t_x} = \frac{B}{x}\frac{\partial}{\partial t_x}.\end{aligned}\right\} \tag{4.17}$$

Hence, having a conical perturbation velocity potential written in the form

$$\varphi = U \sum_m x \mathcal{H}_m^{(1)}(t) \left(A_m \cos m\theta + B_m \sin m\theta \right) \tag{4.18a}$$

the x, r, θ perturbations u,v,w are, respectively, φ_{x_r}, φ_{r_x}, $\frac{1}{r}\varphi_\theta$ namely

$$\left.\begin{aligned} u &= U \sum_m \left(\mathcal{H}_m^{(1)}(t) - t\mathcal{H}_m^{(1)\prime}(t) \right)\left(A_m \cos m\theta + B_m \sin m\theta \right) \\ v &= U \sum_m B \mathcal{H}_m^{(1)\prime}(t) \left(A_m \cos m\theta + B_m \sin m\theta \right) \\ w &= U \sum_m \frac{B}{t} \mathcal{H}_m^{(1)}(t) \left(-m A_m \sin m\theta + m B_m \cos m\theta \right) . \end{aligned}\right\} \tag{4.18b}$$

Evidently the x, r, θ perturbations are, respectively, proportional to the functions

$$\mathcal{H}_m^{(1)}(t) - t\mathcal{H}_m^{(1)\prime}(t) \tag{4.19a}$$

$$B\mathcal{H}_m^{(1)\prime}(t) \tag{4.19b}$$

$$\frac{B}{t}\mathcal{H}_m^{(1)}(t) . \tag{4.19c}$$

It is found that

$$\mathcal{H}_0^{(1)}(t) - t\mathcal{H}_0^{(1)\prime}(t) = \cosh^{-1}\frac{1}{t} \tag{4.20a}$$

$$\mathcal{H}_1^{(1)}(t) - t\mathcal{H}_1^{(1)\prime}(t) = -\frac{2}{t}\sqrt{1-t^2} \tag{4.20b}$$

and for $m \geq 2$ (4.20c)

$$\mathcal{H}_m^{(1)} - t\mathcal{H}_m^{(1)\prime}(t) = (-1)^m \frac{(m-2)!}{2}\left[(m^2-1)(-T^{-m} + T^{-m}) \right] .$$

The explicit forms of $\mathcal{H}_j^{(1)}(t)$ and $\mathcal{H}_j^{(1)\prime}(t)$ have already been given as (4.14a,b,c; and 4.16a,b,c).

A table of modified conical velocity potential functions, calculated from the exact formulae (4.14, 4.16, and 4.20) and appropriately normalized, is presented as Appendix B. The functions tabulated are defined and discussed in Section VII on cone flows.

For analytical considerations of very slender bodies, the three sets of functions appearing in (4.19) may be rather closely approximated. The maximum of t for which the recommended approximation is in error less than 5% is listed with each approximation. The only use to be made of these formulae is in the demonstration of the general impossibility of fulfilling the boundary condition at every point on the surface of a noncircular cone by the superposition of singularities along a line. One has:

	Function	Max t, 5% error	
	$\mathcal{H}_0^{(1)}(t) \doteq \log \frac{2}{t} - 1$	0.37	(4.21a)
	$\mathcal{H}_1^{(1)}(t) \doteq 3t - \frac{1}{t}$	0.28	(4.21b)
$m \geq 2$,	$\mathcal{H}_m^{(1)}(t) \doteq (-1)^m \frac{(m-2)!}{2} \left\{ \frac{(m-1)2^m}{t^m} - 4 \right\}$	0.30	(4.21c)
	$\mathcal{H}_0^{(1)\prime}(t) \doteq -\frac{1}{t}$	0.30	(4.21d)
	$\mathcal{H}_1^{(1)\prime}(t) \doteq \frac{1}{t^2} + \frac{3}{2}$	0.38	(4.21e)
$m \geq 2$,	$\mathcal{H}_m^{(1)\prime}(t) \doteq (-1)^m \frac{(m-2)!}{2} \left\{ \frac{-m(m-1)2^m}{t^{m+1}} \right\}$	0.56	(4.21f)
	$\mathcal{H}_0^{(1)} - t\mathcal{H}_0^{(1)\prime}(t) \doteq \log \frac{2}{t}$	0.49	(4.21g)
	$\mathcal{H}_1^{(1)} - t\mathcal{H}_1^{(1)\prime}(t) \doteq -\frac{2}{t}$	0.30	(4.21h)
$m \geq 2$	$\mathcal{H}_m^{(1)} - t\mathcal{H}_m^{(1)\prime}(t) \doteq (-1)^m \frac{(m-2)!}{2} \frac{(m^2-1)2^m}{t^m}$.	0.30	(4.21i)

V. LORENTZ TRANSFORMATION

The functions obtained and discussed in the previous section represent the perturbation velocity potential and the perturbations associated with a distribution of sources of varying strength and azimuthal intensity located along the axis of the Mach cone from the origin of coordinates. A superposition of these functions is obviously incapable of representing the effects of a body which is yawed to such extent that the Mach cone axis lies outside the body over part or all of the body length. In this event other methods are required: either the line of singularities must be sufficiently yawed to remain wholly inside the body, or the body must be left unyawed to accomplish this end and a secondary "cross-flow" imposed on the free-stream to represent approximately the desired yaw influence.

The mechanism for yawing the line of singularities is the Lorentz transformation. The transformation may, of course, be used to adjust the orientation of any line in the space, but a ray originally inside the Mach cone remains inside, and vice versa.

The Lorentz transformation ("oblique transformation") has been used in aerodynamics by Jones (29), Hayes (1), and by Lagerstrom (23) who gives a rather complete discussion of the various transformations of the wave equation. The present employment of the transformation is different from that presented by the writers referenced, who were interested in the study of planar systems.

The transformation of a differential equation and its solutions may be considered in either of two ways: as a description of the same space in two different coordinate systems, or as an actual mapping of one space

onto another in the same set of coordinates. In the former interpretation, a point retains its absolute position but acquires different numerical coordinates; in the latter the transformation moves a point to new numerical coordinates in the original coordinate system. The latter interpretation is used here.

The hyperbolic distance is defined by (4.6). With this definition in mind, a Lorentz transformation is defined to be a linear transformation of coordinates which leaves the hyperbolic distance (and therefore the wave equation) invariant. The Mach cone is the locus of points of zero hyperbolic distance from the origin of disturbance, hence the Mach cone is invariant under Lorentz transformation.

The invariance of the wave equation guarantees that the transformed solutions of the equation, obtained by literal replacement of the original variables by the transformed variables, are solutions of the original equation. Thus one has a straightforward procedure for constructing, from the original solutions of the wave equation, solutions which vanish on the Mach cone and are singular on any desired ray inside the Mach cone.

The Lorentz transformation may be thought of as a rotation, preserving hyperbolic distances, of the space about any ray through the origin of coordinates. Let the coordinates of a space be as sketched:

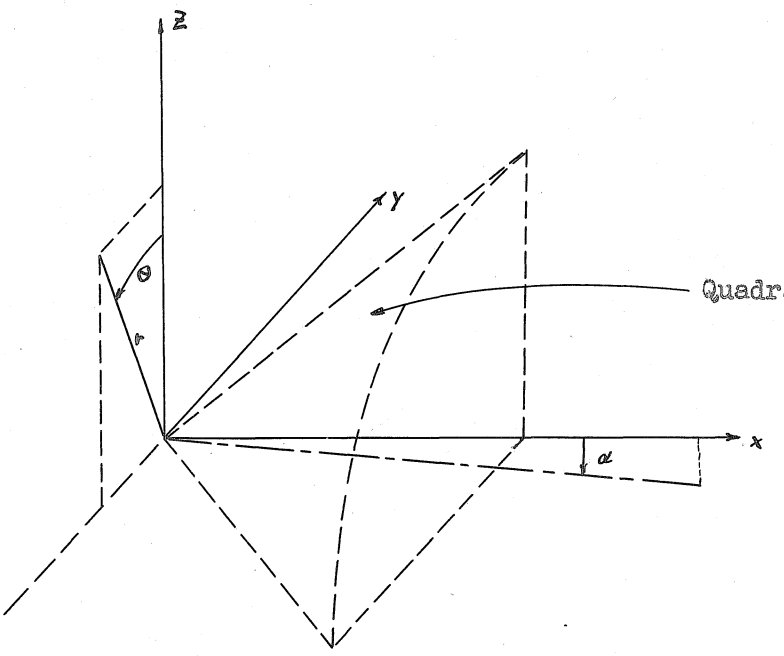

Quadrant of Mach cone.

Denoting by ( )* the coordinates of the transformed point, the Lorentz transformation keeping y fixed is

$$\begin{pmatrix} y^* \\ z^* \\ \frac{x^*}{B} \end{pmatrix} = \begin{pmatrix} 1 & 0 & 0 \\ 0 & \frac{1}{\sqrt{1-a^2}} & \frac{a}{\sqrt{1-a^2}} \\ 0 & \frac{a}{\sqrt{1-a^2}} & \frac{1}{\sqrt{1-a^2}} \end{pmatrix} \begin{pmatrix} y \\ z \\ \frac{x}{B} \end{pmatrix} . \qquad (5.1)$$

This transformation has the properties

i) Determinant of Jacobian $= 1$

ii) $$-B^2\frac{\partial^2}{\partial x^2} + \frac{\partial^2}{\partial y^2} + \frac{\partial^2}{\partial z^2} = -B^2\frac{\partial^2}{\partial x^{*2}} + \frac{\partial^2}{\partial y^{*2}} + \frac{\partial^2}{\partial z^{*2}} \qquad (5.2)$$

iii) $$x^2 - B^2(y^2+z^2) = x^{*2} - B^2(y^{*2}+z^{*2}) .$$

Matrix (5.1) transforms points originally on a line in the x,z plane inclined to the freestream at a positive angle of attack, α, (sketched) into the x axis, where

$$\alpha = \arctan \frac{a}{B} . \tag{5.3}$$

More generally, if it is desired to place the line of singularities at both angle of attack and yaw, the hyperbolic rotation may be accomplished in two steps, keeping first y fixed (angle of attack) and then z* (yaw). The resulting transformation is

$$\begin{pmatrix} y^* \\ z^* \\ \frac{x^*}{B} \end{pmatrix} = \begin{pmatrix} \frac{1}{\sqrt{1-b^2}} & 0 & \frac{b}{\sqrt{1-b^2}} \\ \frac{ab}{\sqrt{(1-a^2)(1-b^2)}} & \frac{1}{\sqrt{1-a^2}} & \frac{a}{\sqrt{(1-a^2)(1-b^2)}} \\ \frac{b}{\sqrt{(1-a^2)(1-b^2)}} & \frac{a}{\sqrt{1-a^2}} & \frac{1}{\sqrt{(1-a^2)(1-b^2)}} \end{pmatrix} \begin{pmatrix} y \\ z \\ \frac{x}{B} \end{pmatrix} . \tag{5.4}$$

This transformation fulfills properties (5.2). The angles of attack and yaw according to (5.4) are

$$\alpha = \arctan \frac{a}{B}$$

$$\beta = \arctan \frac{b}{B}\sqrt{1-a^2}$$

and the line of singularities pierces a plane $x = \text{const.} > 0$ in the quadrant $\frac{\pi}{2} \leq \theta \leq \pi$.

The more general Lorentz transformation (5.4) does not occasion the introduction of any concepts into the following discussion not required by the simpler formula (5.1), hence attention is restricted to (5.1). Hereafter skew orientation of the line of singularities is termed <u>yaw</u>, the parameter is <u>a</u>, and the line of singularities is presumed to lie in the z,x plane.

Writing out (5.1) one finds

$$y^* = y = \frac{-\tau x \sin\theta}{\beta} \tag{5.5a}$$

$$z^* = \frac{z + \frac{a x}{\beta}}{\sqrt{1-a^2}} = \frac{x}{\beta}\left(\frac{\tau\cos\theta + a}{\sqrt{1-a^2}}\right) \tag{5.5b}$$

$$x^* = \frac{a\beta z + x}{\sqrt{1-a^2}} = x\left(\frac{1+a\tau\cos\theta}{\sqrt{1-a^2}}\right) \tag{5.5c}$$

and in addition

$$\left.\begin{aligned} \tau^* \equiv \frac{\beta\sqrt{y^{*2}+z^{*2}}}{x^*} &= \frac{\sqrt{\tau^2(1-a^2\sin^2\theta)+2a\tau\cos\theta+a^2}}{1+a\tau\cos\theta} \\ &= \sqrt{1-\frac{(1-a^2)(1-\tau^2)}{(1+a\tau\cos\theta)^2}} \end{aligned}\right\} \tag{5.5d}$$

$$\theta^* = -\arctan\frac{\beta y\sqrt{1-a^2}}{\beta z + a x} = +\arctan\frac{\tau\sin\theta\sqrt{1-a^2}}{\tau\cos\theta + a}\,. \tag{5.5e}$$

It is instructive to consider the mapping of several specific surfaces by the Lorentz transformation. It has been mentioned that the Mach cone is invariant, although the cone apex is the only stationary point. The map of the cone $\tau = \tau_1 =$ const. is given by the parametric equations

$$\tau^{*2} = 1 - \frac{(1-\tau_1^2)(1-a^2)}{(1+a\tau_1\cos\theta)^2} \tag{5.5d}$$

$$\tan\theta^* = \frac{\tau_1\sin\theta\sqrt{1-a^2}}{\tau_1\cos\theta + a} \tag{5.5e}$$

where θ is the parameter. When these equations are combined to eliminate θ, the complicated equation obtained does not represent any of the familiar contours. The accompanying Fig. 4 shows the traces in the plane $x=1$ of the Mach cone, a cone $\tau_1 = 0.20$, and the transformed cone for $M = \sqrt{2}$ and $a = -0.50$, as calculated numerically. The transformed cone is more slender than the original and rather oblate.

When the yaw parameter, a, is sufficiently small, an approximate equation for the transformed cone may be obtained as follows: Write (5.5d) and (5.5e) in the forms

$$t^{*2} = 1 - \frac{1-t_1^2}{1+2at_1\cos\theta} \tag{5.6}$$

$$\tan\theta^* = \frac{t_1\sin\theta}{t_1\cos\theta + a} \quad ; \tag{5.7}$$

according to (5.6)

$$\cos\theta = \frac{-1}{2at_1}\left[1 - \frac{1-t_1^2}{1-t_1^{*2}}\right] = \frac{-\lambda}{2at_1} \quad (say) \tag{5.8}$$

hence

$$\sin\theta = \pm\sqrt{1 - \frac{\lambda^2}{4a^2t_1^2}}$$

thus, making these substitutions in (5.7) and solving for λ,

$$\lambda = 2a^2\sin^2\theta^* - 2at_1\cos\theta^*.$$

Now by (5.8)

$$\lambda = 1 - \frac{1-t_1^2}{1-t^{*2}}$$

hence

$$t^{*2} = 1 - \frac{1-t_1^2}{1-2a^2\sin^2\theta^* + 2at\cos\theta^*} \quad . \tag{5.9}$$

No approximations other than those implicit in (5.6) and (5.7) have been made in obtaining (5.9). Equation (5.9) is useful for study of the mapping properties of (5.5d and e) for $t_1 < 0.5$ and $|a| < 0.05$. In particular it is observed that the mapped cone $t_1 = \text{const.}$ is not asymptotically circular to first order in the yaw parameter. It follows that within the liberal accuracy requirements of a first order theory, the map of a circular cone is not "approximately" a yawed circular cone. Two consequences of this

fact appear in subsequent paragraphs and are pointed out.

The last example of the mapping to be considered is the trace on a plane $x = x_1 = \text{const.}$ of the locus $\mathcal{X}^* = \mathcal{X}_1^* = \text{const.}$ The trace is an ellipse whose center is at

$$y = 0$$

$$z = -\frac{a x_1}{B}\left(\frac{1-\mathcal{X}_1^{*2}}{1-a^2\mathcal{X}_1^{*2}}\right)$$

whose eccentricity is

$$e = a\sqrt{\frac{1-\mathcal{X}_1^{*2}}{1-a^2\mathcal{X}_1^{*2}}} \tag{5.10}$$

and whose major axis is normal to the plane of yaw. Note that the eccentricity (5.10) is proportional to the parameter a, as was to be expected from the discussion in the preceding paragraph. The equation of the ellipse is

$$y^2(1-a^2)+\left[z+\frac{a x_1}{B}\left(\frac{1-\mathcal{X}_1^{*2}}{1-a^2\mathcal{X}_1^{*2}}\right)\right]^2(1-a^2\mathcal{X}_1^{*2}) = \frac{x_1^2\mathcal{X}_1^{*2}}{B^2}\cdot\frac{(1-a^2)^2}{(1-a^2\mathcal{X}_1^{*2})}\,.$$

The possibility of yawing the solution of a particular problem to obtain the solution of the yawed problem is now to be analyzed. Consider a body whose surface is

$$r = F(x,\theta)\,.$$

The perturbation velocity potential associated with the body must fulfill the equations

$$\Box\varphi = 0 \tag{5.11}$$

$$(\bar{u} + \operatorname{grad}\varphi)\cdot\operatorname{grad}(r - F(x,\theta))\Big|_{r=F} = 0\,. \tag{5.12}$$

Let a Lorentz transformation (5.1) be applied in the space; there is obtained a new function

$$\varphi^* = \varphi(x^*, y^*, z^*) \tag{5.13}$$

which of course satisfies the wave equation (5.11), but which fulfills the condition

$$\left(\bar{U} + \text{grad}^* \varphi^*\right) \cdot \text{grad}^* \left(r^* - F(x^*, \theta^*)\right)\Big|_{r^* = F^*} = 0 \tag{5.14}$$

which is not the boundary condition on the yawed body. In (5.14)

$$\text{grad}^* = \bar{\imath} \frac{\partial}{\partial x^*} + \bar{\jmath} \frac{\partial}{\partial y^*} + \bar{k} \frac{\partial}{\partial z^*} . \tag{5.15}$$

Note that the constant vector $\mathcal{U}$ does not change in the transformation.

Upon introduction of the notation

$$S = r - F(x, \theta) \quad ; \quad S^* = r^* - F(x^*, \theta^*)$$

(5.14) may be written in the form

$$\left(U + \frac{\partial \varphi^*}{\partial x^*}\right)\frac{\partial S^*}{\partial x^*} + \frac{\partial \varphi^*}{\partial y^*}\frac{\partial S^*}{\partial y^*} + \frac{\partial \varphi^*}{\partial z^*}\frac{\partial S^*}{\partial z^*} = 0 . \tag{5.16}$$

According to (5.13)

$$\frac{\partial \varphi^*}{\partial x^{j*}} = \sum_i \frac{\partial \varphi^*}{\partial x^i}\frac{\partial x^i}{\partial x^{j*}} \tag{5.17}$$

and to evaluate (5.16) the inverse of the Lorentz transformation is required, namely

$$\begin{pmatrix} y \\ z \\ \frac{x}{B} \end{pmatrix} = \begin{pmatrix} 1 & 0 & 0 \\ 0 & \frac{1}{\sqrt{1-a^2}} & \frac{-a}{\sqrt{1-a^2}} \\ 0 & \frac{-a}{\sqrt{1-a^2}} & \frac{1}{\sqrt{1-a^2}} \end{pmatrix} \begin{pmatrix} y^* \\ z^* \\ \frac{x^*}{B} \end{pmatrix} . \tag{5.18}$$

Thus

$$\frac{\partial}{\partial x^*} = \frac{1}{\sqrt{1-a^2}}\frac{\partial}{\partial x} - \frac{a}{B\sqrt{1-a^2}}\frac{\partial}{\partial z}$$

$$\frac{\partial}{\partial y^*} = \frac{\partial}{\partial y} \qquad (5.19)$$

$$\frac{\partial}{\partial z^*} = \frac{-aB}{\sqrt{1-a^2}}\frac{\partial}{\partial x} + \frac{1}{\sqrt{1-a^2}}\frac{\partial}{\partial z} .$$

Equations (5.19) are useful in both (5.17) and (5.15).

Upon writing out (5.16) using (5.17) and (5.19), the condition actually fulfilled by the transformed solution, φ^*, is found to be

$$\left(U\sqrt{1-a^2} + \frac{\partial \varphi^*}{\partial x} - \frac{a}{B}\frac{\partial \varphi^*}{\partial z}\right)\left(\frac{\partial S^*}{\partial x} - \frac{a}{B}\frac{\partial S^*}{\partial z}\right) + \frac{\partial \varphi^*}{\partial y}\frac{\partial S^*}{\partial y}(1-a^2) +$$

$$+\left(-aB\frac{\partial \varphi^*}{\partial x} + \frac{\partial \varphi^*}{\partial z}\right)\left(-aB\frac{\partial S^*}{\partial x} + \frac{\partial S^*}{\partial z}\right) = 0 ,$$

which may be written

$$E + \frac{\partial S^*}{\partial z}\left\{-\frac{\partial \varphi^*}{\partial x}\left(\frac{a}{B} + aB\right) + \frac{a^2}{B^2}\frac{\partial \varphi^*}{\partial z} - \frac{a}{B}U\sqrt{1-a^2}\right\}$$

$$+\frac{\partial S^*}{\partial x}\left\{\frac{\partial \varphi^*}{\partial x}a^2B^2 - \frac{\partial \varphi^*}{\partial z}\left(\frac{a}{B} + aB\right)\right\} = 0 \qquad (5.20)$$

In (5.20) the quantity E is

$$E = \left(U\sqrt{1-a^2} + \frac{\partial \varphi^*}{\partial x}\right)\frac{\partial S^*}{\partial x} + \frac{\partial \varphi^*}{\partial y}\frac{\partial S^*}{\partial y}(1-a^2) + \frac{\partial \varphi^*}{\partial z}\frac{\partial S^*}{\partial z}$$

$$= (\bar{U} + \text{grad}\,\varphi^*)\cdot \text{grad}\,S^* + O(a^2U) . \qquad (5.21)$$

For small a ($a^2 << 1$), it follows from (5.21) that the quantity E must vanish at $S^*=0$ if the yawed potential function is to be the solution of the yawed problem. The two brackets in (5.20) indicate the extent to

which the boundary condition is not fulfilled on the transformed body. One observes that the bracketed terms are of order αU, which is the order of the terms in E, and may not, therefore, be ignored. It must be concluded that the yawed solution of a given problem does not solve, even approximately, the yawed problem. See the paragraph preceding (5.10).

The foregoing calculations have served to demonstrate quantitatively the divergence of the yawed solution and the yawed problem. The ultimate conclusion, however, would have been obtained without calculation on the simple observation that the gradient operator is not invariant under Lorentz transformation.

It is natural now to seek that problem which the yawed solution of a particular problem does satisfy. In the study of planar systems, that problem can be found (23), however in general it is impossible to find, by analytical procedures, the yawed solid body to which a yawed solution corresponds. The exception arises when the solution to be yawed is conical, so that the yawed function is also conical. In this event, the boundary condition equation (5.16) becomes an ordinary differential equation defining the function $h(\theta)$, where

$$r = \frac{x}{h(\theta)}$$

represents the surface of the yawed body to be found. The equation is suitable for numerical integration. These questions are of limited interest, hence further discussion is foregone.

The employement of the Lorentz transformation in specific problems is described in the sections on conical and nonconical flows.

VI. GOTHERT TRANSFORMATION

It is well known that any linearized problem at a given supersonic Mach number can, within the scope of the linearized theory, be transformed into an equivalent problem at a different supersonic Mach number. Particularly in wing theory (1)(23), use is made of this fact to transform any given configuration into the equivalent configuration at $M=\sqrt{2}$, where B $(\equiv\sqrt{M^2-1})=1$, the Mach angle is 45°, and the systematization of wing theory is most readily accomplished. The rules for making the transformation were first correctly formulated by Göthert (30), who was concerned with subsonic flow and the transformation to $M=0$. The transformation to $M=\sqrt{2}$ in supersonics is carried out in the same way, with the obvious change of notation. Alternative formulations and proof of the transformation are given by Lagerstrom (23) and Hayes (1).

The Göthert transformation may be stated compactly as follows: To find the perturbation velocity components u,v,w in the x(free stream)y,z directions, respectively, associated with the supersonic motion at Mach number, M, of a slender body the surface of which is

$$S(x,y,z)=0$$

the equivalent body

$$S(Bx',y',z')=0$$

may be solved at $M_0=\sqrt{2}$. Then at corresponding points

$$x'=\frac{x}{B}$$

$$y'=y$$

$$z'=z$$

$$u = \frac{u'}{\beta^2}$$

$$v = \frac{v'}{\beta}$$

$$w = \frac{w'}{\beta}$$

$$\varphi = \frac{\varphi'}{\beta}$$

where the primed quantities correspond to $M_0 = \sqrt{2}$, and the free stream velocity is invariant.

The convenience afforded in wing theory by the Göthert transformation to $M_0 = \sqrt{2}$ does not materialize in solid body theory and, except for the simplest bodies, the rule is of little utility. It is apparent that the Göthert rule requires the velocity potential and the perturbations at $M_0 = \sqrt{2}$ to be explicitly expressible in terms of the configuration dimensions, which is, for solid bodies, in general impractical. For example, suppose it be desired to study, by means of the Göthert transformation, the variation with M of the perturbation field surrounding a specific cone, the surface of which is

$$r = \delta x h(\theta)$$

Considering the cone at $M_0 = \sqrt{2}$, assume it is found that

$$\varphi' = U f_1\left(\frac{r'}{x'}, \theta, \delta h(\theta)\right)$$

$$u' = U f_2\left(\frac{r'}{x'}, \theta, \delta h(\theta)\right)$$

$$v' = U f_3\left(\frac{r'}{x'}, \theta, \delta h(\theta)\right) .$$

Then the same body at Mach number M is characterized by

$$\varphi = \frac{U\tau}{B} f_1\left(\frac{Br}{x}, \theta, B\delta h(\theta)\right)$$

$$u = \frac{U\tau}{B^2} f_2\left(\frac{Br}{x}, \theta, B\delta h(\theta)\right)$$

$$v = \frac{U\tau}{B} f_3\left(\frac{Br}{x}, \theta, B\delta h(\theta)\right).$$

It will be found in this study that in practical calculations involving noncircular cones and nonconical bodies it is seldom feasible to calculate the explicit dependence of the functions $f_1, f_2, \ldots$ on the configuration parameters $\delta, h(\theta), \ldots$, and usually more efficient either to use the approximation described below, or to calculate numerically the function of interest at several Mach numbers, and interpolate for the Mach number variation.

For solid bodies of nearly circular cross-section having, say, a maximum radius variation of 10% on either side of the mean at any station along the axis, numerical calculations verify, as would be expected, that the dependence of the longitudinal perturbation on M is sensibly the same as that for a circular body of the same cross section area and meridian contour. The lateral perturbations are practically independent of M. At portions of the body which are nearly conical or nearly circular, the Göthert rule provides the following formulae for comparing the same body at different Mach numbers:

$$\frac{\varphi_2}{\varphi_1} = \frac{B_1}{B_2}\left(\frac{1 - \log\frac{2}{B_2\delta}}{1 - \log\frac{2}{B_1\delta}}\right) \qquad \text{(conical portion)} \quad (6.1)$$

$$\frac{u_2}{u_1} = \frac{\log\frac{2}{B_2\delta}}{\log\frac{2}{B_1\delta}} \qquad \text{(conical portion)} \quad (6.2)$$

$$\frac{\varphi_2}{\varphi_1} = \frac{B_1}{B_2}\,\frac{Y_0(B_2\tau)}{Y_0(B_1\tau)} \qquad \text{(cylindrical portion)} \quad (6.3)$$

$$\frac{u_2}{u_1} = \frac{B_1^2}{B_2^2} \frac{Y_0(B_2 r)}{Y_0(B_1 r)} \qquad \text{(cylindrical portion)} \quad (6.4)$$

$$v_2 = v_1 \; ; \; w_2 = w_1 \qquad \text{(cylindrical or conical)} \quad (6.5)$$

the free stream velocity being the same at both Mach numbers. In these formulae, δ is the tangent of the mean half cone angle, and τ is the fineness ratio (< 1).

VII. FLOW OVER SOLID CONES

Attention is now given to the systematic analysis of the flow over conical solid bodies. The velocity distribution is considered first, then the calculation of the forces and moments is described.

Solid bodies in supersonic flow naturally fall into one of two categories, namely simple or nonsimple. A simple (nonsimple) solid body is defined to be one which does (does not) contain the Mach cone axis throughout the length of the body. If the Mach cone axis lies in the surface of the body, the body is by definition nonsimple. The distinction between simple and nonsimple solid bodies is quite important and has not been adequately appreciated. As mentioned in Section V, it is impossible to represent a nonsimple body by singularities distributed along the axis of the Mach cone unless further simplifications are made. All methods applicable to nonsimple bodies apply as well to simple bodies, but not vice versa.

1. Simple Cones

Consider a simple cone on whose surface

$$r = \frac{x}{h(\theta)} \tag{7.1}$$

where the coordinates are as sketched:

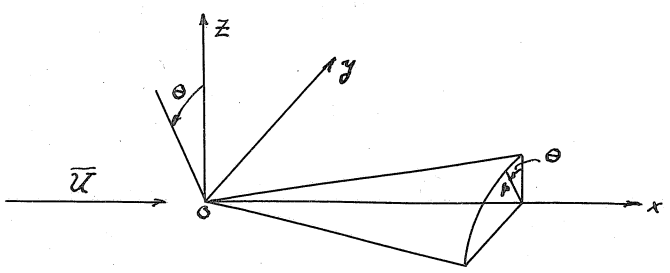

The potential of the perturbation velocity associated with the body satisfies the differential equation

$$\Box \varphi = 0 \qquad (1.1,\ 3.2)$$

and the boundary conditions

$$(\vec{U} + \text{grad}\,\varphi)\cdot \text{grad}\, S\Big|_{S=0} = 0 \qquad (1.2)$$

where

$$S = r - \frac{x}{h(\theta)} \,. \qquad (7.2)$$

The boundary condition is hereafter used in the approximate form in which the longitudinal perturbation, u, is ignored in comparison with the free stream speed, U. As mentioned in Section I, the error so introduced tends to counterbalance the errors inherent in the linearized theory. Thus (1.2) becomes

$$U\frac{\partial S}{\partial x} + \frac{\partial \varphi}{\partial r}\frac{\partial S}{\partial r} + \left(\frac{1}{r}\frac{\partial \varphi}{\partial \theta}\right)\left(\frac{1}{r}\frac{\partial S}{\partial \theta}\right)\Big|_{S=0} = 0$$

which equation, upon elimination of S by (7.2) becomes

$$-U + \frac{\partial \varphi}{\partial r}h(\theta) + \left(\frac{1}{r}\frac{\partial \varphi}{\partial \theta}\right)h'(\theta)\Big|_{r=\frac{B}{h(\theta)}} = 0 \,. \qquad (7.3)$$

With reference to equations (4.18), (7.3) is explicitly

$$\begin{aligned} &-1 + h(\theta)B\sum_m \mathcal{H}_m^{(1)\prime}(t)\left(A_m \cos m\theta + B_m \sin m\theta\right) \\ &+ h(\theta)h'(\theta)\sum_m \mathcal{H}_m^{(1)}(t)\left(-mA_m \sin m\theta + mB_m \cos m\theta\right) = 0 \,. \end{aligned} \qquad (7.4)$$

It is now to be shown that it is in general impossible to fulfill the boundary condition (7.4) at every point on the surface of a non-circular solid cone. The word impossible is used in the sense that the fulfillment of (7.4) at every point on the cone surface leads to an algebraic problem for whose resolution no methods are available.

For simplicity, assume that the cone is symmetrical with respect to the z,x plane, so that h(θ) is even. Then the velocity potential

$$\varphi = U \times \sum_m \mathcal{H}_m^{(1)}(t) \left(A_m \cos m\theta + B_m \sin m\theta \right) \qquad (4.18a)$$

is also even, and $B_m \equiv 0$.

To fulfill (7.4) at every point on the cone surface, the equation must be an identity in θ. Taking the cone to be sufficiently slender to permit the use of expressions (4.21), the $\mathcal{H}_m^{(1)}(t)$ functions in (7.4) may be written explicitly in terms of $t = \frac{B}{h(\theta)}$, and after some rearrangement, there appears

$$1 + A_0 h(\theta) + A_1 \left[-\cos\theta \left(\frac{h^3(\theta)}{B} + \frac{3}{2} B h(\theta) \right) + \sin\theta \left(3Bh'(\theta) - \frac{h^2(\theta) h'(\theta)}{B} \right) \right]$$

$$- 4 \sum_{m \geq 2} (-1)^m m A_m \frac{(m-2)!}{2} h(\theta) h'(\theta) \sin m\theta \qquad (7.5)$$

$$+ \sum_{m \geq 2} (-1)^m A_m m! \, 2^{m-1} \frac{h^{m+1}(\theta)}{B^m} \left[h'(\theta) \sin m\theta + h(\theta) \cos m\theta \right] = 0 .$$

Assume now that $h(\theta)$ is the simplest admissible nontrivial function,

$$h(\theta) = \beta (1 + \alpha \cos n\theta)$$

where $|\alpha| < 1$, and write all the terms in (7.5) as cosine trigonometric series. It can be shown that

$$h^m(\theta) = \beta^m \left(1 + \frac{1}{2} D_0^{(m)} + \sum_{l=1}^{m} D_l^{(m)} \cos ln\theta \right)$$

where

$$D_l^{(m)} = 2 \sum_{k=0}^{\left[\frac{m-l}{2}\right]} \left(\frac{\alpha}{2}\right)^{2k+l} \binom{m}{2k+l} \binom{2k+l}{k}$$

with the square brackets denoting the largest integer and

$$\binom{j}{s} = \frac{j!}{s!\,(j-s)!} .$$

The sine functions in (7.5) may be eliminated by the elementary addition formulae of the trigonometric functions. Finally, collecting all terms, (7.5) has the form

$$\sum_{j=0}^{\infty} C_j \cos j n\theta = 0 \qquad (0 \le \theta \le 2\pi)$$

hence

$$C_j = 0 \qquad (j = 0, 1, \cdots) .$$

The calculations show that each C_j is an infinite series of the form

$$C_j = c_0(j, n, \alpha, \beta) A_j + c_2(j, n, \alpha, \beta) A_{j+2} + c_4(j, n, \alpha, \beta) A_{j+4} + \cdots$$

where the $c_i(j, n, \alpha, \beta)$ do not necessarily decrease absolutely with increasing i, and are not apparently systematic. Thus one has an infinite set of linear algebraic equations in as many unknowns, A_i. There appears to be no practical method of solution; consequently resort must be taken to the fulfillment of the boundary condition on only a finite number of rays in the cone surface.

The procedure for this approximate fulfillment of the boundary condition is purely algebraic. A ray in the cone surface is completely specified by its azimuth, θ; thus, making the fullest use of whatever symmetries the problem has, several values, θ_i, of θ are selected and, having computed the numbers

$$h(\theta_i), \quad h'(\theta_i), \quad x_i = \frac{B}{h(\theta_i)}, \quad \mathcal{H}_m^{(1)}(x_i), \quad \mathcal{H}_m^{(1)\prime}(x_i)$$

equation (7.4) is written anew for each θ_i and the resulting linear simultaneous algebraic equations are solved for the coefficients A_m. Examples are to be presented.

The velocity potential obtained by this procedure is, of course, only an approximation to the solution. There is no way of determining which values of θ_i lead to the best approximation for a given number

of terms in the assumed solution (4.18a).

It happens that the $\mathcal{H}_m^{(j)}(t)$ functions are numerically very large for small t. To facilitate numerical computations, such as the foregoing schedule, tables of $\mathcal{H}_m^{(1)}(t)$ functions ($0 \leq m(1) \leq 10$; $0.04 \leq t(0.02) \leq 0.30 \leq t(0.05) \leq 1.00$) have been computed and, for $m \geq 2$, suitably normalized so that the tabulated numbers are not large. The normalization is permissible because the differential equation of the H functions is linear and homogeneous. The normalized functions are

$$H_m(t) = \begin{cases} \mathcal{H}_m^{(1)}(t) & (m = 0, 1) \\ \dfrac{\mathcal{H}_m^{(1)}(t)}{\mathcal{H}_m^{(1)}(0.20)} & (m \geq 2) \end{cases} . \tag{7.6}$$

The derivatives of the $\mathcal{H}_m^{(1)}(t)$ have, of course, been normalized by the same factor, namely

$$H_m'(t) = \begin{cases} \mathcal{H}_m^{(1)\prime}(t) & (m = 0, 1) \\ \dfrac{\mathcal{H}_m^{(1)\prime}(t)}{\mathcal{H}_m^{(1)}(0.20)} & (m \geq 2) \end{cases} . \tag{7.7}$$

The tables are presented as Appendix B. The functions tabulated are

$$\begin{aligned} &H_m(t) && (0 \leq m \leq 10) \\ &H_m'(t) \\ &H_m(t) - t\,H_m'(t) \end{aligned} .$$

Thus, referring to equations (4.18b) all the perturbation components for a given conical flow may be inferred directly from the tables, once the coefficients A_m, B_m are known. For each $m \geq 2$, the number $\mathcal{H}_m^{(1)}(0.20)$ is also given, so that the tables may be used in conjunction with formula (4.15) to obtain the values of $\mathcal{H}_m^{(j)}(t)$ for $j > 1$.

For reference, equation (7.4) is here rewritten in terms of the new H functions

$$-1+h(\theta)\,B\sum_m H_m'(t)\,(A_m\cos m\theta+B_m\sin m\theta)$$
$$+h(\theta)h'(\theta)\sum_m H_m(t)(-mA_m\sin m\theta+mB_m\cos m\theta)\Big]_{t=\frac{B}{h(\theta)}}=0\,. \tag{7.8}$$

Several examples of simple cone flows are now presented.

A. Right circular cone.

According to (4.18a) the perturbation velocity potential is simply

$$\varphi = U A_0 \times H_0(t)\,.$$

If the cone half vertex angle is arctan ε, then

$$h(\theta)=\frac{1}{\varepsilon}$$

and condition (7.8) is

$$-1+A_0\,\frac{B}{\varepsilon}\,H_0'(B\varepsilon)=0$$

hence

$$A_0=\frac{\varepsilon}{B\,H_0'(B\varepsilon)}$$

and

$$\varphi=\frac{\varepsilon U x\,H_0(t)}{B\,H_0'(B\varepsilon)}\,, \tag{7.9a}$$

According to (4.18b) the perturbation components are

$$u=\frac{\varepsilon U\{H_0(t)-tH_0'(t)\}}{B\,H_0'(B\varepsilon)} \tag{7.9b}$$

$$v=\frac{\varepsilon U\,H_0'(t)}{H_0'(B\varepsilon)} \tag{7.9c}$$

$$w=0\,. \tag{7.9d}$$

The surface pertubations ($t = B\varepsilon$) are simply

$$u = \frac{\varepsilon U}{B}\left\{\frac{H_o(B\varepsilon) - B\varepsilon H_o'(B\varepsilon)}{H_o'(B\varepsilon)}\right\} \qquad (7.9e)$$

$$v = \varepsilon U \qquad (7.9f)$$

$$w = 0 \quad . \qquad (7.9g)$$

These are the familiar fundamental functions used by Kármán and Moore (2), compactly expressed without approximation in terms of the new tabulated H(t) functions. Observe that the dependence of the perturbations on the Mach number is explicit, but that if the solution had been worked out at $M = \sqrt{2}$ and the Göthert transformation (Section VI) applied, precisely the above results would have been found.

B. Slightly yawed circular cone.

Assume that the perturbation velocity potential is adequately approximated by

$$\varphi = U A_o \times H_o(t) + U A_1 \times H_1(t) \cos\theta$$

and fulfill the boundary condition at two points, say $\theta = 0$ and $\theta = \pi$. The results to be obtained are of accuracy comparable to those of Tsien (3), which will appear subsequently in the criticism of the cross flow method.

The boundary condition (7.8) is

$$B h(\theta)\left(A_o H_o'(t) + A_1 H_1'(t)\cos\theta\right) = 1 \qquad (\theta = 0, \pi) \quad . \qquad (7.10a)$$

When $\theta = \theta_1 = 0$, $t = t_1 = \dfrac{B}{h(\theta_1)}$

and $h(\theta_1) = \dfrac{1 + \varepsilon \tan\alpha}{\varepsilon - \tan\alpha} = h_1$.

When $\theta = \theta_2 = \pi$, $\lambda = \lambda_2 = \frac{B}{k(\theta_2)}$

and $k(\theta_2) = \frac{1-\varepsilon \tan\alpha}{\varepsilon + \tan\alpha} = k_2$.

The fulfillment of (7.10a) at θ_1 and θ_2 requires

$$A_0 = \frac{k_2 H_1'(\lambda_2) + k_1 H_1'(\lambda_1)}{\Delta} \tag{7.10b}$$

$$A_1 = \frac{-k_1 H_0'(\lambda_1) + k_2 H_0'(\lambda_2)}{\Delta} \tag{7.10c}$$

with

$$\Delta = B k_1 k_2 \left(H_0'(\lambda_1) H_1'(\lambda_2) + H_0'(\lambda_2) H_1'(\lambda_1) \right). \tag{7.10d}$$

For each Mach number of interest, A_0 and A_1 can be calculated from the tables in Appendix B and the perturbation velocities then inferred from the tables and formulae (4.18b).

If more than two coefficients A_1 are to be calculated, it is inconvenient to write the explicit forms for them as in (7.10b,c) because the expressions become lengthy. It is more efficient to consider the boundary condition as a set of numerical equations from the outset. The present solution is compared graphically with the exact, slender body, and cross flow solutions of the same problem on subsequent pages (Fig.5).

C. Unyawed square cone.

The following last example demonstrates the maximum exploitation of the symmetry of a problem. Consider an unyawed cone of square cross section in the orientation sketched (looking upstream).

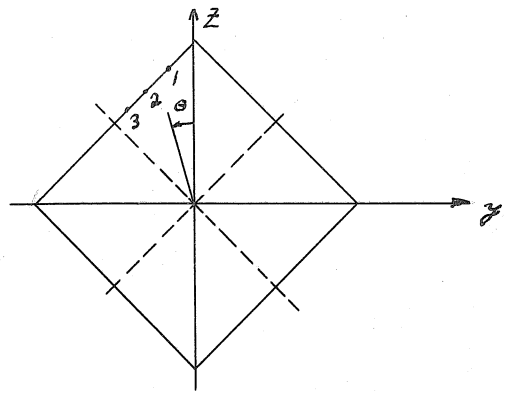

The velocity potential of the perturbations must obviously be periodic of period $\frac{\pi}{2}$, hence only harmonics of order 0, 4, 8, 12,... can appear in the solution. Furthermore the velocity potential must be even in θ with respect to all of the four lines of symmetry of the square, therefore if the boundary condition is fulfilled at, say, the three points 1, 2, 3 (sketched) then it will be fulfilled at all the images of these points, and their images, with respect to the four lines of symmetry. There are clearly 24 such points. Thus if one writes

$$\varphi = U \times \left(A_0 H_0(t) + A_4 H_4(t) \cos 4\theta + A_8 H_8(t) \cos 8\theta \right)$$

and fulfills (7.8) at the points 1, 2, 3, which entails the solution of only three simultaneous linear equations, then the boundary condition is actually being satisfied on 24 rays in the cone surface. A numerical example involving a square cone is presented in detail as a portion of Appendix D.

It is worth mentioning that in general there exists no necessary relationship between the Fourier coefficients of the radius of a simple cone

$$r = x \left(\frac{a_0}{2} + a_1 \cos\theta + a_2 \cos 2\theta + \dots \right)$$

and the coefficients, $UA_m H_m(t)$, in the perturbation velocity potential

$$\varphi = x\left(UA_0 H_0(t) + UA_1 H_1(t)\cos\theta + UA_2 H_2(t)\cos 2\theta + \cdots\right)$$

associated with the cone. If the numbers A_i are so selected that at the median cone $\left(r_0 = \frac{B a_0}{2}\right)$

$$UA_0 H_0(t_0) = \frac{a_0}{2}$$

$$UA_i H_i(t_0) = a_i \qquad (i = 1, 2, \cdots)$$

then the potential obtained represents a body both slenderer and more eccentric than the original cone.

A method of superposition of a number of yawed source lines, having a common vertex, to study the flow over noncircular cones at zero yaw has been worked out separately by the writer and by S. H. Maslen (25). Maslen obtained the velocity potential associated with a yawed source line by actually integrating a linearly increasing source intensity along the line. Precisely the same functions are obtained by applying the Lorentz transformation to the potential for an unyawed conical source line, as described in Section V. For the study of such noncircular cones, the writer has found it more efficient to proceed by the methods of the present Section than to consider yawed source lines. If the cone has a well-defined axis (intersection of two planes of symmetry) which is yawed, it is recommended that the unyawed solution be calculated by the present simple-body method, and the yaw contribution accounted for by the modified Tsien procedure described in the following paragraphs.

2. Nonsimple Cones

Methods applicable to nonsimple bodies are now to be discussed,

namely, the cross-flow methods of Tsien (3) and Jones (6, 7), and the method of inclined source lines using the Lorentz transformation. The assumptions of Tsien and Jones are criticized, and the accuracy of the two methods is evaluated. In this and the following sections, some extension of the methods is offered. The cross flow procedures are applicable as well to simple bodies as to nonsimple bodies, and are in fact usually to be recommended, because of their simplicity, for the aerodynamic study of any admissible body having a well-defined axis at yaw.

It has been found experimentally (31) that a slender cone may be yawed until the cone generatrix closest to the Mach cone axis is inclined to the axis at an angle as large as arctan $\frac{0.35}{\sqrt{M^2-1}}$ before flow separation occurs. For example, at M = 2, a circular cone of 5^0 half angle may be yawed approximately 17^0 and maintain a continuous flow field. Thus the methods presently discussed may be expected to yield quantitatively interesting results for such cases.

The fundamental assumption of the cross flow methods is that, within the scope of the linearized theory, the small component of the free stream velocity normal to the axis of a slightly yawed body may be considered as a secondary "cross flow" separate from the supersonic free stream in which the body is unyawed. The consequence is that insofar as the flow in the vicinity of the body surface is concerned, the slight yawing of the Mach cone with respect to the body is ignored. The cross flow technique in subsonic flow is not of present concern.

M. J. Lighthill (5), without stating his assumptions in full, made implicit use of the cross flow approximation in his consideration of the higher order solution of the problem of a circular body at yaw. He reached the conclusion that ignoring the yaw of the bow wave with respect to the body is inconsequential until terms of the order $\alpha^i \tau^j$ $(i(\geq 0)+j(\geq 0)=5)$ are considered. Here α is the yaw angle, and τ is the fineness ratio ($\tau \ll 1$). This conclusion appears to contrast with the theoretical and numerical calculations of A. H. Stone (32, 33) who showed that the cross flow approximation applied to a cone amounts to a neglect of the vorticity in the flow between the bow wave and the body surface, that this vorticity is proportional to the yaw, for small yaw, and that it significantly effects the pressure distribution on the cone surface. In strictness, therefore, the cross flow approximation must only be regarded as a highly plausible simplifying assumption.

The accompanying sketch shows the relationship between a yaw problem and its cross flow equivalent:

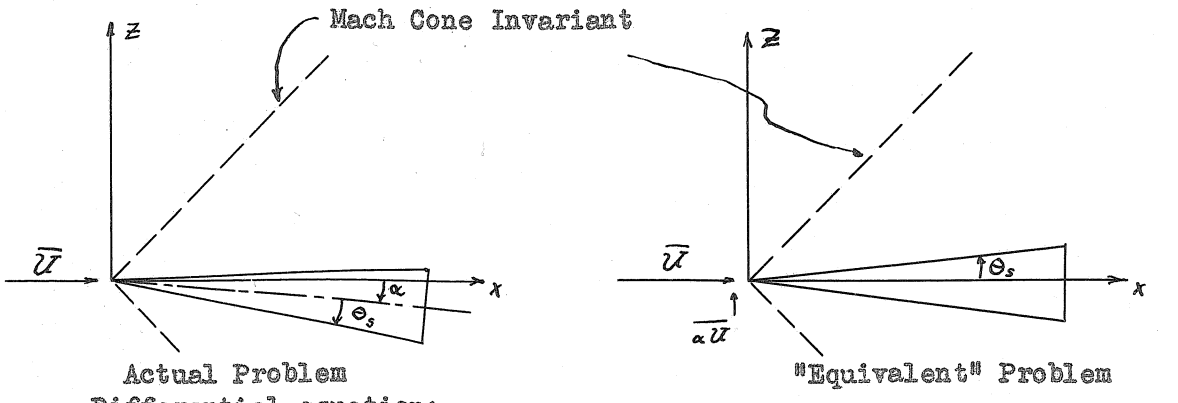

Boundary condition

$$U S_{1_{x_r}} + \varphi_{r_x} + \frac{\varphi_\theta}{r}\frac{S_{1_\theta}}{r}\Big]_{S_1=0} = 0 \qquad U^x S_{2_{x_r}} + (U^r + \varphi_{r_x}) S_{2_{r_x}} + (U^\theta + \frac{\varphi_\theta}{r})\frac{1}{r} S_{2_\theta}\Big]_{S_2=0} = 0 \qquad (7.11a,\ 7.11b)$$

Here the expressions $S_1 = 0$, $S_2 = 0$ represent the same body in the two different orientations. In the cross flow boundary condition, the components U^r and U^θ of the free stream are

$$U^r = \sin\alpha\, U \cos\theta$$
$$U^\theta = -\sin\alpha\, U \sin\theta . \qquad (7.12)$$

The difference between the Tsien and Jones cross flow theories is that Tsien assumes the cross flow compressible and three dimensional, and calculates the pressure from the velocities, whereas Jones considers the cross flow incompressible and two dimensional, and deduces the pressures by means of the nonstationary Bernoulli equation. The elements of the two theories are found in the references (3, 6, 7) and are hereafter presumed known. The application to nonconical bodies is discussed presently. Equation (7.11b) is the boundary condition to be used for the Tsien cross flow method.

For example, if one writes

$$S = r - \frac{x}{h(\theta)}$$

the Tsien-type boundary condition may be written

$$-1 + h(\theta_i)\Big[\sin\alpha\cos\theta_i + B\sum_m A_m H_m'(t_i)\cos m\theta_i\Big] - h'(\theta_i)\Big[\sin\alpha\sin\theta_i + h(\theta_i)\sum_m m A_m H_m(t_i)\sin m\theta_i\Big]_{t_i = \frac{B}{h(\theta_i)}} = 0 .$$

For a circular cone of half angle $\arctan\varepsilon$ at angle of attack α one thus has, with $h(\theta) = \frac{1}{\varepsilon}$, $h'(\theta) = 0$,

$$-1 + \frac{1}{\varepsilon}\Big(\sin\alpha\cos\theta_i + B\sum_{m=0}^{1} A_m H_m'(B\varepsilon)\cos m\theta_i\Big) = 0$$

hence

$$A_0 = \frac{\varepsilon}{B H_0'(B\varepsilon)}$$

$$A_1 = \frac{-\sin\alpha}{B H_1'(B\varepsilon)} . \qquad (7.13)$$

These coefficients may be compared with those obtained by the simple body method, equations (7.10). Apparently only a two term solution of a circular cone at yaw is possible on the basis of the present method. Simple body theory can yield a closer approximation with higher harmonics at the expense of additional labor.

A cone which is asymptotically elliptic may be studied at zero or finite angle of attack by setting $h(\theta) = \varepsilon(1-\delta\cos 2\theta)$. The eccentricity is

$$e = \frac{2\sqrt{\delta}}{1+\delta} .$$

Of course it is not necessary to determine the analytical expression of h(θ) for a given problem; it may frequently be more efficient to measure the numbers $h(\theta_i)$, $h'(\theta_i)$ from a drawing of the contour.

On the simple premise that the Tsien procedure considers the cross flow compressible and three dimensional, it must be presumed closer to the truth than the Jones procedure. In particular, the results of the Tsien theory are that for an admissible body at small yaw, the drag is independent of yaw but a function of M and body shape, the normal force and moment are proportional to the yaw and a function of M and body shape and, for nonconical bodies, that there is a normal force on cylindrical portions of the body. By numerical comparison of solutions of the Tsien type with more exact solutions such as the Kopal tables (10,33), it is found that the Tsien theory is qualitatively correct on all but

two counts: the dependence of the lift and moment coefficients of cones on the Mach number is inverted in that the Tsien theory predicts a decrease of these coefficients as M increases, whereas the coefficients actually increase with M, though slowly; and the drag is not independent of the yaw. The Tsien theory slightly overestimates the lift and moment at low supersonic speeds. The drag may be over - or underestimated depending on the body shape and the Mach number (see Fig. 1).

It is curious that Tsien and those who have since enlarged his theory dismissed the drag due to yaw as being second order in the yaw angle. The drag is known to be of second order in the apex half angle, but there is nothing in the Tsien approximation forbidding the yaw to be as large or larger than the apex half angle, provided the body is sufficiently slender. Experimental evidence in support of this statement has been mentioned. The following simple and approximate calculation demonstrates the trend of the drag due to yaw for a cone:

Obviously the drag coefficient, based on projected frontal area, of a slightly yawed circular cone is given by the formula

$$C_D = \frac{1}{2\pi \tan^2 \theta_{s0}} \int_0^{2\pi} C_p(\beta) \tan^2 \theta_s(\beta)\, d\beta$$

where β is the azimuth angle around the Mach cone axis, θ_{s0} is the apex half angle of the cone, and $\theta_s(\beta)$ is the inclination to the Mach cone axis of the cone generatrix at azimuth β. Now it is found that, very nearly

$$C_p(\beta) = C_{p0} - \Delta C_p \cos\beta$$

where C_{p_o} corresponds to the cone at zero yaw, and ΔC_p is a number proportional to the yaw. Furthermore, for small yaw, α,

$$\tan \theta_s(\beta) \doteq \tan \theta_{so} - \tan \alpha \cos \beta$$

Inserting these expressions in (7.13), it is found that

$$C_D \equiv C_{D_o} + \Delta C_D = C_{p_o} + \frac{\tan \alpha}{\tan \theta_{so}} \Delta C_p$$

hence

$$\Delta C_D = \frac{\tan \alpha}{\tan \theta_{so}} \Delta C_p$$

Apparently ΔC_D is important if α is not negligible in comparison with θ_{so}. For the typical case of a 10^o cone yawed 5^o at M = 2.075, one finds the drag due to yaw amounts to about 13% of the total drag. This figure increases rapidly as $\alpha \to \theta_{so}$, for then $\Delta C_p \to C_{p_o}$.

In Tsien's original paper (14), the linear pressure formula

$$C_p = -\frac{2u}{U} \qquad (2.2)$$

is used, hence the pressure contributions of the axial flow and the cross flow are linearly superimposed. However in Section II it is shown that formula (2.2) is inapplicable to the flow over slender bodies. This formula is the source of much of the error which has led to the criticism of the predictions of the linear theory. The foregoing evaluation of the Tsien theory is based upon a series of numerical calculations using the recommended pressure formula

$$C_p = 1 - \frac{g^2}{U^2} + M^2 \frac{u^2}{U^2} \qquad (2.5)$$

which leads to very much improved lift drag and moment predictions.

The principal results of the Jones method are: the lift and moment

are propostional to the yaw and a function of body shape, and are independent of M; for nonconical bodies, there is no lift force on a cylindrical portion of the body. The independence of M of the Jones results permits the theory to be used at sub-, trans- and supersonic speeds, but at supersonic speeds the predictions of the theory become less and less reliable as M increases. It is obvious that the aerodynamic coefficients must, actually, show some Mach number dependence, for as M (> 1) increases the body occupies relatively more of the volume within the bow wave. The Jones method overestimates the lift and moment, the error increasing as M (> 1) increases. The theory does not yield a direct drag estimate. The drag is presumed to be that found by the Kármán-Moore method (2) for the unyawed body. The approximate boundary condition and the quadratic pressure formula (2.5) should be used.

The evaluations presented in this section are based on a set of calculations of which the accompanying Figure 5 is an example. The figure compares the pressure distributions on the surface of a cone of 10° half angle, yawed 5° at M = 2.075. The various curves are: the exact first order value according to Stone and Kopal (32, 33), the pressure based on Tsien's assumption, but using the recommended pressure formula (2.5), the pressure according to Jones' slender body theory, and the pressure according to simple body theory (Section VII·1). The erratic behavior of the last mentioned curve for $0 < \theta < 45^{\circ}$ is due to the fact that the solutions of the linearized equation are not asymptotic to the solutions of the exact equation for points very near the line of singularities.

On the basis of the Jones theory, a thumb rule for the calculation of the lift and moment of slender bodies has appeared. The rule is: The lift and the moment of a slender body all of whose cross-section contours are similar are the same as those of a flat plate of the same projected area at the same yaw. The rule is true for all cones of elliptical cross section, of which the circular cone (7) and flat plate are limiting cases. For contours of other shape the rule is quantitatively incorrect but qualitatively valuable for purposes of estimation, because the error is not large. For slender square and triangular cones, departure of the thumb rule prediction from the true Jones value is less than 10%, and Spreiter (7) has found the error to be less than 8% for a circular cone with thin wing-like excrescences. The lift and moment are underestimated.

If the distribution of velocity due to yaw is desired in the vicinity of the body surface, the calculation is most simply carried out on the basis of Jones' assumption. For bodies of circular cross section with or without thin radial excrescences, or bodies of oval or elliptical contour, the velocities can be calculated by suitable conformal transformation in the usual way. If the body has a polygonal cross section contour, the mapping functions which arise in general define transcendental functions which cannot be written down explicitly, and numerical methods are required. Two cross section contours of current aerodynamic interest are the equilateral triangle and the square. The solutions of these problems have been obtained and are presented in Appendix C.

There is an upper limit of body size beyond which the Jones cross flow assumption is untenable. The approximation amounts to the replacement of the wave equation by the two dimensional Laplacian in planes normal to the free stream. One may thus determine the maximum of the variable t beyond which the harmonic solutions of the wave equation, $H_m(t)$, and their derivatives, cease to be proportional within specified error to the corresponding two dimensional harmonic solutions of the Laplace equation. Establishing the bound of error as 5%, the least maximum of t is found to be about 0.23. Thus the Jones theory should not be used for a body whose surface slope, σ, is greater than

$$\sigma_{max} = \frac{0.23}{\sqrt{M^2-1}} .$$

Of course, neither cross flow theory should be expected to yield an acceptable quantitative description of the flow field between the body surface and bow wave beyond t = 0.50 (say), owing to the neglect of the Mach cone yaw.

The theory of the representation of a non-simple body by superposition of the yawed solutions (Section V) is, with the few requisite changes of notation, word for word the same as that for the representation of a simple body in terms of the unyawed solutions. Specifically, the velocity potential of the perturbations is written

$$\varphi = U \sum_m x^* H_m(x^*)\left(A_m \cos m\theta^* + B_m \sin m\theta^*\right)$$

where

$$x^* = \frac{x(1+a\,t\cos\theta)}{\sqrt{1-a^2}}$$

$$t^* = \sqrt{1-\frac{(1-a^2)(1-t^2)}{(1+a\,t\cos\theta)^2}}$$

$$\theta^* = \arctan\frac{t\sin\theta\sqrt{1-a^2}}{a+t\cos\theta}$$

and $a = B \tan \alpha$, α being the angle of attack.

Thus, for example

$$\varphi = U \sum_m \frac{x(1+at\cos\theta)}{\sqrt{1-a^2}} H_m\left(\sqrt{1-\frac{(1-a^2)(1-t^2)}{(1+at\cos\theta)^2}}\right) A_m \cos\left\{m \tan^{-1} \frac{t\sin\theta\sqrt{1-a^2}}{a+t\cos\theta}\right\} . \quad (7.14)$$

The boundary condition to be fulfilled is

$$(\bar{u} + \text{grad}\,\varphi)\cdot \text{grad}\, S\Big|_{S=0} = 0 ,$$

which equation can be fulfilled only along a finite number of rays in the cone surface. Observe that the function S must represent the yawed body with respect to the original x,r,θ coordinates. For example, a circular cone of half angle θ_s at angle of attack α may be represented by

$$S = r^2\left[\cos^2\theta_s \sin^2\theta + \cos(\alpha-\theta_s)\cos(\alpha+\theta_s)\cos^2\theta\right] + r x \sin 2\alpha \cos\theta$$

$$+ x^2 \sin(\alpha+\theta_s)\sin(\alpha-\theta_s) = 0 ,$$

In forming the derivatives of the velocity potential, equations (4.17) must be kept in mind.

Owing to the obvious algebraic complication associated with the yawed solutions and the boundary condition, their use as a practical computation tool cannot be recommended. The solution of the flow about a yawed cone in terms of the yawed solution does, however, represent the closest approximation to the truth attainable by the linear theory. For this reason the pressure has been calculated at several points on the surface of the cone on which Fig. 5 is based. The results were not significantly different from the modified Tsien-type results, which suggests the adequacy of the Tsien procedure for moderate-yaw problems.

In summary, the procedures recommended for the study of circular or noncircular cones are:

(1) If the entire cone surface lies in the band of admissibility on Fig. 1, use simple body theory.

(2) If the mean cone surface of the unyawed cone lies in the band, but parts of the surface do not so qualify when the cone is yawed, use the modified Tsien method.

(3) If the mean cone surface lies below the band, use Jones' slender-body method provided the requisite conformal transformations can be found; if they cannot, resort to the thumb rule. Except for a single special case (34) the Jones method is the only recourse if the cone has thin excrescences (7).

3. Lift, Drag, Moment of Cones

Formulae giving the aerodynamic properties of yawed and unyawed circular cones, based on the linear pressure formula (2.2) are well known (2, 3). Quite elegant formulae for the characteristics of non-circular cones can also be obtained using the linear pressure formula, but these are not presented or recommended, even for use in qualitative comparisons, because in consequence of the discussion in Section II the linear formula is known to be unreliable. Except for those problems which are satisfactorily studied by the Jones theory (7), there appears to be no substitute for the numerical integration over the cone surface of the pressure according to the quadratic formula (2.5).

VIII NONCONICAL BODIES

To study by linearized theory the aerodynamics of slender nonconical bodies, one may proceed by any one of four methods, each having its advantages and disadvantages and a circumscribed domain of applicability as regards body shape and Mach number within which the results obtained are quantitatively acceptable. The methods are:

1. Superposition of conical flows so as to satisfy the surface boundary condition at an optional number of points. This is a generalization of the Kármán-Moore method (2, 3) applicable to noncircular bodies.

2. Jones slender body theory (7), a zero-order approximate method of determining the effects of yaw and which does not lead directly to an estimation of pressure distribution for drag.

3. Analysis of nonconical velocity distributions by study of the fundamental nonconical solutions of the wave equation.

4. Needle theory (17, 4, 35), a generalization of methods 1 and 3 in which the analysis is very much simplified by assuming that the radius of the body is vanishingly small throughout the body length.

For circular bodies, methods 1, 2 and 4 have been adequately developed in the literature, particularly in the cited references. For particular noncircular bodies, methods 2 (7) and 4 (35) have been used. The concern of this section is the development of method 1 for rather general noncircular solid bodies, and of method 3 for both circular and noncircular solid bodies.

In contrast with the state of affairs in the consideration of cone flow, the evaluation of the several methods must be only

qualitative for no exact solutions of nonconical flow over solid bodies for use in comparison are known. The criticism of methods 1 and 2 presented in Section VII seems to hold when these methods are applied to nonconical flows, with the exception that the inverted dependence of the lift and moment coefficients on Mach number does not persist (36). The features of needle theory are that the predicted aerodynamic coefficients are independent of Mach number and can usually be expressed in closed form in terms of the body shape parameters. The Kármán-Lighthill drag formula (17, 4),

$$D = \frac{\rho V^2}{4\pi} \int_0^l \int_0^l \log \frac{1}{|x-y|} S''(x) S''(y) \, dx \, dy ,$$

where $S(\xi)$ is the body cross section at station ξ, is a typical needle theory result. Lighthill obtained this formula taking great care to estimate the order of magnitude of all approximations made. The writer feels, however, that order-of-magnitude arguments may be misleading (viz. Section II) and does not regard the results of needle theory as quantitatively reliable except for the study of the flow over needles. As to method 3, it is subject to the same limitations as the simple body method for conical flows.

It is of course more difficult to analyze the flow over a noncircular body than that over a circular body. Before going to the extra effort, it is wise to inquire as to the utility of the results to be obtained. Certainly if a description of the local flow between the body surface and the bow wave is required, the complete noncircular solution must be obtained. Consider now the drag on the body. Kármán (17) has shown how the drag of a circular body may be calculated

approximately by integration of the flux of longitudinal momentum through a circular cylinder surrounding the body and extending to infinity downstream:

$$D \doteq -\int_0^\infty dx \int_0^{2\pi} \rho u v \, r \, d\theta . \tag{8.1}$$

In this formula the density is considered constant and it is easily seen that this approximation amounts to the integration over the body surface of the pressure according to the linear formula (2.2). Thus the formula is quantitatively unreliable; however it is useful for the derivation of a few important generalizations.

Consider a body all of whose cross section contours are similar and, for simplicity, symmetrical about the vertical (z,x) plane. It will appear subsequently that the perturbations u and v in the flow over such a body may be written in the form

$$\begin{aligned} u &= u_0(B,r,x) + U \sum_{m\geq 1} A_m f_m(B,r,x) \cos m\theta \\ v &= v_0(B,r,x) + U \sum_{m\geq 1} A_m g_m(B,r,x) \cos m\theta . \end{aligned} \tag{8.2}$$

Thus

$$\begin{aligned} D &= -\rho \int_0^\infty dx \int_0^{2\pi} u v \, r \, d\theta \\ &= -2\pi\rho \int_0^\infty r u_0(B,r,x) v_0(B,r,x) dx - \pi\rho U^2 \sum_{m\geq 1} A_m^2 \int_0^\infty r f_m(B,r,x) g_m(B,r,x) dx . \end{aligned}$$

The integral of $u_0 v_0$ is improper, but the integral of $f_m g_m$ is absolutely convergent. This formula shows that the noncircularity, which gives rise to the small terms in the summation, usually has very little influence on the drag. For the typical case of a square contour, the numbers

$A_1 = A_2 = A_3 = 0$, and $\dfrac{A_4^2 f_4 g_4}{u_0 v_0} \simeq \dfrac{1}{900}$

and hence the contribution of the noncircularity to the drag in this example is inconsequential.

The functions u_0 and v_0 are cylindrically symmetrical and may be thought of as arising from a circular body "equivalent" to the noncircular body. In reference (35), E. W. Graham has considered the drag of noncircular bodies from the viewpoint of needle theory and found that the equivalent body has the same distribution of cross section area as the original body. When the needle theory assumptions are not made, it is found that the two areas are not exactly the same. But it appears that the error committed in assuming the two areas to be the same is no more important than ignoring the small drag contribution of the noncircularity.

Let the perturbation velocity potential associated with the flow over a given noncircular cone be

$$\varphi = U x \left[A_0 H_0(x) + A_1 H_1(x) \cos\theta + A_2 H_2(x) \cos 2\theta + \cdots \right] .$$

If one imagines a nonconical body to be represented by a superposition of these functions at points along the body axis in the manner of Kármán-Moore, the u_0 and v_0 functions associated with the equivalent body are the result of the superposition of the functions

$$u = U A_0 \left(H_0(x) - x H_0'(x) \right)$$

$$v = U B A_0 H_0'(x) .$$

Now if the equivalent body has the same area at any station as the original body, the coefficient A_0 of the fundamental cone solution must be the same as the coefficient A_0' in the solution for a circular cone of the same

cross section area. However in general it is found that $A_0 \neq A_0'$. The error is minor. It is difficult to formulate a theorem relating A_0 and A_0' to the noncircular contour shape, inasmuch as A_0 depends upon both the number of rays in the cone surface at which the boundary condition is satisfied and on the location chosen for these rays. However the following suggestion seems to be correct: the original and equivalent contours have the same area when both are subjected to the Tschaplygin transformation,

$$T = \frac{1-\sqrt{1-x^2}}{x}.$$

This suggestion is inferred from the observation that it is in terms of the variable T that the solutions of the wave equation are naturally expressed. For small t, T and t are proportional:

$$T \doteq \frac{t}{2}$$

hence for very slender bodies, the equivalent and actual bodies have the same area with negligible error.

In considering the lift of the body, if the compressible cross flow assumption is made, the form of the perturbation v (8.2) is unchanged, and by the momentum theorem

$$L = \rho \int_0^\infty dx \int_0^{2\pi} v^2 \cos\theta \, r \, d\theta$$

$$= \rho\pi \int_0^\infty r \{ 2A_1 v_0(B,r,x) g_1(B,r,x) + \sum_{m\geq 2} A_m A_{m-1} g_m(B,r,x) g_{m-1}(B,r,x) \} dx .$$

By inspection of this formula, bearing in mind that the functions $A_1 g_1$, $A_2 g_2, \cdots$ are in general absolutely much smaller than $v_0(B,r,x)$, it is apparent that most of the lift arises from the term $A_1 g_1(B,r,x)\cos\theta$

in v, and that, as with the drag, the higher harmonics make little lift contribution. Although it is difficult to express unalytically, it is also implicit in the lift formula that the relative contribution to lift of the higher harmonics is more important than their contribution to the drag.

The conclusions drawn from these rather qualitative arguments are: for estimating the net aerodynamic action on a solid body, it is usually adequate to consider the circular equivalent body having the same distribution of cross section area and having the same orientation in the stream. For detailed study of the aerodynamic characteristics, for a more reliable quantitative determination of the pressure distribution, and for a description of the flow field in the vicinity of the body surface, the complete noncircular flow field should be worked out. The method recommended for the study of the equivalent body is that of reference (3) using, however, the approximate boundary condition, the quadratic pressure formula (2.5) and the tables of Appendix B. A rough estimate of the velocities due to yaw is available by the Jones incompressible cross flow method. The velocity distribution over circular, elliptic, and oval cross sections, and over certain circular cross sections with thin excrescences may be calculated by two-dimensional potential flow theory as mentioned in Section VII. The cross flow associated with slender bodies of square and triangular cross sections is tabulated in Appendix C.

1. Superposition Procedure for Nonconical Noncircular Solid Bodies.

For simplicity, attention is first directed to bodies all of whose cross sections contours are similar and similarly oriented with respect to the x-axis. If the body is yawed, the cross flow boundary condition is to be used. The yaw, α, is taken to be small enough that $\cos\alpha = 1$, $\sin\alpha = \alpha$. If the body of interest is not yawed, $\alpha = 0$ in the following equations. In virtue of the similarity of the cross section contours, the function S may be written

$$S = r - \frac{f(x)}{h(\theta)}$$

where $f(0) = 0$ and $f'(0+) = 1$. The equation of the body surface is

$$r = \frac{f(x)}{h(\theta)} .$$

According to (7.11b) the boundary condition to be fulfilled is

$$U f'(x) + h(\theta)\left[\alpha U \cos\theta + \varphi_{r_x}\right] + h'(\theta)\left[\alpha U \sin\theta - \frac{1}{r}\varphi_\theta\right]_{t = \frac{Bf(x)}{x h(\theta)}} = 0 . \qquad (8.3)$$

As $x \to 0$, (8.3) tends to exactly the boundary condition on the perturbation velocity potential associated with the cone tangent to the body at the apex, as would be expected.

The idea now is to solve this cone flow problem and then, at a number of points along the axis downstream from the nose, to add correction solutions to the initial solution in order to deform the flow streamlines to the contours of the body surface. In view of the assumption that all the cross section contours of the body are similar and similarly positioned with respect to the body axis, it is reasonable that the correction solutions to be superimposed should be the same function, in coordinates originating at the selected points along the axis, as the solution

associated with the initial tangent cone. In general this assertion is not strictly true, as will be indicated parenthetically in the description of the procedure; but the error entailed by its rise is clearly minor for a reasonably shaped body.

The superposition is accomplished as follows:

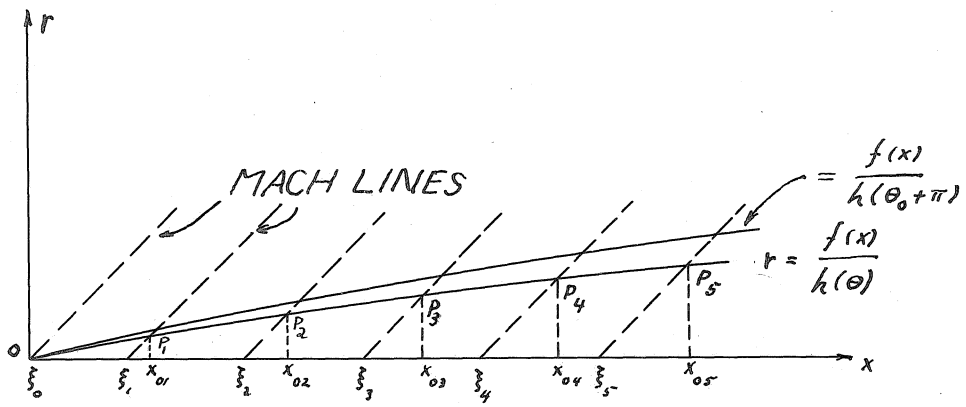

1. Select a set of points $\xi_0 = 0$, ξ_1, (near ξ_0), ξ_2, ξ_3, $\cdots$ along the body (x) axis, and a value θ_0 of θ such that $\frac{\partial r}{\partial \theta}$ is continuous in θ at θ_0. The continuity of $\frac{\partial r}{\partial \theta}$ insures that the velocity potential and its derivatives are not singular on the plane $\theta = \theta_0$. Draw the body contour $r = \frac{f(x)}{h(\theta_0)}$ and construct Mach lines from the points ξ_i $(i = 1, 2, \ldots)$ intersecting this contour at the points P_i. Now establish an x_i, t_i, θ coordinate system at each ξ_i, such that $x_i = x - \xi_i$, $t_i = \frac{\beta r}{x - \xi_i}$, and $\theta = \theta$. Let the coordinates of P_i in the j coordinate system be $(x_{j,i}, t_{j,i}, \theta_0)$, which will be written (j,i) for brevity.

2. Solve the conical flow problem of the flow about the cone tangent to the body at the nose using the methods of Section VII. Let the velocity potential obtained be $\tilde{\varphi}(x, t, \theta)$

3. At ξ_1 add the function $c_1\bar{\varphi}(x_1, t_1, \theta)$ and determine the coefficient c_1 by imposing the boundary condition (8.3) at P_2:

$$U f'(x_{02}) + h(\theta_0)\left[\alpha U \cos\theta_0 + \tilde{\varphi}_{r_x}(0,2) + c_1\bar{\varphi}_{r_x}(1,2)\right] + h'(\theta_0)\left[\alpha U \sin\theta_0 - \frac{1}{r}\tilde{\varphi}_\theta(0,2) - \frac{c_1}{r}\tilde{\varphi}_\theta(1,2)\right] = 0 . \tag{8.4}$$

(Remark: The number c_1 obtained by solving this simple algebraic equation should not depend on the choice of θ_0. Suppose, for example, that $h(\theta)$ is even about $\theta = 0$ and $\theta = \pi$ and continuously differentiable at these points. In this event $\bar{\varphi}_\theta(i,j) = 0$. Let $c_1\big|_{\theta_0 = 0} = c_1$ and $c_1\big|_{\theta_0 = \pi} = c_1'$. Then according to (8.4)

$$c_1 = \frac{-\{U f'(x_{02}) + h(0)[\alpha U + \tilde{\varphi}_{r_x}(0,2)]\}}{h(0)\,\bar{\varphi}_{r_x}(1,2)} \tag{8.5a}$$

$$c_1' = \frac{-\{U f'(x_{02'}) + h(\pi)[-\alpha U + \bar{\varphi}_{r_x}(0,2')]\}}{h(\pi)\,\bar{\varphi}_{r_x}(1,2')} . \tag{8.5b}$$

For the argument, take $h(\pi) < h(0)$. This is the condition depicted on the figure. For this condition

$$x_{02'} > x_{02}$$

$$t_{(0,2')} > t_{(0,2)}$$

$$t_{(1,2')} > t_{(1,2)} .$$

Now $\bar{\varphi}(x, t, \theta)$ and its first derivatives decrease absolutely as t increases, and for the solution associated with a simple cone, $\frac{\partial\varphi}{\partial x_r} < 0$ and $\frac{\partial\varphi}{\partial r_x} > 0$. With these observations, comparison of (8.5a) and (8.5b) shows that the variations of the numerator and denominator of c_1' have been such as to preserve the value of c_1. The variations tend to counterbalance,

and the net change of C_1 is very small. This argument is necessarily intuitive; its only purpose is to indicate that even though the constants C_1 and C_1' are clearly not necessarily equal, that the difference is unimportant. This is the justification for the superposition of the noncircular conical flows. It is mentioned in passing that if the nonconical body is circular, the C_i are completely independent of θ_0.)

4. Then at ξ_2 add a second correction function $C_2\bar{\varphi}(x_2, r_2, \theta)$ and determine C_2 by imposing the boundary condition at P_3:

$$U f'(x_{03}) + h(\theta_0)\left[\alpha U \cos\theta_0 + \bar{\varphi}_{r_x}(0,3) + C_1\bar{\varphi}_{r_x}(1,3) + C_2\bar{\varphi}_{r_x}(2,3)\right] \qquad (8.6)$$
$$+ h'(\theta_0)\left[\alpha U \sin\theta_0 - \frac{1}{r}\bar{\varphi}_\theta(0,3) - \frac{C_1}{r}\bar{\varphi}_\theta(1,3) - \frac{C_2}{r}\bar{\varphi}_\theta(2,3)\right] = 0.$$

5. One continues in this manner adding a correction function at each ξ_i and determining the constants C_i.

If the body has a plane of symmetry at which $h'(\theta)$ is continuous, the foregoing calculations may be considerably simplified by setting $\theta = \theta_0$ to be this plane, which reduces the number of terms in the boundary conditions by one-third.

The practical execution of this method is quite simple and rapid when use is made of the tables in Appendix B. It is recommended that the contour $r = \frac{f(x)}{h(\theta_0)}$ be plotted on a small scale (i.e. large figure) and the coordinates x_{ij}, r_{ij} tabulated by direct measurement; then the derivatives of the $\bar{\varphi}$ functions can be interpolated from the tables and the successive equations for the C_i's written and inverted by inspection. An example of the method is worked out in detail in Appendix D.

It turns out to be difficult completely to close a body downstream

by this method because the boundary condition becomes an equation involving the difference of large numbers which are almost equal. The solution of such equations is troubled by considerable numerical uncertainty in actual calculation. Aerodynamically, this shortcoming is unimportant because a supersonic stream cannot converge completely behind a three-dimensional body however well it be faired, as was proven by D. R. Chapman (37).

3. Superposition of Nonconical Potentials

It is assumed that the cross section contours of the body are not necessarily similar but are, for simplicity, symmetrical about the (z,x) plane which also contains the free stream velocity. For angle of attack, the cross flow approximation is made. The surface, $S=0$, of the body is given by

$$r = F(x,\theta)$$

and the approximate boundary condition to be fulfilled by the nonconical velocity potential

$$\varphi = \mathcal{U} \sum_{j=1} \sum_{m=0} A_m^{(j)} x^j H_m^{(j)}(t) \cos m\theta \qquad (3.12)$$

is, according to equation (1.2)

$$\mathcal{U} F F_x - (\alpha \mathcal{U} \cos\theta + \varphi_{r_x}) F + (-\alpha \mathcal{U} \sin\theta + \tfrac{1}{r}\varphi_\theta) F_\theta \Big|_{r=F} = 0. \qquad (8.8)$$

If the body does not have lateral symmetry, terms of the form

$$\mathcal{U} \sum_{j=1} \sum_{m=0} B_m^{(j)} x^j H_m^{(j)}(t) \sin m\theta$$

must be annexed to the velocity potential. Now

$$\varphi_{r_x} = \mathcal{U} \sum_{j=1} \sum_{m=0} A_m^{(j)} x^{j-1} B H_m^{(j)\prime}(t) \cos m\theta$$

and

$$\frac{1}{r} \varphi_\theta = -\mathcal{U} \sum_{j=1} \sum_{m=0} m A_m^{(j)} x^{j-1} \frac{B}{t} H_m^{(j)}(t) \sin m\theta$$

there being no question of convergence or the validity of termwise differentiation, for both summations are ultimately to be extended over only a finite number of terms. Inserting these representations into (8.8), the boundary condition becomes

$$F^2 F_x - \alpha \cos\theta F^2 - \alpha \sin\theta F F_\theta$$

$$- F^2 \sum_{j=1} \sum_{m=0} A_m^{(j)} x^{j-1} B H_m^{(j)\prime}(t) \cos m\theta \qquad (8.9)$$

$$- F_\theta \sum_{j=1} \sum_{m=0} m A_m^{(j)} x^j H_m^{(j)}(t) \sin m\theta \Big]_{t = \frac{BF(x,\theta)}{x}} = 0 .$$

It is in general impossible to fulfill (8.9) identically in x and θ at every point on the body surface for reasons the same as those mentioned in Section VII. It is possible, however, to satisfy the boundary condition at an arbitrary number of points on the body surface, relying on the continuity of the functions involved to produce satisfactory values of the velocities and the pressure at intermediate points.

Consider for a moment the inverse problem of determining the function $F(x,\theta)$ specifying the body defined by a set of coefficients $A_m^{(j)}$ and suppose the variation of t_s with x may be ignored. In order for the boundary condition to be an identity in x, it is necessary that the power series representation of $F(x,\theta)$

$$F(x,\theta) = x g_1(\theta) + x^2 g_2(\theta) + \cdots$$

be of order at least as great as the largest value of the index j for which $A_m^{(j)}$ does not vanish, and this is true a fortiori if the variation of t with x on S = 0 cannot be ignored. Consequently in the direct problem of determining (approximately) the coefficients $A_m^{(j)}$ the largest value of the index of summation with respect to j cannot be less than the order in x of a satisfactory polynomial approximation to F(x,θ). This criterion is very important.

Let it be assumed that a satisfactory approximation to F(x,θ) is

$$F(x,\theta) = \sum_{j=1}^{M} x^j g_j(\theta)$$

and that a trigonometric series of N terms affords a satisfactory representation of the velocity potential as a function of θ for all x along the body. Then one may write

$$\varphi = \mathcal{U} \sum_{j=1}^{M} \sum_{m=0}^{N-1} A_m^{(j)} x^j H_m^{(j)}(t) \cos m\theta$$

and the boundary condition is

$$\begin{aligned} & F^2 F_x(x,\theta) - \alpha \cos\theta F^2(x,\theta) - \alpha \sin\theta F F_\theta(x,\theta) + \\ & - F^2(x,\theta) \sum_{j=1}^{M} \sum_{m=0}^{N-1} A_m^{(j)} x^{j-1} B H_m^{(j)}(t) \cos m\theta \\ & - F_\theta(x,\theta) \sum_{j=1}^{M} \sum_{m=1}^{N-1} m A_m^{(j)} x^j H_m^{(j)}(t) \sin m\theta \Big]_{t = \frac{B F(x,\theta)}{x}} = 0 . \end{aligned} \tag{8.10}$$

The N constants $A_m^{(1)}$ $(m = 0, 1, \cdots, N-1)$ are very easily found, for

they are simply the coefficients associated with the conical flow over the hypothetical cone tangent to the body at the nose, and may be calculated by the methods of Section VII. This assertion is easily proven, for if the body has a tangent cone at the nose, then

$$F(x,\theta) = x g_1(\theta) + F_1(x,\theta)$$

where

$$\lim_{x\to 0} \frac{F_1(x,\theta)}{x} = 0 .$$

Thus, for $x \ll 1$,

$$F(x,\theta) \doteq x g_1(\theta)$$

and upon making this substitution in (8.10) there appears

$$\begin{aligned} & x^2 g_1^3(\theta) - \alpha \cos\theta\, x^2 g_1^2(\theta) - \alpha \sin\theta\, x^2 g_1(\theta) g_1'(\theta) \\ & - x^2 g_1^2(\theta) \sum_{m=0}^{N-1} A_m^{(1)} B H_m^{(1)\prime}(t) \cos m\theta \\ & - x^2 g_1'(\theta) \sum_{m=1}^{N-1} m A_m^{(1)} H_m^{(1)}(t) \sin m\theta \qquad = 0 . \end{aligned}$$

When x^2 is cancelled from each term of this equation there is obtained precisely the boundary condition on the flow over the tangent cone.

To calculate the remaining $(M-1)N$ constants $A_m^{(j)}$ ($j = 2,3,\ldots,M$; $m = 0,1,\ldots,N-1$), $(M-1)$ stations $x = x_i$ ($i = 1,2,\ldots,M-1$) are selected along the axis (say at equal intervals) and the N values, θ_k, of θ used in the calculation of the $A_m^{(1)}$ are retained. Then the boundary condition is imposed at the $(M-1)N$ points

$$(x_i, t_{ik}, \theta_k) = \left(x_i, \frac{BF(x_i,\theta_k)}{x_i}, \theta_k\right)$$

and the resulting simultaneous linear algebraic equations are solved for the unknowns $A_m^{(j)}$. It is apparent that the labor involved in this calculation increases sharply as either of the indices M, N increases. It is thus particularly desirable that the function $F(x,\theta)$ be simple so that the representation

$$F(x,\theta) = x g_1(\theta) + x^2 g_2(\theta) + \cdots$$

has four or fewer terms.

There is no simple method of determining the particular set of points which leads to the best approximating coefficients $A_m^{(j)}$; the adequacy of the approximation attained through the use of a given set of points can and should be checked by calculating the flow at a few intermediate points on the body surface and comparing the local flow direction with the orientation of the local surface.

Two special cases may be recognized in which the boundary condition assumes a simplified form:

a) All cross section contours of the body are geometrically similar and similarly oriented with respect to the body axis. In this case

$$F(x,\theta) = f(x) g(\theta) \quad .$$

b) The body surface is very nearly a cone. The two cases are now discussed.

a) Cross sections cimilar and similarly oriented.

Unless f(x) is a polynomial of degree less than or equal to three, this case probably should be handled by the superposition procedure for nonconical flows previously described. If, however, f(x) is suitably simple, the present method is feasible. The boundary condition may be

written

$$f(x)f'(x)g^3(\theta) - \alpha\cos\theta\, f(x)g^2(\theta) - \alpha\sin\theta\, f(x)g(\theta)g'(\theta)$$
$$- f(x)g^2(\theta)\sum_{j=1}^{3}\sum_{m=0}^{N-1} A_m^{(j)} x^{j-1} BH_m^{(j)\prime}(t)\cos m\theta$$
$$- g'(\theta)\sum_{j=1}^{3}\sum_{m=1}^{N-1} m A_m^{(j)} x^j H_m^{(j)}(t)\sin m\theta \quad = 0 .$$

The simplification achieved is that $g(\theta)$ and $g'(\theta)$ are calculated once for all in the determination of the coefficients $A_m^{(j)}$ and are used unchanged when the boundary condition is written out at the points (x_i, t_{ik}, θ_k) downstream from the nose.

b) Body surface nearly a cone.

Even if the cross section contours are all similar, this case is usually not handled successfully by the superposition of conical flows because the small longitudinal curvature of the surface requires the summation of a large number of weak conical flows to satisfy the boundary condition. Such a procedure usually entails considerable numerical uncertainty. On the other hand the small meridian curvature justifies ignoring the variation of t_s with x at S = 0 and pursuing one of two alternatives: either approximate the actual body by a median cone of the same cross section contour, if all the contours are similar; or study the flow as a limitedly nonconical problem by a method to be described.

The former option requires no further exposition at this point; the latter permits the boundary condition to be written as an identity in x, and separated into a set of independent equations in θ by equating to zero the coefficient of each power of x. Letting e_j be the equation

obtained by equating to zero the coefficient of x^{j+1} in the boundary condition, it develops that the only unknowns in e_1 are the $A_m^{(1)}$, and these are calculated by assigning N distinct values to θ and solving the resulting simultaneous equations. (Again, there is no method of determining the best N values of θ to use, but of course values of θ for which $F_\theta(x,\theta)$ is discontinuous should be avoided.) Equation e_2 contains the $A_m^{(1)}$ which are now known, and in addition $A_m^{(2)}$ $(m = 0,1,\cdots,N-1)$ which are determined by assigning to θ the same N values used before. Each succeeding equation contains only N new unknowns, so that the calculation of all the $A_m^{(j)}$ is quite simple in comparison with the general noncircular nonconical problem, involving M·N constants, of which number (M-1)·N must be determined by the solution of as many simultaneous equations.

The formalism of the preceding discussion is as follows:

Let

$$F(x,\theta)\ (=r) = x g_1(\theta) + x^2 g_2(\theta) + \cdots$$

then

$$F^2(x,\theta) = x^2 b_2(\theta) + x^3 b_3(\theta) + x^4 b_4(\theta) + \cdots$$

$$F^2 F_x(x,\theta) = x^2 c_2(\theta) + x^3 c_3(\theta) + x^4 c_4(\theta) + \cdots$$

where

$$b_2(\theta) = g_1^2(\theta) + \cdots$$

$$b_3(\theta) = 2 g_1(\theta) g_2(\theta) + \cdots$$

$$b_4(\theta) = g_2^2(\theta) + 2 g_1(\theta) g_3(\theta) + \cdots$$

and

$$c_2(\theta) = g_1^3(\theta) + \cdots$$

$$c_3(\theta) = 4 g_1^2(\theta) g_2(\theta) + \cdots$$

$$c_4(\theta) = 7 g_1(\theta) g_2^2(\theta) + 5 g_1^2(\theta) g_3(\theta) + \cdots .$$

The boundary condition then is

$$x^2 c_2(\theta) + x^3 c_3(\theta) + \cdots - \alpha \cos\theta \{x^2 b_2(\theta) + x^3 b_3(\theta) + \cdots\}$$

$$- \alpha \sin\theta \{x^2 g_1 g_1' + x^3 (g_1' g_2 + g_1 g_2') + x^4 (g_1' g_3 + g_1 g_3' + g_2' g_2 + \cdots)\}$$

$$- \left[x^2 b_2(\theta) + x^3 b_3(\theta) + \cdots\right] \sum_{j=1}^{M} \sum_{m=0}^{N-1} A_m^{(j)} x^{j-1} B H_m^{(j)\prime}(t) \cos m\theta$$

$$- \left[x^2 g_1'(\theta) + x^3 g_2'(\theta) + \cdots\right] \sum_{j=1}^{M} \sum_{m=1}^{N-1} m A_m^{(j)} x^{j-1} H_m^{(j)}(t) \sin m\theta = 0.$$

By comparison of the coefficients of like powers of x there appears

$$e_1: \quad c_2(\theta) - \alpha \cos\theta\, b_2(\theta) - \alpha \sin\theta\, g_1(\theta) g_1'(\theta)$$

$$- b_2(\theta) \sum_{m=0}^{N-1} A_m^{(1)} B H_m^{(1)}(t) \cos m\theta - g_1'(\theta) \sum_{m=1}^{N-1} m A_m^{(1)} H_m^{(1)}(t) \sin m\theta = 0$$

$$e_2: \quad c_3(\theta) - \alpha \cos\theta\, b_3(\theta) - \alpha \sin\theta \left(g_1'(\theta) g_2(\theta) - g_1(\theta) g_2'(\theta)\right)$$

$$- b_3(\theta) \sum_{m=0}^{N-1} A_m^{(1)} B H_m^{(1)\prime}(t) \cos m\theta - g_2'(\theta) \sum_{m=1}^{N-1} m A_m^{(1)} H_m^{(1)}(t) \sin m\theta$$

$$- b_2(\theta) \sum_{m=0}^{N-1} A_m^{(2)} B H_m^{(2)\prime}(t) \cos m\theta - g_1'(\theta) \sum_{m=1}^{N-1} m A_m^{(2)} H_m^{(2)}(t) \sin m\theta = 0$$

and so on.

The value of t in these equations is a function of θ and a median value with respect to x.

Yawed Nonconical Bodies, Lorentz Transformation.

The theory of the representation of yawed nonconical solid bodies by superposition of the yawed conical or nonconical solutions (Section V) is, with the few obvious requisite changes of notation, word for word the same as that for the representation of unyawed nonconical bodies in terms of the unyawed solutions as presented in this section. The writer

has tried a few calculations using the yawed solutions for nonconical bodies and found the algebraic complication to be formidable, owing to the involved structure of the yawed functions, especially the yawed nonconical functions. For this reason the method is neither presented nor recommended. For very slender bodies, the Jones method may be used, and for less slender bodies, the superposition procedures described above, employing the cross flow boundary conditions.

REFERENCES

1. W. D. Hayes: "Linearized Supersonic Flow," Doctoral Dissertation, Calif. Inst. Technol., Pasadena, Calif., June, 1947
2. Th. von Kármán and N. B. Moore: "Resistance of Slender Bodies Moving with Supersonic Velocities, with Special Reference to Projectiles," Transactions Amer. Soc. Mech. Engrs. (1932) 54 303
3. H. S. Tsien: "Supersonic Flow over an Inclined Body of Revolution," Journ. Aero. Sci. (1938) 5 480
4. M. J. Lighthill: "Supersonic Flow Past Bodies of Revolution," British A.R.C. R.and M. 2003, 1945
5. M. J. Lighthill: "Supersonic Flow Past Slender Pointed Bodies of Revolution at Yaw", Quart. Journ. Mech. and Appl. Math. (1948) 1 76
6. R. T. Jones: "Properties of Low-Aspect-Ratio Pointed Wings at Speeds Below and Above the Speed of Sound", NACA TR No. 835, 1946
7. J. R. Spreiter: "Aerodynamic Properties of Slender Wing-Body Combinations at Subsonic, Transonic and Supersonic Speeds," NACA TN No. 1662, 1948
8. H. W. Liepmann and A. E. Puckett: Aerodynamics of a Compressible Fluid, Wiley and Sons, New York, 1947
9. R. Sauer: Theoretische Einführung in die Gasdynamik, Edwards Bros. Inc., Ann Arbor, 1945
10. Z. Kopal: Supersonic Flow of Air Around Cones, Tech. Rep't. No. 1 M.I.T. Dept. Electr. Eng'g., Center of Analysis, Cambridge, 1947
11. M. Van Dyke: Doctoral Dissertation, Calif. Inst. Technol. Pasadena, Calif. 1949 (To be published)

12. A. Busemann: "Drücke auf kegelformige Spitzen bei Bewegung mit Überschallgeschwindigkeit," A. Angen. Math. Mech. (1929) 9 496

13. A. Busemann: "Die Achsensymmetrische kegelige Überschallströmung", Luftf. Forschg. (1942) 19 137

14. G. I. Taylor and J. W. Maccoll: "The Air Pressure on a Cone Moving at High Speeds", Proc. Roy. Soc. A (1937) 139 278

15. W. Hantzsche and H. Wendt: "Mit Überschallgeschwindigkeit angeblasene Kegelspitzen," Jahrb. der. deut. Luftf. Forschg. (1942) p. 180

16. E. Kamke: Differentialgleichungen Lösungsmethoden und Lösungen, Edwards Bros. Inc., Ann Arbor, 1945

17. Th. von Kármán: "The Problem of Resistance in Compressible Fluids," Real. Accad. d'Italia (1936) 14 222 (Fifth Volta Congress).

18. R. T. Jones: "Flow over a Slender Body of Revolution at Supersonic Velocities," NACA TN No. 1081, 1946

19. W. R. Sears: "On Projectiles of Minimum Wave Drag," Quart. Appl. Math. (1947) 4 361

20. M. J. Lighthill: "Supersonic Flow Past Slender Bodies of Revolution the Slope of whose Meridian Section is Discontinuous," Quart. Journ. Mech. and Appl. Math. (1948) 1 90

21. R. Courant and D. Hilbert: Methoden der Mathematischen Physik, Vol. 2, Interscience Inc. New York, 1943

22. Fremberg: Generalized Hyperbolic Potentials, Dissertation, Lund, Sweden, 1947; or B. B. Baker and E. T. Copson: The Mathematical Theory of Huygens' Principle. Oxford, 1939, p. 54 ff.

23. P. A. Lagerstrom: Linearized Supersonic Theory of Conical Wings, Jet Propulsion Lab., Calif. Inst. Tech. Prog.Rept 4-36, 1947

24. O. Laporte and R. C. F. Bartels: "An Investigation of the Exact Solutions of the Linearized Equations for the Flow Past Conical Bodies," Bumblebee Series, Rept. No. 75, 1948.

25. S. H. Maslen: "Method for Calculation of Pressure Distributions on Thin Conical Bodies of Arbitrary Cross Section in a Supersonic Stream". NACA TN No. 1659, 1948

26. H. J. Stewart: "The Lift of a Delta Wing at Supersonic Speeds," Quart. Appl. Math. (1946) 4 246

27. Whittaker and Watson: A Course of Modern Analysis, 6th Ed., Cambridge, 1940

28. Jahnke and Emde: Tables of Functions, Dover, New York, 1945

29. R. T. Jones: "Thin Oblique Airfoils at Supersonic Speeds," NACA TN No. 1107, 1946

30. B. Göthert: "Plane and Three-Dimensional Flow at High Subsonic Speeds," NACA TM No. 1105, 1946

31. B. H. Young: Private communication

32. A. H. Stone: "On Supersonic Flow Past a Slightly Yawing Cone," Journ. Math. and Phys. (1948) 27 67

33. Z. Kopal: Supersonic Flow Around Yawing Cones, Tech. Rept. No. 3, MIT Dept. Elect. Eng'g. Center of Analysis, Cambridge, 1947

34. S. H. Browne, L. Friedman, I. Hodes: "A Wing-Body Problem in Supersonic Conical Flow". Inst. Aeronaut. Sci. Preprint No. 133

35. E. W. Graham: "The Pressure on a Slender Body of Nonuniform Cross Sectional Shape in Axial Supersonic Flow", Douglas Aircraft Inc. Rep't. No. SM-13346; also

E. W. Graham: "The Pressure on Slender Bodies of Uniform Cross Sectional Shape in Axial Supersonic Flow", Douglas Aircraft Inc. Rep't. No. SM-13377

36. C. C. Lin: "Supersonic Lift and Moment Characteristics of a Shell with a Conical Nose," Jet Propulsion Laboratory, Calif. Inst. Technol. Prog. Rep't. 4-14, 1945

37. D. R. Chapman: "Theory of Base Pressure," Doctoral Dissertation, Calif. Inst. Technol., 1948

38. H. Lamb: Hydrodynamics, 6th Ed., Dover, New York, 1945

APPENDIX A

Tabulation of Associated Legendre Functions, Argument Greater than One.

The functions listed stem from the definition

$$Q_j^m(u) = (u^2-1)^{\frac{m}{2}} \left(\frac{d}{du}\right)^m Q_j(u)$$

and the recurrence relation

$$Q_{j+1}^m(u) = u\,Q_j^m(u) + (j+m)\sqrt{u^2-1}\;Q_j^{m-1}(u).$$

It is found

$$Q_1(u) = \frac{1}{2}\,u \log\frac{u+1}{u-1} - 1$$

$$Q_1'(u) = \frac{\sqrt{u^2-1}}{2}\log\frac{u+1}{u-1} - \frac{u}{\sqrt{u^2-1}}$$

$m \geq 2$,

$$Q_1^m(u) = (-1)^m \frac{(m-2)!}{2}\left[(m+u)\left(\frac{u-1}{u+1}\right)^{\frac{m}{2}} + (m-u)\left(\frac{u+1}{u-1}\right)^{\frac{m}{2}}\right]$$

$$Q_2(u) = \frac{1}{4}(3u^2-1)\log\frac{u+1}{u-1} - \frac{3u}{2}$$

$$Q_2'(u) = \frac{3u\sqrt{u^2-1}}{2}\log\frac{u+1}{u-1} - \frac{(3u^2-2)}{\sqrt{u^2-1}}$$

$$Q_2^2(u) = \frac{3}{2}(u^2-1)\log\frac{u+1}{u-1} - \frac{u(3u^2-5)}{u^2-1}$$

$m \geq 3$

$$Q_2^m(u) = (-1)^m \frac{(m-3)!}{2}(u^2-1)^{\frac{m}{2}}\left[\frac{-3u(m+u)-(m^2-1)}{(u+1)^m} + \frac{-3u(m-u)+(m^2-1)}{(u-1)^m}\right]$$

$$Q_3(u) = \frac{1}{4}(5u^3-3u)\log\frac{u+1}{u-1} - \frac{5u^2}{2} + \frac{2}{3}$$

$$Q_3'(u) = \frac{3}{4}(5u^2-1)\sqrt{u^2-1}\log\frac{u+1}{u-1} - \frac{(15u^3-13u)}{2\sqrt{u^2-1}}$$

$$Q_3^2(u) = \frac{15u}{2}(u^2-1)\log\frac{u+1}{u-1} - \frac{(10u^4-15u^2+3)}{u^2-1}$$

$$Q_3^3(u) = \frac{15}{2}(u^2-1)^{3/2}\log\frac{u+1}{u-1} - \frac{(15u^5-40u^3+33u)}{(u^2-1)^{3/2}}$$

$m \geq 4$

$$Q_3^m(u) = (-1)^m \frac{(m-4)!}{2}(u^2-1)^{\frac{m}{2}}\left[\frac{15u^3+15mu^2+(6m^2-9)u+m(m^2-4)}{(u+1)^m} + \frac{-15u^3+15mu^2-(6m^2-9)u+m(m^2-4)}{(u-1)^m}\right]$$

$$Q_4(u) = \frac{1}{16}(35u^4-30u^2+3)\log\frac{u+1}{u-1} - \frac{(35u^3)}{8} + \frac{55u}{24}$$

$$Q_4^1(u) = \frac{5}{4}(7u^3-3u)\sqrt{u^2-1}\log\frac{u+1}{u-1} - \frac{(420u^4-405u^2+64)}{24\sqrt{u^2-1}}$$

$$Q_4^2(u) = \frac{15}{4}(7u^2-1)(u^2-1)\log\frac{u+1}{u-1} - \frac{u(105u^4-190u^2+81)}{2(u^2-1)}$$

$$Q_4^3(u) = \frac{105}{2}u(u^2-1)^{3/2}\log\frac{u+1}{u-1} - \frac{(420u^6-1120u^4+924u^2-192)}{4(u^2-1)^{3/2}}$$

$$Q_4^4(u) = \frac{105}{2}(u^2-1)^2\log\frac{u+1}{u-1} - \frac{u}{(u^2-1)2}(105u^6-385u^4+511u^2-279)$$

$m \geq 5$

$$Q_4^m(u) = (-1)^m\frac{(m-5)!}{2}(u^2-1)^{\frac{m}{2}}\left[\left\{-105u^4-(124m+45)u^3-(57m^2+45m-63)u^2+ -(9m^3+18m^2-37m-27)u-(m^4+3m^3-4m^2-12m)\right\}\frac{1}{(u+1)^m} + \left\{105u^4+(-124m+45)u^3+(57m^2-45m-63)u^2 +(-9m^3+18m^2+37m-27)u+(m^4-3m^3-4m^2+12m)\right\}\frac{1}{(u-1)^m}\right].$$

The essentially polynomial character of the Legendre functions appears if the binomials in any of the explicit general forms above are expanded and the terms properly arranged. For example, for $m \geq 2$

$$Q_1^m(u) = (-1)^m 2(m-2)!(u^2-1)^{-\frac{m}{2}}\sum_{s=1}^{\left[\frac{m}{2}\right]} s\binom{m+1}{2s+1}u^{m-2s}$$

$[\,]$ being the greatest integer symbol.

APPENDIX B

Tables of Conical Harmonic Functions for Wave Equation

1. Description.

The functions tabulated are

$$H_m(t)$$
$$H_m(t) - t H_m'(t)$$
$$H_m'(t)$$

$$(0\,m(1)10\,;\ 0.04t(0.02)0.30t(0.05)1\,;\ 5d)$$

which appear in the series for the perturbation velocity potential and the perturbation components of flows described in conical coordinates, or in a superposition of conical coordinates (Section VIII) according to equations (4.18). The functions are defined as follows:

$$H_m(t) = \begin{cases} \mathcal{H}_m^{(1)}(t) & (m = 0, 1) \\ \dfrac{\mathcal{H}_m^{(1)}(t)}{\mathcal{H}_m^{(1)}(0.20)} & (m \geq 2) \end{cases} \tag{7.6}$$

$$H_m'(t) = \begin{cases} \mathcal{H}_m^{(1)\prime}(t) & (m = 0, 1) \\ \dfrac{\mathcal{H}_m^{(1)\prime}(t)}{\mathcal{H}_m^{(1)}(0.20} & (m \geq 2) \end{cases} \tag{7.7}$$

$$H_m - t H_m'(t) = \begin{cases} \mathcal{H}_m^{(1)}(t) - t\,\mathcal{H}_m^{(1)\prime}(t) & (m = 0, 1) \\ \dfrac{\mathcal{H}_m^{(1)}(t) - t\,\mathcal{H}_m^{(1)\prime}(t)}{\mathcal{H}_m^{(1)}(0.20)} & (m \geq 2)\,. \end{cases}$$

The definitions of the $\mathcal{H}_m^{(1)}(t)$ functions is to be found in Section IV, equations (4.16) and (4.14).

2. Accuracy

All calculations in the construction of the tables were carried out on a Marchant calculator to an accuracy of eight decimals. The powers of T were built up on the machine, and the even powers checked to six figures by logarithms. The tabular entires were rounded to five figures as the last operation. All reasonable precautions have been taken to find and eliminate errors, but a very few may have escaped detection.

3. Use

The use of the tables, based on equations (4.18), in the analysis of conical and nonconical flows over solid bodies is described in Sections VII and VIII.

4. Normalization Factor

The divisor $\mathcal{V}_m^{(1)}(0.20)$ (see equations 7.6 and 7.7) is required in order to infer the numerical values of $\mathcal{V}_m^{(j)}(t)$ $(j>1)$ from the tables by use of relation (4.15). The divisors are listed on the first page of the tables.

5. Interpolation.

The graphs of the absolute value of all the functions presented are very nearly straight lines on semi-log paper. Hence in general logarithmic interpolation is preferable over algebraic interpolation; however the latter is usually more rapid if a table of Lagrangian interpolation coefficients (at least 4-point) is available.

Logarithmic interpolation is now described. If log f(t) is very nearly a linear function of t, then

$$\log f(a+\delta) \doteq \log f(a) + \frac{\delta}{b-a}\left[\log f(b) - \log f(a)\right]$$

$$= \log\left[\left(\frac{f(b)}{f(a)}\right)^{\frac{\delta}{b-a}} f(a)\right]$$

Hence

$$f(a+\delta) = f(a)\left(\frac{f(b)}{f(a)}\right)^{p}$$

where

$$p = \frac{\delta}{b-a}$$

For example, if f(0.10) and f(0.12) are known, and f(0.11) is required, one has $p = \frac{0.01}{0.02} = \frac{1}{2}$ and

$$f(0.11) = \sqrt{f(0.10)\, f(0.12)}$$

Normalization Divisor: $\mathfrak{H}_m^{(1)}(0.20)$

m	Divisor
2	+47.0306
3	-940.620
4	+28030.6
5	$-111182 \cdot 10^{1}$
6	$+550870 \cdot 10^{2}$
7	$-327409 \cdot 10^{4}$
8	$+226985 \cdot 10^{6}$
9	$-179830 \cdot 10^{8}$
10	$+160250 \cdot 10^{10}$

$m = 0$				$m = 1$			
t	$H_0(t)$	$+[H_0 - tH_0']$	$-H_0'(t)$	t	$-H_1(t)$	$-[H_1 - tH_1']$	$+H_1'(t)$
0.04	2.9124	3.9116	24.980	0.04	24.824	49.960	628.41
0.06	2.5075	3.5057	16.637	0.06	16.426	33.273	280.78
0.08	2.2205	3.2173	12.460	0.08	12.203	24.920	158.97
0.10	1.9982	2.9932	9.9499	0.10	9.6506	19.900	102.49
0.12	1.8170	2.8098	8.2731	0.12	7.9359	16.546	71.752
0.14	1.6642	2.6543	7.0725	0.14	6.7009	14.145	53.172
0.16	1.5321	2.5193	6.1695	0.16	5.7664	12.339	41.079
0.18	1.4161	2.3997	5.4648	0.18	5.0329	10.930	32.760
0.20	1.3126	2.2924	4.8990	0.20	4.4405	9.7980	26.787
0.22	1.2174	2.1929	4.4339	0.22	3.9514	8.8677	22.347
0.24	1.1348	2.1055	4.0449	0.24	3.5396	8.0898	18.959
0.26	1.0573	2.0229	3.7139	0.26	3.1879	7.4278	16.307
0.28	0.98591	1.9459	3.4286	0.28	2.8837	6.8571	14.191
0.30	0.91988	1.8738	3.1798	0.30	2.6177	6.3596	12.473
0.35	0.77409	1.7108	2.6764	0.35	2.0776	5.3529	9.3578
0.40	0.65028	1.5668	2.2913	0.40	1.6646	4.5826	7.2950
0.45	0.54366	1.4367	1.9845	0.45	1.3380	3.9690	5.8467
0.50	0.45093	1.3170	1.7321	0.50	1.0736	3.4641	4.7811
0.55	0.36981	1.2050	1.5185	0.55	0.85574	3.0370	3.9659
0.60	0.29861	1.0986	1.3333	0.60	0.67417	2.6667	3.3208
0.65	0.23613	0.99606	1.1691	0.65	0.52169	2.3383	2.7947
0.70	0.18145	0.89559	1.0202	0.70	0.39329	2.0404	2.3530
0.75	0.11482	0.76626	0.86858	0.75	0.29389	1.7372	1.9244
0.80	$0.93147 \cdot 10^{-1}$	0.69315	0.75000	0.80	0.19548	1.5000	1.6307
0.85	$0.58899 \cdot 10^{-1}$	0.58568	0.61975	0.85	0.12192	1.2395	1.3148
0.90	$0.31255 \cdot 10^{-1}$	0.46715	0.48432	0.90	$0.63891 \cdot 10^{-1}$	0.96864	1.0053
0.95	$0.10787 \cdot 10^{-1}$	0.32304	0.32868	0.95	$0.21799 \cdot 10^{-1}$	0.65737	0.66902
1.00	0	0	0	1.00	0	0	0

m = 2				m = 3			
t	$H_2(t)$	H_2-tH_2'	$-H_2'(t)$	t	$H_3(t)$	H_3-tH_3'	$-H_3'(t)$
0.04	26.515	79.671	1328.9	0.04	132.57	530.93	9958.9
0.06	11.749	35.374	393.75	0.06	39.163	157.08	1965.2
0.08	6.5809	19.869	166.10	0.08	16.473	66.147	620.93
0.10	4.1889	12.694	85.048	0.10	8.3778	33.765	253.87
0.12	2.8896	8.7955	49.216	0.12	4.8159	19.475	122.16
0.14	2.1062	6.4449	30.991	0.14	3.0088	12.216	65.764
0.16	1.5978	4.9192	20.759	0.16	1.9972	8.1462	38.431
0.18	1.2492	3.8732	14.578	0.18	1.3880	5.6916	23.909
0.20	1.0000	3.1250	10.625	0.20	1.0000	4.1250	15.625
0.22	0.81216	2.5607	7.9478	0.22	0.73682	3.0600	10.560
0.24	0.67544	2.1502	6.1447	0.24	0.56286	2.3547	7.4658
0.26	0.56639	1.8224	4.8307	0.26	0.43569	1.8375	5.3916
0.28	0.47990	1.5622	3.8652	0.28	0.34278	1.4586	3.9851
0.30	0.41017	1.3522	3.1401	0.30	0.27344	1.1749	3.0049
0.35	0.28536	0.97560	1.9721	0.35	0.16306	0.72054	1.5928
0.40	0.20462	0.73078	1.3154	0.40	0.10231	0.46769	0.91346
0.45	0.14956	0.56262	0.91790	0.45	$0.66473\cdot10^{-1}$	0.31653	0.55568
0.50	0.11048	0.44193	0.66290	0.50	$0.46851\cdot10^{-1}$	0.22362	0.35354
0.55	$0.81892\cdot10^{-1}$	0.35222	0.49151	0.55	$0.29779\cdot10^{-1}$	0.15786	0.23288
0.60	$0.60481\cdot10^{-1}$	0.28350	0.37170	0.60	$0.20160\cdot10^{-1}$	0.11466	0.15750
0.65	$0.44173\cdot10^{-1}$	0.22947	0.28507	0.65	$0.13591\cdot10^{-1}$	$0.84194\cdot10^{-1}$	0.10862
0.70	$0.31609\cdot10^{-1}$	0.18593	0.22046	0.70	$0.90371\cdot10^{-2}$	$0.62161\cdot10^{-1}$	$0.75891\cdot10^{-1}$
0.75	$0.20196\cdot10^{-1}$	0.14077	0.16077	0.75	$0.52111\cdot10^{-2}$	$0.41936\cdot10^{-1}$	$0.48967\cdot10^{-1}$
0.80	$0.14352\cdot10^{-1}$	0.10685	0.11562	0.80	$0.35881\cdot10^{-2}$	$0.33489\cdot10^{-1}$	$0.37376\cdot10^{-1}$
0.85	$0.86043\cdot10^{-2}$	$0.93018\cdot10^{-1}$	$0.99310\cdot10^{-1}$	0.85	$0.20245\cdot10^{-2}$	$0.23910\cdot10^{-1}$	$0.25748\cdot10^{-1}$
0.90	$0.43480\cdot10^{-2}$	$0.68654\cdot10^{-1}$	$0.71451\cdot10^{-1}$	0.90	$0.96623\cdot10^{-3}$	$0.16222\cdot10^{-1}$	$0.16951\cdot10^{-1}$
0.95	$0.14345\cdot10^{-2}$	$0.44140\cdot10^{-1}$	$0.44953\cdot10^{-1}$	0.95	$0.30200\cdot10^{-3}$	$0.12398\cdot10^{-1}$	$0.97816\cdot10^{-2}$
1.00	0	0	0	1.00	0	0	0

	m = 4			m = 5			
t	$H_4(t)$	$H_4 - tH'_4$	$-H'_4(t)$	t	$H_5(t)$	$H_5 - tH'_5$	$-H'_5(t)$
0.04	667.13	3339.2	66802.	0.04	3362.7	20227.	$42160 \cdot 10^{+1}$
0.06	131.34	658.28	8782.3	0.06	441.17	2653.0	36864.
0.08	41.362	207.70	2079.2	0.08	104.14	627.35	6540.1
0.10	16.840	84.766	679.26	0.10	33.893	204.64	1707.5
0.12	8.0610	40.697	271.97	0.12	13.508	81.786	568.98
0.14	4.3130	21.852	125.28	0.14	6.1881	37.592	224.31
0.16	2.5025	12.731	63.930	0.16	3.1377	19.134	99.978
0.18	1.5442	7.8930	35.271	0.18	1.7186	10.526	48.932
0.20	1.0000	5.1384	20.692	0.20	1.0000	6.1554	25.777
0.22	0.66751	3.4503	12.649	0.22	0.60449	3.7417	14.260
0.24	0.47056	2.4360	8.1895	0.24	0.38826	2.4179	8.4568
0.26	0.33359	1.7481	5.4405	0.26	0.25510	1.5994	5.1702
0.28	0.24326	1.2848	3.7199	0.28	0.17233	1.0884	3.2717
0.30	0.18076	0.96295	2.6073	0.30	0.11921	0.75899	2.1326
0.35	$0.91889 \cdot 10^{-1}$	0.50174	1.1710	0.35	$0.51572 \cdot 10^{-1}$	0.33600	0.81265
0.40	$0.50123 \cdot 10^{-1}$	0.28201	0.57971	0.40	$0.24408 \cdot 10^{-1}$	0.16351	0.34776
0.45	$0.28738 \cdot 10^{-1}$	0.16759	0.30856	0.45	$0.12318 \cdot 10^{-1}$	$0.85317 \cdot 10^{-1}$	0.16222
0.50	$0.17054 \cdot 10^{-1}$	0.10381	0.17351	0.50	$0.65055 \cdot 10^{-2}$	$0.45940 \cdot 10^{-1}$	$0.78869 \cdot 10^{-1}$
0.55	$0.10352 \cdot 10^{-1}$	$0.66326 \cdot 10^{-1}$	0.10177	0.55	$0.35441 \cdot 10^{-2}$	$0.26783 \cdot 10^{-1}$	$0.42253 \cdot 10^{-1}$
0.60	$0.63592 \cdot 10^{-2}$	$0.43339 \cdot 10^{-1}$	$0.61633 \cdot 10^{-1}$	0.60	$0.19509 \cdot 10^{-2}$	$0.15606 \cdot 10^{-1}$	$0.22759 \cdot 10^{-1}$
0.65	$0.38408 \cdot 10^{-2}$	$0.28677 \cdot 10^{-1}$	$0.38210 \cdot 10^{-1}$	0.65	$0.10994 \cdot 10^{-2}$	$0.94233 \cdot 10^{-2}$	$0.12806 \cdot 10^{-1}$
0.70	$0.23855 \cdot 10^{-2}$	$0.19228 \cdot 10^{-1}$	$0.24060 \cdot 10^{-1}$	0.70	$0.61092 \cdot 10^{-3}$	$0.57015 \cdot 10^{-2}$	$0.72722 \cdot 10^{-2}$
0.75	$0.12339 \cdot 10^{-2}$	$0.11446 \cdot 10^{-1}$	$0.13616 \cdot 10^{-1}$	0.75	$0.28115 \cdot 10^{-3}$	$0.29854 \cdot 10^{-2}$	$0.36056 \cdot 10^{-2}$
0.80	$0.80671 \cdot 10^{-3}$	$0.85286 \cdot 10^{-2}$	$0.96524 \cdot 10^{-2}$	0.80	$0.17303 \cdot 10^{-3}$	$0.20702 \cdot 10^{-2}$	$0.23715 \cdot 10^{-2}$
0.85	$0.42180 \cdot 10^{-3}$	$0.55191 \cdot 10^{-2}$	$0.59968 \cdot 10^{-2}$	0.85	$0.82959 \cdot 10^{-4}$	$0.12074 \cdot 10^{-2}$	$0.13229 \cdot 10^{-2}$
0.90	$0.18698 \cdot 10^{-3}$	$0.33856 \cdot 10^{-2}$	$0.35540 \cdot 10^{-2}$	0.90	$0.33727 \cdot 10^{-4}$	$0.66314 \cdot 10^{-3}$	$0.69935 \cdot 10^{-3}$
0.95	$0.54378 \cdot 10^{-4}$	$0.18012 \cdot 10^{-2}$	$0.18388 \cdot 10^{-2}$	0.95	$0.89899 \cdot 10^{-5}$	$0.31278 \cdot 10^{-3}$	$0.31978 \cdot 10^{-3}$
1.00	0	0	0	1.00	0	0	0

	m = 6				m = 7		
t	$H_6(t)$	H_6-tH_6'	$-H_6'(t)$	t	$H_7(t)$	$H_7(t)-tH_7'(t)$	$-H_7'(t)$
0.04	16962.	$11885\cdot10^{1}$	25471.10^{2}	0.04	85582.	$68530\cdot10^{1}$	$14993\cdot10^{3}$
0.06	1482.8	10402.	14866.10^{1}	0.06	4985.6	39969.	$58305\cdot10^{1}$
0.08	262.35	1843.6	19765.	0.08	661.12	5308.8	58096.
0.10	68.253	480.66	4124.1	0.10	137.48	1106.3	9688.5
0.12	22.645	159.90	1143.8	0.12	37.972	306.36	2236.6
0.14	8.8815	62.915	385.95	0.14	12.750	103.18	645.95
0.16	3.9351	27.978	150.27	0.16	4.9358	40.089	219.71
0.18	1.9129	13.658	65.249	0.18	2.1293	17.365	84.643
0.20	1.0000	7.1740	30.870	0.20	1.0000	8.1932	35.966
0.22	0.54733	3.9477	15.456	0.22	0.49554	4.0811	16.298
0.24	0.32223	2.3376	8.3973	0.24	0.26738	2.2146	8.1134
0.26	0.19497	1.4235	4.7253	0.26	0.14898	1.2417	4.2026
0.28	0.12199	0.89700	2.7679	0.28	$0.86326\cdot10^{-1}$	0.72442	2.2789
0.30	$0.78547\cdot10^{-1}$	0.58201	1.6782	0.30	$0.51729\cdot10^{-1}$	0.43732	1.2853
0.35	$0.27992\cdot10^{-1}$	0.21800	0.54287	0.35	$0.16180\cdot10^{-1}$	0.13975	0.35306
0.40	$0.11857\cdot10^{-1}$	$0.92337\cdot10^{-1}$	0.20095	0.40	$0.57526\cdot10^{-2}$	$0.50985\cdot10^{-1}$	0.11308
0.45	$0.52616\cdot10^{-2}$	$0.42256\cdot10^{-1}$	$0.82209\cdot10^{-1}$	0.45	$0.22436\cdot10^{-2}$	$0.20508\cdot10^{-1}$	$0.40588\cdot10^{-1}$
0.50	$0.24698\cdot10^{-2}$	$0.20601\cdot10^{-1}$	$0.36262\cdot10^{-1}$	0.50	$0.93545\cdot10^{-3}$	$0.88700\cdot10^{-2}$	$0.15869\cdot10^{-1}$
0.55	$0.12058\cdot10^{-2}$	$0.10522\cdot10^{-1}$	$0.16938\cdot10^{-1}$	0.55	$0.40893\cdot10^{-3}$	$0.40504\cdot10^{-2}$	$0.66208\cdot10^{-2}$
0.60	$0.60346\cdot10^{-3}$	$0.55581\cdot10^{-2}$	$0.82578\cdot10^{-2}$	0.60	$0.18436\cdot10^{-3}$	$0.19238\cdot10^{-2}$	$0.28990\cdot10^{-2}$
0.65	$0.30552\cdot10^{-3}$	$0.30040\cdot10^{-2}$	$0.41515\cdot10^{-2}$	0.65	$0.84447\cdot10^{-4}$	$0.93842\cdot10^{-3}$	$0.13138\cdot10^{-2}$
0.70	$0.15430\cdot10^{-3}$	$0.16440\cdot10^{-2}$	$0.21281\cdot10^{-2}$	0.70	$0.38695\cdot10^{-4}$	$0.46446\cdot10^{-3}$	$0.60823\cdot10^{-3}$
0.75	$0.62888\cdot10^{-4}$	$0.75656\cdot10^{-3}$	$0.92490\cdot10^{-3}$	0.75	$0.13932\cdot10^{-4}$	$0.18783\cdot10^{-3}$	$0.23186\cdot10^{-3}$
0.80	$0.36264\cdot10^{-4}$	$0.48784\cdot10^{-3}$	$0.56447\cdot10^{-3}$	0.80	$0.75070\cdot10^{-5}$	$0.11259\cdot10^{-3}$	$0.13135\cdot10^{-3}$
0.85	$0.15835\cdot10^{-4}$	$0.27627\cdot10^{-3}$	$0.28236\cdot10^{-3}$	0.85	$0.29725\cdot10^{-5}$	$0.53051\cdot10^{-4}$	$0.58916\cdot10^{-4}$
0.90	$0.58509\cdot10^{-5}$	$0.12528\cdot10^{-3}$	$0.13270\cdot10^{-3}$	0.90	$0.99188\cdot10^{-6}$	$0.23111\cdot10^{-4}$	$0.24577\cdot10^{-4}$
0.95	$0.14119\cdot10^{-5}$	$0.51864\cdot10^{-4}$	$0.53107\cdot10^{-4}$	0.95	$0.21458\cdot10^{-6}$	$0.83486\cdot10^{-5}$	$0.85621\cdot10^{-5}$
1.00	0	0	0	1.00	0	0	0

m = 8				m = 9			
t	$H_8(t)$	H_8-tH_8'	$-H_8'(t)$	t	$H_9(t)$	H_9-tH_9'	$-H_9'(t)$
0.04	$43189\cdot10^{1}$	$38906\cdot10^{2}$	$86468\cdot10^{3}$	0.04	$21797\cdot10^{2}$	$21817\cdot10^{3}$	$49093\cdot10^{4}$
0.06	16765.	$15120\cdot10^{1}$	$22406\cdot10^{2}$	0.06	56382.	$56497\cdot10^{1}$	$84764\cdot10^{2}$
0.08	1666.3	15052.	$16732\cdot10^{1}$	0.08	4199.9	47196.	$53745\cdot10^{1}$
0.10	276.97	2507.1	22301.	0.10	558.00	5611.6	50536.
0.12	63.682	577.91	4285.2	0.12	106.80	1076.8	8083.0
0.14	18.304	166.61	1059.3	0.14	26.279	265.74	1710.4
0.16	6.1914	56.555	314.77	0.16	7.7663	79.515	443.99
0.18	2.3702	21.738	107.60	0.18	2.6384	26.877	134.66
0.20	1.0000	9.2128	41.064	0.20	1.0000	10.232	46.160
0.22	0.44863	4.1543	16.844	0.22	0.40595	4.1748	17.131
0.24	0.22186	2.0657	7.6827	0.24	0.18406	1.9032	7.1629
0.26	0.11382	1.0663	3.6634	0.26	$0.86946\cdot10^{-1}$	0.90446	3.1443
0.28	$0.61076\cdot10^{-1}$	0.57602	1.8391	0.28	$0.43203\cdot10^{-1}$	0.45240	1.4614
0.30	$0.34058\cdot10^{-1}$	0.32355	0.96497	0.30	$0.22418\cdot10^{-1}$	0.23644	0.71339
0.35	$0.90549\cdot10^{-2}$	$0.87843\cdot10^{-1}$	0.22511	0.35	$0.50658\cdot10^{-2}$	$0.54538\cdot10^{-1}$	0.14135
0.40	$0.27891\cdot10^{-2}$	$0.27749\cdot10^{-1}$	$0.62400\cdot10^{-1}$	0.40	$0.13516\cdot10^{-2}$	$0.14917\cdot10^{-1}$	$0.33914\cdot10^{-1}$
0.45	$0.95576\cdot10^{-3}$	$0.98001\cdot10^{-2}$	$0.19654\cdot10^{-1}$	0.45	$0.40687\cdot10^{-3}$	$0.46254\cdot10^{-2}$	$0.93745\cdot10^{-2}$
0.50	$0.35383\cdot10^{-3}$	$0.37602\cdot10^{-2}$	$0.68128\cdot10^{-2}$	0.50	$0.13372\cdot10^{-3}$	$0.15745\cdot10^{-2}$	$0.28816\cdot10^{-2}$
0.55	$0.13844\cdot10^{-3}$	$0.15352\cdot10^{-2}$	$0.25395\cdot10^{-2}$	0.55	$0.46813\cdot10^{-4}$	$0.57471\cdot10^{-3}$	$0.95981\cdot10^{-3}$
0.60	$0.56191\cdot10^{-4}$	$0.65557\cdot10^{-3}$	$0.99896\cdot10^{-3}$	0.60	$0.17101\cdot10^{-4}$	$0.22066\cdot10^{-3}$	$0.33926\cdot10^{-3}$
0.65	$0.23270\cdot10^{-4}$	$0.28861\cdot10^{-3}$	$0.40822\cdot10^{-3}$	0.65	$0.63996\cdot10^{-5}$	$0.87676\cdot10^{-4}$	$0.12504\cdot10^{-3}$
0.70	$0.96652\cdot10^{-5}$	$0.12919\cdot10^{-3}$	$0.17075\cdot10^{-3}$	0.70	$0.24081\cdot10^{-5}$	$0.35496\cdot10^{-4}$	$0.47268\cdot10^{-4}$
0.75	$0.30690\cdot10^{-5}$	$0.45909\cdot10^{-4}$	$0.57120\cdot10^{-4}$	0.75	$0.67371\cdot10^{-6}$	$0.11083\cdot10^{-4}$	$0.13879\cdot10^{-4}$
0.80	$0.15429\cdot10^{-5}$	$0.25579\cdot10^{-4}$	$0.30045\cdot10^{-4}$	0.80	$0.31569\cdot10^{-6}$	$0.57398\cdot10^{-5}$	$0.67801\cdot10^{-5}$
0.85	$0.55248\cdot10^{-6}$	$0.10826\cdot10^{-4}$	$0.12087\cdot10^{-4}$	0.85	$0.10204\cdot10^{-6}$	$0.21819\cdot10^{-5}$	$0.24469\cdot10^{-5}$
0.90	$0.16576\cdot10^{-6}$	$0.41921\cdot10^{-5}$	$0.44737\cdot10^{-5}$	0.90	$0.27443\cdot10^{-7}$	$0.75065\cdot10^{-6}$	$0.80356\cdot10^{-6}$
0.95	$0.31908\cdot10^{-7}$	$0.13168\cdot10^{-5}$	$0.13525\cdot10^{-5}$	0.95	$0.46733\cdot10^{-8}$	$0.20463\cdot10^{-6}$	$0.21048\cdot10^{-6}$
1.00	0	0	0	1.00	0	0	0

m = 10

t	$H_{10}(t)$	$H_{10}-tH'_{10}$	$-H'_{10}(t)$
0.04	11003.10^{3}	$12114\cdot10^{4}$	$27534\cdot10^{5}$
0.06	$18965\cdot10^{1}$	$20903\cdot10^{2}$	$31677\cdot10^{3}$
0.08	10588.	$11688\cdot10^{1}$	$13287\cdot10^{2}$
0.10	1124.4	12437.	$11313\cdot10^{1}$
0.12	179.14	1986.6	15062.
0.14	37.734	419.67	2728.1
0.16	9.7433	108.73	618.68
0.18	2.9372	32.907	166.50
0.20	1.0000	11.253	51.263
0.22	0.36769	4.1581	17.229
0.24	0.15271	1.7362	6.5979
0.26	$0.66420\cdot10^{-1}$	0.53445	1.8001
0.28	$0.30561\cdot10^{-1}$	0.35181	1.1473
0.30	$0.14757\cdot10^{-1}$	0.17108	0.52107
0.35	$0.28338\cdot10^{-2}$	$0.33528\cdot10^{-1}$	$0.87698\cdot10^{-1}$
0.40	$0.65488\cdot10^{-3}$	$0.79401\cdot10^{-2}$	$0.18213\cdot10^{-1}$
0.45	$0.17316\cdot10^{-3}$	$0.21617\cdot10^{-2}$	$0.44190\cdot10^{-2}$
0.50	$0.50512\cdot10^{-4}$	$0.65281\cdot10^{-3}$	$0.12046\cdot10^{-2}$
0.55	$0.15820\cdot10^{-4}$	$0.21304\cdot10^{-3}$	$0.35858\cdot10^{-3}$
0.60	$0.52000\cdot10^{-5}$	$0.73640\cdot10^{-4}$	$0.11390\cdot10^{-3}$
0.65	$0.17580\cdot10^{-5}$	$0.26373\cdot10^{-4}$	$0.37869\cdot10^{-4}$
0.70	$0.59904\cdot10^{-6}$	$0.96563\cdot10^{-5}$	$0.12939\cdot10^{-4}$
0.75	$0.14757\cdot10^{-6}$	$0.26493\cdot10^{-5}$	$0.33357\cdot10^{-5}$
0.80	$0.64411\cdot10^{-7}$	$0.12754\cdot10^{-5}$	$0.15137\cdot10^{-5}$
0.85	$0.18771\cdot10^{-7}$	$0.43542\cdot10^{-6}$	$0.49017\cdot10^{-6}$
0.90	$0.45158\cdot10^{-8}$	$0.13307\cdot10^{-6}$	$0.14284\cdot10^{-6}$
0.95	$0.67731\cdot10^{-9}$	$0.30837\cdot10^{-6}$	$0.32389\cdot10^{-6}$
1.00	0	0	0

APPENDIX C.

Two Dimensional Cross Flow; Triangle and Square

The velocity distribution at the surface, and in the vicinity of the surface, of two cylinders of polygonal cross section are here tabulated. These data are useful in the consideration of the upwash field surrounding pointed slender solid bodies at small angle of attack in a rectilinear stream of either subsonic or supersonic speed, and are mentioned in this respect in Section VII. The corresponding solutions for bodies of circular, oval, elliptical and a few other families of contours are well known (7, 38).

The loci of the net points at which the velocities are tabulated are indicated on the accompanying figures. If one desires the contour in an orientation with respect to the free stream different from that presented, the solution can easily be obtained by a superposition of a rotation of the present solution upon itself in the obvious way. Thus supposing known the function

$$u^{\xi} - i u^{\eta} = \mathcal{U} f(\xi + i\eta)$$

which is the complex velocity distribution about an equilateral triangular cylinder when the free stream is normal to a side, let be required the complex velocity distribution when the free stream is parallel to a side. The solution is simply

$$u^{\xi} - i u^{\eta} = \frac{2}{\sqrt{3}} \mathcal{U} f(\xi + i\eta) + \frac{\mathcal{U}}{\sqrt{3}} f\{(\xi + i\eta) e^{-i\frac{2\pi}{3}}\}.$$

A. Triangular Cylinder

The triangular contour has been mapped conformally onto a circle by the appropriate Schwarz-Christoffel integral transformation, which entailed numerical integration. The velocity field about the circle was then transformed back to the triangle. Letting $\zeta = \xi + i\eta$ be the complex variable in the plane of the equilateral triangle in the orientation sketched, and $S = e^{(\rho + i\theta)}$ be the complex variable in the plane of the circle, the coordinate and velocity functions are found to be

$$\xi - \xi_0 = -\frac{2}{3} 2^{\frac{2}{3}} k \int_0^{\frac{3\theta}{2}} \left(\sinh^2 \frac{3\rho}{2} + \sin^2 \beta \right)^{\frac{1}{3}} \sin \gamma(\rho, \beta)\, d\beta$$

$$\eta - \eta_0 = \frac{2}{3} 2^{\frac{2}{3}} k \int_0^{\frac{3\theta}{2}} \left(\sinh^2 \frac{3\rho}{2} + \sin^2 \beta \right)^{\frac{1}{3}} \cos \gamma(\rho, \beta)\, d\beta$$

$$\frac{u^{\xi}}{u_0^{\xi}} = \frac{2^{1/3} \left[\sinh\rho \cos\theta \cos\gamma(\rho,\beta) + \cosh\rho \sin\theta \sin\gamma(\rho,\beta) \right]}{\left(\sinh^2 \frac{3\rho}{2} + \sin^2 \frac{3\theta}{2} \right)^{1/3}}$$

$$\frac{u^{\eta}}{u_0^{\xi}} = \frac{2^{1/3} \left[\sinh\rho \cos\theta \sin\gamma(\rho,\beta) - \cosh\rho \sin\theta \cos\gamma(\rho,\beta) \right]}{\left(\sinh^2 \frac{3\rho}{2} + \sin^2 \frac{3\theta}{2} \right)^{1/3}}$$

where

$$\gamma(\rho, \beta) = \frac{2}{3} \arctan \left(\coth \frac{3\rho}{2} \tan \beta \right)$$

and k is a scale factor selected to make convenient the size of the triangle transformed from a unit circle.

$$k = \frac{3\sqrt{3}}{2^{8/3} \int_0^{\pi/2} (\sin\beta)^{3/3}\, d\beta} \doteq 0.73098.$$

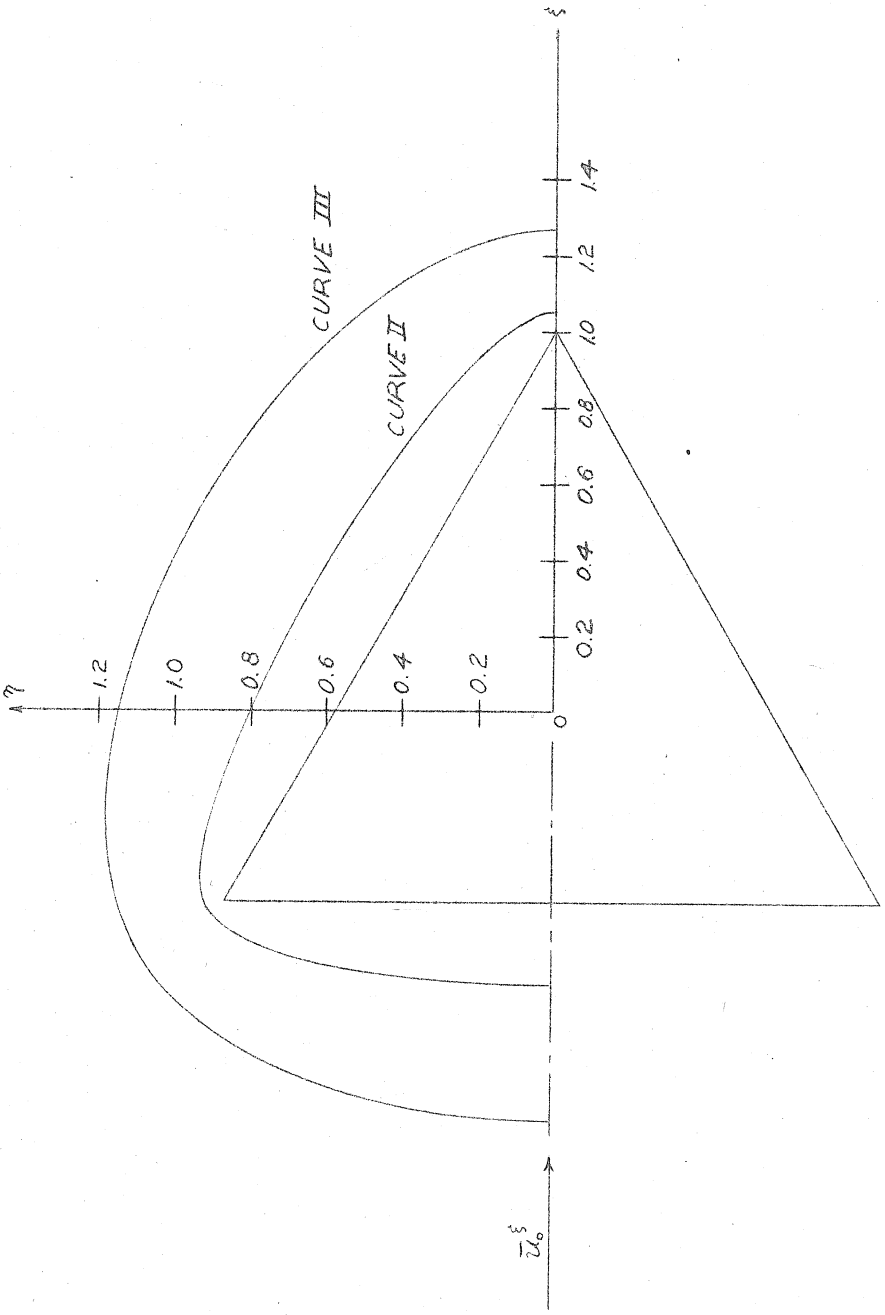
ξ
1.4
1.2
1.0
0.8
0.6
0.4
0.2
0
η
1.2
1.0
0.8
0.6
0.4
0.2
CURVE III
CURVE II
$\bar{u}_0^{\xi}$

Surface

$\beta = \frac{3\theta}{2}$	ξ	η	$\frac{u^\xi}{u_0^\xi}$	$\frac{u^\eta}{u_0^\xi}$
0	1.00000	0.00000	0	0
5	0.99360	0.00524	0.32271	-0.18632
10	0.97861	0.01235	0.40697	-0.23496
20	0.93136	0.03963	0.51452	-0.29706
30	0.86565	0.07757	0.59239	-0.34202
40	0.78504	0.12411	0.65747	-0.37959
50	0.69234	0.17763	0.71618	-0.41349
60	0.59008	0.23667	0.77195	-0.44568
70	0.48068	0.29983	0.82725	-0.47761
80	0.36653	0.36574	0.88419	-0.51049
90	0.25000	0.43302	0.94495	-0.54556
100	0.13347	0.50029	1.01217	-0.58438
110	0.01931	0.56620	1.08953	-0.62904
120	-0.09008	0.62936	1.18269	-0.68283
130	-0.19235	0.68841	1.30110	-0.75119
140	-0.28505	0.74193	1.46248	-0.84436
150	-0.36565	0.78846	1.70574	-0.98481
160	-0.43136	0.82640	2.13729	-1.23397
170	-0.47862	0.85368	3.21892	-1.85844
175	-0.49360	0.86310	4.96012	-2.86372
180	-0.50000	0.86603	∞	∞
185	-0.50000	0.85786	0	5.35136
190	-0.50000	0.84133	0	3.24693
200	-0.50000	0.78677	0	1.87382
210	-0.50000	0.71090	0	1.28559
220	-0.50000	0.61782	0	0.92954
230	-0.50000	0.51078	0	0.67541
240	-0.50000	0.39270	0	0.47428
250	-0.50000	0.26637	0	0.30286
260	-0.50000	0.13456	0	0.14776
265	-0.50000	0.06745	0	0.07344
270	-0.50000	0.00000	0	0

Curve II

$\beta = \frac{3\theta}{2}$	ξ	η	$\frac{u^{\xi}}{u_0^{\xi}}$	$\frac{u^{\eta}}{u_0^{\xi}}$
0	1.05365	0.00000	0.54382	0.00000
10	1.04133	0.05802	0.56627	-0.10647
20	1.00603	0.11925	0.61387	-0.18653
30	0.95093	0.18470	0.66763	-0.24492
40	0.87903	0.25396	0.71823	-0.29046
50	0.79300	0.32609	0.76991	-0.32807
60	0.69530	0.39988	0.85477	-0.38480
70	0.58829	0.47408	0.87180	-0.38923
80	0.47438	0.54729	0.93167	-0.41756
90	0.35601	0.61812	0.99367	-0.44357
100	0.23549	0.68521	1.06348	-0.47802
110	0.11513	0.74728	1.14125	-0.49032
120	-0.00264	0.80297	1.24381	-0.51112
130	-0.11539	0.85068	1.36185	-0.52507
140	-0.22087	0.88912	1.53535	-0.52342
150	-0.31686	0.91675	1.76773	-0.43958
160	-0.40104	0.93174	2.09835	-0.32949
170	-0.47171	0.93170	2.48227	+0.14091
180	-0.52813	0.91336	2.39780	+1.07037
190	-0.57221	0.87368	1.55413	1.53559
200	-0.60759	0.81249	0.90922	1.35706
210	-0.63671	0.73205	0.60247	1.12637
220	-0.66074	0.63515	0.42167	0.82427
230	-0.68018	0.52457	0.33057	0.61740
240	-0.69524	0.40305	0.27751	0.44085
250	-0.70599	0.27325	0.24591	0.28313
260	-0.71244	0.13796	0.23271	0.21189
270	-0.71460	0.00000	0.22536	0.00000

Curve III

$\beta = \frac{3\theta}{2}$	ξ	η	$\frac{u^{\xi}}{u_0^{\xi}}$	$\frac{u^{\eta}}{u_0^{\xi}}$
0	1.26573	0.00000	0.73438	0.00000
10	1.25495	0.11288	0.74043	-0.05376
20	1.22303	0.22549	0.75745	-0.10366
30	1.17094	0.33729	0.78294	-0.14775
40	1.10022	0.44751	0.81450	-0.18552
50	1.01312	0.55456	0.85053	-0.21818
60	0.91086	0.65816	0.89029	-0.24388
70	0.79601	0.75643	0.93377	-0.26511
80	0.67085	0.84793	0.98207	-0.28177
90	0.53772	0.93121	1.03334	-0.29244
100	0.39904	1.00485	1.09190	-0.29705
110	0.25723	1.06750	1.15511	-0.29257
120	0.11469	1.11782	1.22227	-0.27623
130	-0.02616	1.15458	1.30530	-0.24264
140	-0.16242	1.17649	1.38850	-0.18340
150	-0.29323	1.18262	1.46756	-0.08835
160	-0.41611	1.17184	1.52294	+0.05083
170	-0.52958	1.14318	1.52310	+0.22801
180	-0.63273	1.09607	1.44055	0.41534
190	-0.72510	1.03029	1.28266	0.53691
200	-0.80666	0.94635	1.09445	0.58567
210	-0.87744	0.84533	0.92079	0.56321
220	-0.93753	0.72898	0.78200	0.49606
230	-0.98669	0.60002	0.67957	0.40667
240	-1.02528	0.45943	0.60809	0.30764
250	-1.05296	0.30985	0.56145	0.20541
260	-1.06962	0.15538	0.53570	0.10276
270	-1.07518	0.00000	0.52679	0.00000

B. Square Cylinder

The square contour has been oriented with a diagonal parallel to the free stream, as shown on the accompanying figure. In this figure, the loci of the tabulated net points are also streamlines. The flow field has been studied by mapping the part of the contour and its exterior on one side of the diagonal onto the boundary and points of a half plane. Inasmuch as the flow over the square is symmetrical with respect to both diagonals, only the flow description in one quadrant is required.

Letting $\zeta = \xi + i\eta$ be the complex variable in the plane of the square, in the orientation sketched, and $S = \sigma + i\tau$ be the complex variable in the mapped half plane where the mapped flow is simply rectilinear, the coordinate and velocity functions are found to be

$$\xi = k \int_0^{\sigma} \frac{(\sigma^2+\tau^2)^{1/4} \cos\beta(\sigma,\tau)\, d\sigma}{\left[\sigma^4 + 2\sigma^2(\tau^2-1) + (\tau^2+1)^2\right]^{1/8}}$$

$$\eta - \eta_0 = k \int_0^{\sigma} \frac{(\sigma^2+\tau^2)^{1/4} \sin\beta(\sigma,\tau)\, d\sigma}{\left[\sigma^4 + 2\sigma^2(\tau^2-1) + (\tau^2+1)^2\right]^{1/8}}$$

$$\frac{u^{\xi}}{u_0^{\xi}} = \frac{\left[\sigma^4 + 2\sigma^2(\tau^2-1) + (\tau^2+1)^2\right]^{1/8} \cos\beta(\sigma,\tau)}{(\sigma^2+\tau^2)^{1/4}}$$

$$\frac{u^{\eta}}{u_0^{\xi}} = \frac{\left[\sigma^4 + 2\sigma^2(\tau^2-1) + (\tau^2+1)^2\right]^{1/8} \sin\beta(\sigma,\tau)}{(\sigma^2+\tau^2)^{1/4}}$$

where

$$\beta(\sigma,\tau) = \tfrac{1}{2} \arctan\frac{\tau}{\sigma} - \tfrac{1}{4} \arctan\frac{2\sigma\tau}{\sigma^2-\tau^2-1}$$

and k is a scale factor chosen to give the mapped square a diagonal length of 2. It is found

$$k = \frac{2\sqrt{2}\,\Gamma(\frac{3}{2})}{\Gamma^2(\frac{3}{4})} \doteq 1.66910 .$$

The appearance of the gamma functions in k is due to the fact that the Schwarz-Christoffel mapping function for the present problem, namely

$$\zeta - \zeta_0 = H\int_{S_0}^{S} \frac{S^{1/2}\,dS}{(S^2-1)^{1/4}} \qquad (H = \text{const.})$$

is formally similar to the incomplete beta function when the transformation

$$S^2 = T$$

is made. Indeed

$$\zeta - \zeta_0 = \frac{H}{(i)^{1/4}}\int_{S_0^2}^{S^2} T^{-1/4}(1-T)^{-1/4}\,dT$$

$$= \frac{H}{(i)^{1/4}}\left[B_{S^2}(\tfrac{3}{4},\tfrac{3}{4}) - B_{S_0^2}(\tfrac{3}{4},\tfrac{3}{4})\right]$$

where the incomplete beta function has the definition

$$B_x(p,q) = \int_0^x t^{p-1}(1-t)^{q-1}\,dt .$$

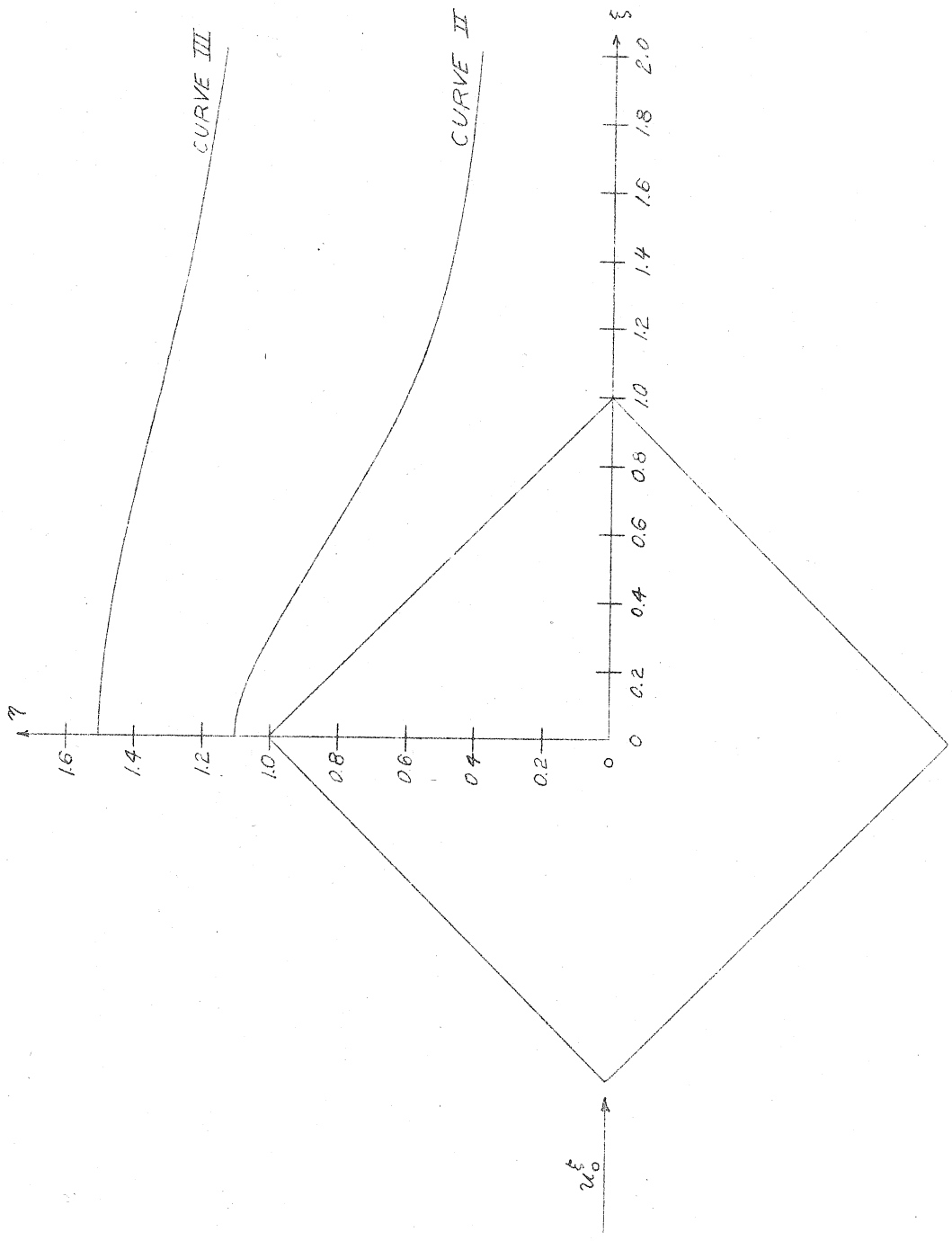
CURVE III
CURVE II
η
ξ
1.6
1.4
1.2
1.0
0.8
0.6
0.4
0.2
0
0.2
0.4
0.6
0.8
1.0
1.2
1.4
1.6
1.8
2.0
u_0^ξ

Surface

	ξ	η	$\frac{u^{\xi}}{u_{\infty}^{\xi}}$	$\frac{u^{\eta}}{u_{\infty}^{\xi}}$
0	0.00000	1.00000	∞	∞
.10	0.02386	0.97614	2.23048	-2.23048
.20	0.06969	0.93031	1.56509	-1.56509
.30	0.12965	0.87035	1.26091	-1.26091
.40	0.20185	0.79815	1.07033	-1.07033
.50	0.28573	0.71427	0.93061	-0.93061
.60	0.38165	0.61835	0.81650	-0.81650
.70	0.49105	0.50895	0.71421	-0.71421
.80	0.61715	0.38285	0.61238	-0.61238
.90	0.76821	0.23179	0.49210	-0.49210
1.00	1.00000	0.00000	0.00000	0.00000

Curve II

1000α	ξ	η	$\frac{u}{u_0}^{\xi}$	$\frac{u}{u_0}^{\eta}$
0	0.00000	1.09908	2.25810	0.00000
10	0.07418	1.09040	2.07786	-0.46928
20	0.15355	1.06537	1.75256	-0.68529
30	0.24026	1.02664	1.47619	-0.73136
40	0.33578	0.97603	1.27013	-0.70814
50	0.44140	0.91516	1.11502	-0.65806
60	0.55865	0.84522	0.99403	-0.59545
70	0.68867	0.76745	0.89704	-0.52382
80	0.83670	0.68399	0.82015	-0.44192
90	1.00580	0.59964	0.76690	-0.34755
100	1.19791	0.52440	0.74872	-0.24722
110	1.40361	0.46899	0.76646	-0.16385
120	1.61099	0.43326	0.79858	-0.10964
130	1.81358	0.41035	0.82930	-0.07681
140	2.01068	0.39494	0.85527	-0.05605
150	2.20312	0.38403	0.87530	-0.04276
160	2.39183	0.37594	0.89189	-0.03350
170	2.57754	0.36976	0.90524	-0.02673
180	2.76078	0.36491	0.91815	-0.02180
190	2.94205	0.36094	0.92550	-0.01800
200	3.12176	0.35775	0.93325	-0.01508

Curve III

100σ	ξ	η	$\frac{u}{u_0}^{\xi}$	$\frac{u}{u_0}^{\eta}$
0	0.00000	1.50000	1.39416	0
10	0.12009	1.49634	1.38090	-0.08352
20	0.24159	1.48552	1.34344	-0.15642
30	0.36581	1.46797	1.29141	-0.21208
40	0.49394	1.44441	1.23084	-0.24807
50	0.62703	1.41573	1.16943	-0.26578
60	0.76592	1.38305	1.11188	-0.26820
70	0.91122	1.34768	1.06107	-0.25867
80	1.06323	1.31110	1.01864	-0.24017
90	1.22185	1.27484	0.98531	-0.21667
100	1.38647	1.24041	0.96106	-0.19017
110	1.55607	1.20895	0.94506	-0.16351
120	1.72936	1.18115	0.93590	-0.13858
130	1.90507	1.15720	0.93186	-0.11651
140	2.08215	1.13690	0.93135	-0.09737
150	2.25978	1.11984	0.93295	-0.08218
160	2.43756	1.10552	0.93584	-0.06907
170	2.61488	1.09348	0.93934	-0.05848
180	2.79183	1.08333	0.94308	-0.04983
190	2.96823	1.07471	0.94680	-0.04270
200	3.14406	1.06735	0.95040	-0.03682

APPENDIX D

Detailed Solution of Typical Problem by Superposition of Conical Flows; Unyawed solid body of square cross section with a parabolic meridian contour.

The methods of Sections VII and VIII are illustrated in this Appendix.

Let $M = \sqrt{2}$, so that $B = 1$, and consider the body whose surface in the quadrant $0 \le \theta \le \frac{\pi}{2}$ is given by

$$r = \frac{f(x)}{h(\theta)} = \frac{2.5\left[1-(1-\frac{x}{5})^2\right]}{\frac{10}{3}(\cos\theta+\sin\theta)} \qquad (0 \le x \le 5)$$

$$= \frac{2.5}{\frac{10}{3}(\cos\theta+\sin\theta)} \qquad (x > 5)$$

and whose surface in the remaining quadrands is the image of this surface in the coordinate planes. The body nose has a square cross section and a parabolic meridian contour, and is followed by a cylinder of the same cross section. The solution is desired from the nose to the beginning of the cylindrical portion.

In accordance with the schedule and notation presented in Section VIII, the first step is the selection of the points at which the boundary condition is to be fulfilled. The midpoint, $\theta = \frac{\pi}{4} = \theta_0$, of a side is taken as the reference contour; this contour is plotted on a large figure, as sketched in Section VIII. The curve is

$$r\Big|_{\theta_0} = 0.53033\left[1-(1-\tfrac{x}{5})^2\right] \qquad (0 \le x \le 5)$$

$$= 0.53033 \qquad (x > 5).$$

The points ξ_i at which the conical solutions are to be added are taken as

$$\xi_i = i \qquad (i = 0, 1, 2, 3, 4).$$

The Mach lines from the points ξ_i to the contour are drawn, and points P_i designated as in the sketch. The coordinates of P_i in the j conical coordinate system $(x_{ji}, r_{ji}, \theta_0)$, written (j,i), are then found to be

$$(0,1) = (1.235,\ 0.185,\ \tfrac{\pi}{4})$$
$$(0,2) = (2.395,\ 0.162,\ \tfrac{\pi}{4})$$
$$(0,3) = (3.480,\ 0.139,\ \tfrac{\pi}{4})$$
$$(0,4) = (4.525,\ 0.115,\ \tfrac{\pi}{4})$$
$$(0,5) = (5.535,\ 0.090,\ \tfrac{\pi}{4})$$
$$(1,2) = (1.375,\ 0.275,\ \tfrac{\pi}{4})$$
$$(1,3) = (2.480,\ 0.195,\ \tfrac{\pi}{4})$$
$$(1,4) = (3.525,\ 0.145,\ \tfrac{\pi}{4})$$
$$(1,5) = (4.535,\ 0.110,\ \tfrac{\pi}{4})$$
$$(2,3) = (1.480,\ 0.330,\ \tfrac{\pi}{4})$$
$$(2,4) = (2.525,\ 0.207,\ \tfrac{\pi}{4})$$
$$(2,5) = (3.535,\ 0.148,\ \tfrac{\pi}{4})$$
$$(3,4) = (1.525,\ 0.344,\ \tfrac{\pi}{4})$$
$$(3,5) = (2.535,\ 0.208,\ \tfrac{\pi}{4})$$
$$(4,5) = (1.535,\ 0.345,\ \tfrac{\pi}{4})$$

Next the conical flow about the square cone tangent to the body at the apex is calculated. As shown in Section VIII, the boundary condition can be fulfilled on 24 rays in the cone surface if the velocity potential

is written

$$\varphi = Ux\left[A_0 H_0(t) + A_4 H_4(t)\cos 4\theta + A_8 H_8(t)\cos 8\theta\right]$$

and the boundary condition

$$-1 + h(\theta) B \sum_m H_m'(t) A_m \cos m\theta$$

$$+ h(\theta) h'(\theta) \sum_m H_m(t) (-m A_m) \sin m\theta \Big]_{t=\frac{B}{h(\theta)}} = 0$$

is fulfilled at the points 1, 2, 3 indicated on the following sketch.

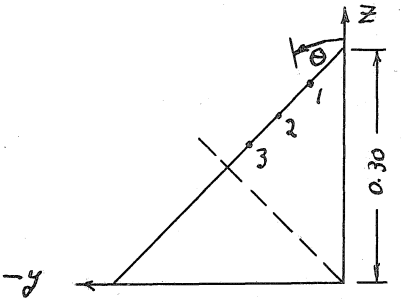

Select, for convenience $\theta_1 = 7^0.5$, $\theta_2 = 22^0.5$, $\theta_3 = 37^0.5$. Now

$$h(\theta) = \frac{10}{3}(\cos\theta + \sin\theta)$$

$$h'(\theta) = \frac{10}{3}(\cos\theta - \sin\theta)$$

$$t_s = \frac{B}{h(\theta)}$$

and thus the following table may be prepared

	θ	$\sin\theta$	$\cos\theta$	$\cos\theta+\sin\theta$	$\cos\theta-\sin\theta$	$h(\theta)$	$h'(\theta)$	t_i
θ_1	$7^0.5$	0.13053	0.99144	1.12197	0.86091	3.7399	2.8697	0.26739
θ_2	$22^0.5$	0.38268	0.92388	1.30656	0.54120	4.3552	1.8040	0.22961
θ_3	$37^0.5$	0.60876	0.79335	1.40211	0.18459	4.6737	0.61530	0.21396

From the tables in Appendix B it is found:

at t_1

$H_0 = 1.0359$ $\qquad$ $H_0' = -3.6283$

$H_4 = 0.30649$ $\qquad$ $H_4' = -4.9243$

$H_8 = 0.09800$ $\qquad$ $H_8' = -3.1161$

at t_2

$H_0 = 1.1782$ $\qquad$ $H_0' = -4.2491$

$H_4 = 0.57396$ $\qquad$ $H_4' = -10.531$

$H_8 = 0.34091$ $\qquad$ $H_8' = -12.492$

at t_3

$H_0 = 1.2507$ $\qquad$ $H_0' = -4.5967$

$H_4 = 0.78388$ $\qquad$ $H_4' = -15.464$

$H_8 = 0.64161$ $\qquad$ $H_8' = -25.321$

Thus the boundary condition invoked at point 1 leads to the equation

$$1 + 3.7399\left[3.6283\ A_0 + (4.9243)(0.86603)\ A_4 + (3.1161)(0.50)\ A_8\right] + (3.7399)(2.8697)\left[4(0.30649)(0.50)A_4 + 8(0.09800)(0.86603)\ A_8\right] = 0$$

or

$$13.5695\ A_0 + 22.5278\ A_4 + 13.1139\ A_8 = -1.$$

Similarly at points 2 and 3, respectively,

$$18.5057\ A_0 + 18.0379\ A_4 - 54.4052\ A_8 = -1$$

$$21.4836\ A_0 - 58.0830\ A_4 + 46.3881\ A_8 = -1$$

The solutions of these simultaneous equations are

$A_0 = -0.05803$

$A_4 = -0.007249$

$A8 = -0.003760$

With reference to equations (4.18) and (2.5) the complete linearized

velocity and pressure distributions between the apex Mach cone and the conical body surface are now known.

In proceeding to the nonconical body and the third step in the solution, it is observed that $h'(\theta_0)=0$, hence according to equation (8.4), the condition to be fulfilled at P_2 is simply

$$\mathcal{U} f'(x_{02}) + h(\theta_0)\left[\bar{\varphi}_{r_x}(0,2) + c_1 \bar{\varphi}_{r_x}(1,2)\right] = 0.$$

Apparently only the velocity distribution

$$v = \frac{\partial \bar{\varphi}}{\partial r_x}$$

need be calculated from the foregoing conical solution. By (4.18b)

$$v_0 \equiv v(\theta=\theta_0=\tfrac{\pi}{4}) = \mathcal{U}\left[A_0 H_0'(x) - A_4 H_4'(x) + A_8 H_8'(x)\right]$$

Using this formula, Table DI is prepared. From this table the numbers $\frac{1}{\mathcal{U}} \frac{\partial \bar{\varphi}}{\partial r_x}(y;i)$ may be determined by interpolation, using the logarithmic interpolation formula described in Appendix B. The work is conveniently arranged as shown on Table DII, using the notation of Appendix B.

Calculation of c_1 : The equation is

$$\mathcal{U} f'(x_{02}) + h(\theta_0)\left[\bar{\varphi}_{r_x}(0,2) + c_1 \bar{\varphi}_{r_x}(1,2)\right] = 0 \qquad (8.4)$$

or

$$0.52100 + 4.71405\left[0.991390 + 0.181585\, c_1\right] = 0$$

$$c_1 = -6.06829 .$$

Subsequent equations are written as described in Section VIII; each contains only one new unknown, hence the solutions are immediate. One finds

$$C_2 = -15.4749$$

$$C_3 = -16.3560$$

$$C_4 = +158.990 \ .$$

The values of C_1, C_2, and C_3 are reliable, but that of C_4, which is determined by the boundary condition applied on the cylindrical portion of the body, is obviously not. The unacceptable value of C_4 is evidence of the numerical uncertainty encountered in the solution of equations involving the difference of large numbers which are almost equal. In order to fulfill the boundary condition more accurately on the cylindrical portion of the present body by this method the reference points ξ_i would have to be more closely positioned and greater care exercised in the determination of the coordinates (j,i).

The aerodynamic characteristics of this body may now be determined by the methods described in Section VIII.

Table D I

t	$A_0 H_0'(t)$	$A_4 H_4'(t)$	$A_8 H_8'(t)$	$\frac{v_0}{U}$
0.08	0.72305	15.0721	629.123	614.774
0.10	0.57739	4.92396	83.8518	79.5052
0.12	0.48009	1.97151	16.1124	14.6209
0.14	0.41042	0.90815	3.98297	3.48524
0.16	0.35802	0.46343	1.18354	1.07813
0.18	0.31712	0.25568	0.40458	0.46602
0.20	0.28429	0.15000	0.15440	0.28869
0.22	0.25730	0.09169	0.06333	0.22894
0.24	0.23473	0.05937	0.02889	0.20425
0.26	0.21552	0.03944	0.01377	0.18985
0.28	0.19896	0.02697	0.00692	0.17891
0.30	0.18452	0.01890	0.00363	0.16925
0.35	0.15531	0.00849	0.00085	0.14767

Table D II

t	$\frac{f(b)}{f(a)}$	$\log_{10}\frac{f(b)}{f(a)}$	p	p log	antilog	$f(a)$	$f(a+\delta)$	(i,j)
0.090	0.129324	9.1116791	0.50	9.5558396	0.359616	614.774	221.082	(0,5)
0.110	0.183899	9.2645793	0.50	9.6322897	0.428734	79.5052	34.0866	(1,5)
0.115	"	"	0.75	9.4484345	0.280824	"	22.3270	(0,4)
0.139	0.238373	9.3772571	0.85	9.4706685	0.295576	14.6209	4.32160	(0,3)
0.145	0.309342	9.4904389	0.25	9.8726097	0.745778	3.48524	2.59922	(1,4)
0.148	"	"	0.40	9.7961756	0.625426	"	2.17976	(2,5)
0.162	0.432248	9.6357330	0.10	9.9635733	0.919546	1.07813	0.991390	(0,2)
0.185	0.619480	9.7920273	0.25	9.9480068	0.887170	0.46602	0.413439	(0,1)
0.195	"	"	0.75	9.8440205	0.698265	"	0.325405	(1,3)
0.207	0.793031	9.8992902	0.35	9.9647516	0.922044	0.28869	0.266185	(2,4)
0.208	"	"	0.40	9.9597161	0.911415	"	0.263116	(3,5)
0.275	0.942376	9.9742243	0.75	9.9806682	0.956463	0.18985	0.181585	(1,2)
0.330	0.872496	9.9407634	0.60	9.9644580	0.921421	0.16925	0.155951	(2,3)
0.344	"	"	0.88	9.9478718	0.886894	"	0.150107	(3,4)
0.345	"	"	0.90	9.9466871	0.884478	"	0.149698	(4,5)

FIGURE I

RANGE OF APPLICABILITY OF LINEARIZED THEORY FOR 10% MAX. ERROR IN VELOCITY PREDICTION. $t_s = \sqrt{M^2-1}\tan\theta_s$.

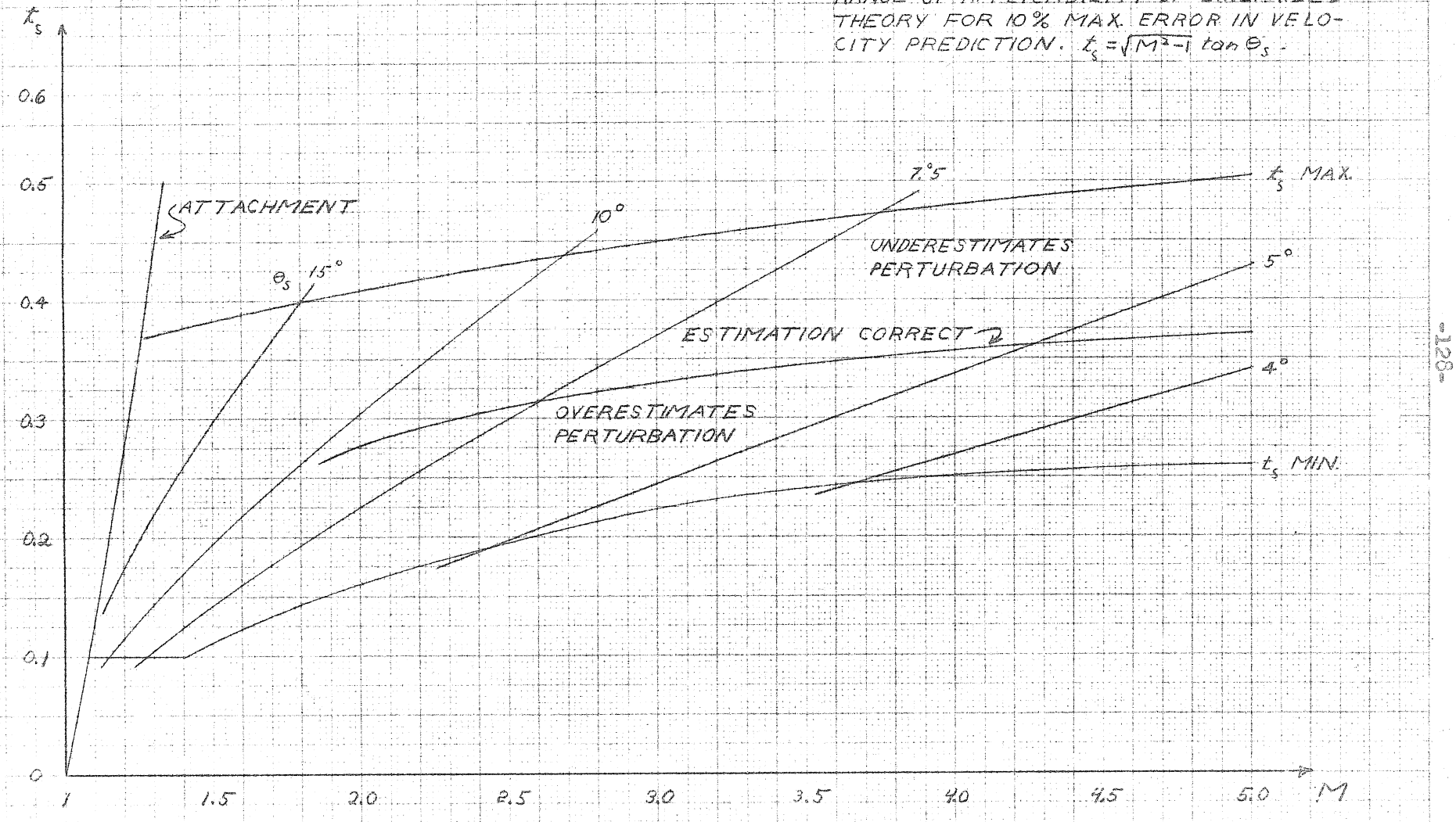

FIGURE II

COMPARISON OF LINEARIZED AND EXACT PREDICTIONS OF VELOCITY AT SURFACE OF CONES OF VARIOUS HALF-ANGLE

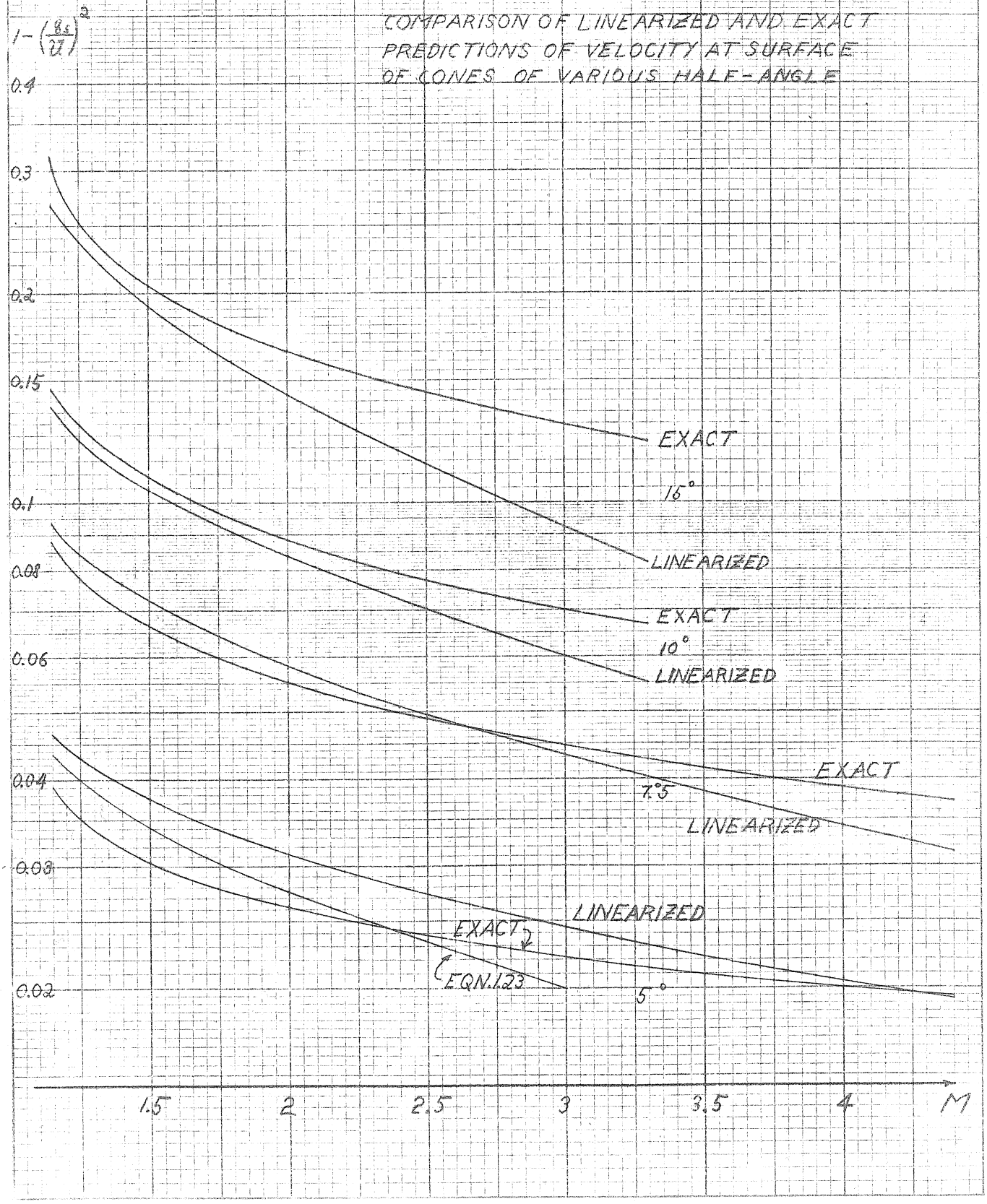

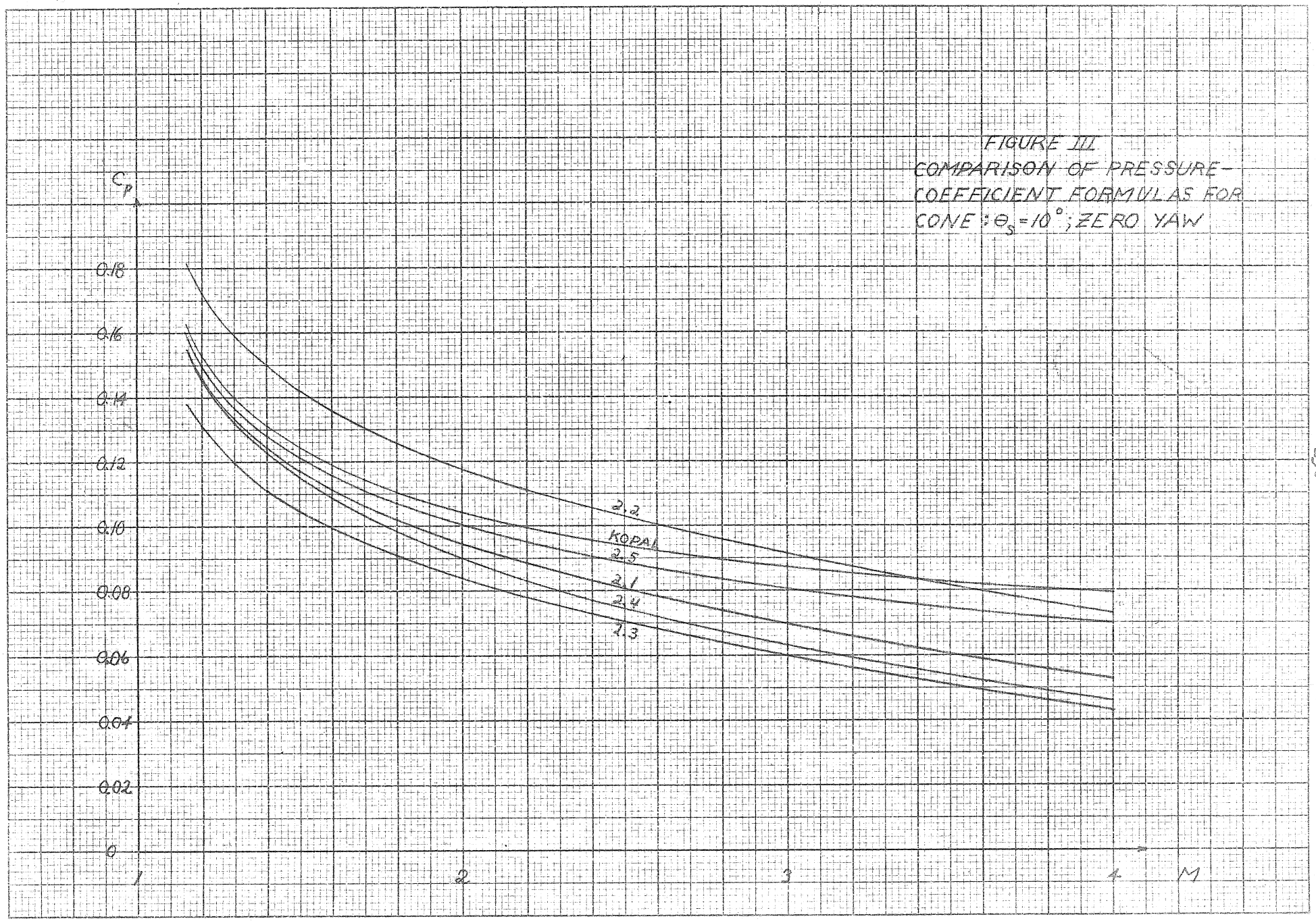

FIGURE III
COMPARISON OF PRESSURE-COEFFICIENT FORMULAS FOR CONE; $\theta_s = 10^\circ$; ZERO YAW

FIGURE IV

LORENTZ MAPPING OF CIRCULAR CONE

$\tau_s = 0.20$; $a = -0.50$

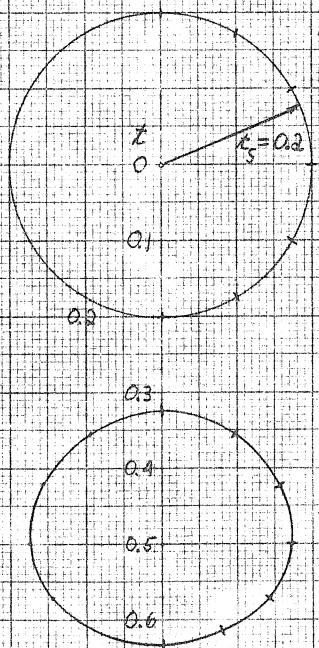

TRACE OF MACH CONE

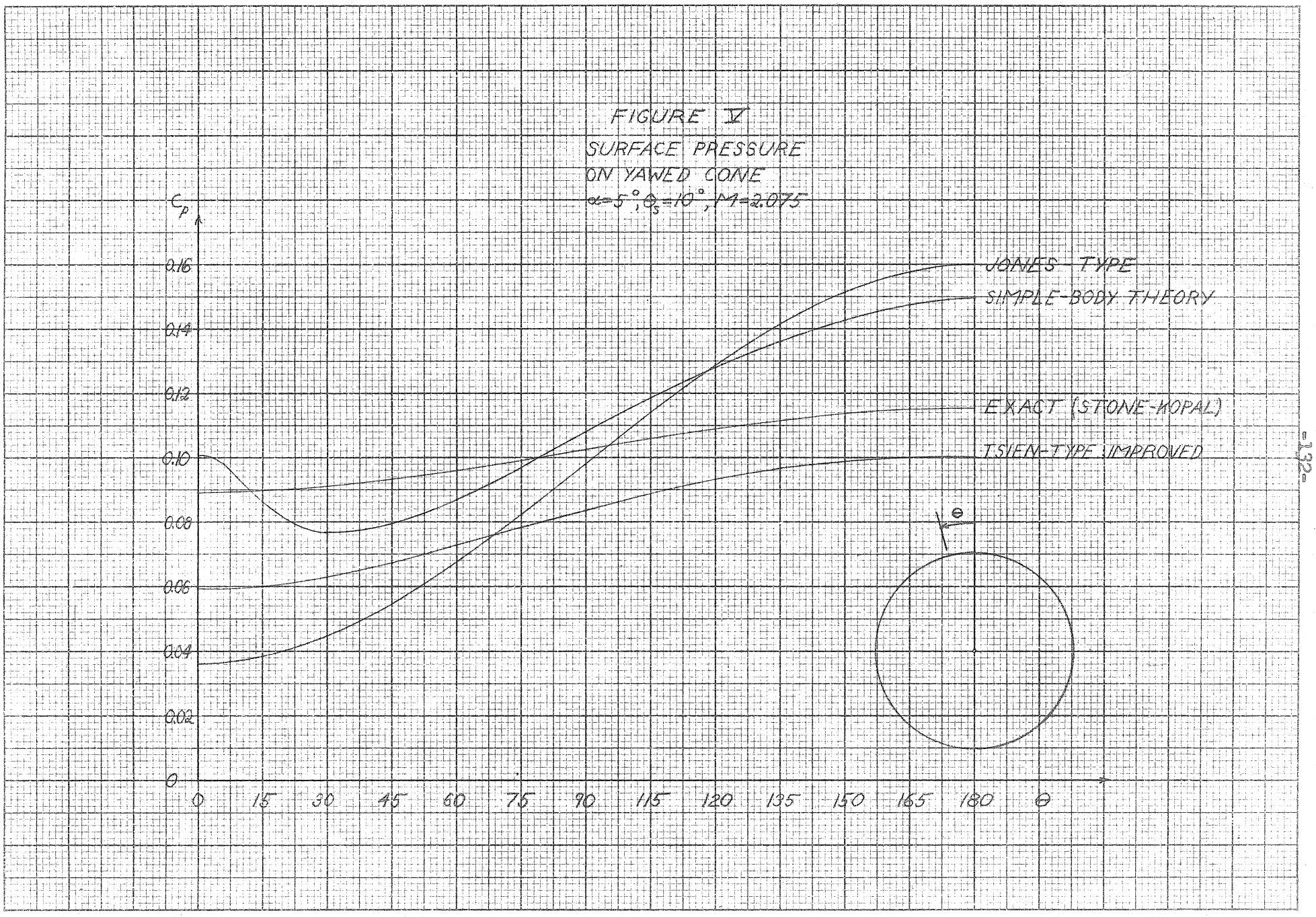
FIGURE V
SURFACE PRESSURE
ON YAWED CONE
$\alpha = 5^\circ, \theta_s = 10^\circ, M = 2.075$
C_p
0.16
0.14
0.12
0.10
0.08
0.06
0.04
0.02
0
0
15
30
45
60
75
90
115
120
135
150
165
180
θ
JONES - TYPE
SIMPLE-BODY THEORY
EXACT (STONE-KOPAL)
TSIEN-TYPE IMPROVED
θ